

**Improving safety and  
establishing episomal maintenance of  
Adeno-associated viral vectors**

Inaugural-Dissertation

zur

Erlangung des Doktorgrades

der Mathematisch-Naturwissenschaftlichen Fakultät

der Universität zu Köln

vorgelegt von

Maria Angelika Schnödt

aus Auerbach i.d.OPf.

Köln, 2016

Berichterstatterin: Prof. Dr. Dagmar Mörsdorf

Prof. Dr. Mirka Uhlířova

Prof. Dr. Hildegard Büning

Tag der mündlichen Prüfung: 24.10.2016

## Kurzzusammenfassung

Adeno-assoziierte virale (AAV) Vektoren sind eine der am häufigsten verwendeten Gentransfersysteme in der Grundlagen- und der präklinischen Forschung und wurden bereits in mehr als 160 klinischen Studien angewendet. Üblicherweise werden sie durch Kotransfektion eines sogenannten Vektorplasmids und zweier, oder wie in meiner Arbeit, eines Helferplasmids in einer Produktionszelllinie hergestellt. Das Vektorplasmid enthält die Transgenexpressionskassette („transgene cassette of interest“ (TEC)) flankiert von den viralen „inverted terminal repeats“ (ITRs), palindromischen Sequenzen, die als Verpackungssignale fungieren, während das Helferplasmid die notwendigen AAV- und Helfervirusgene *in trans* bereitstellt. Ein entscheidender Aspekt der AAV-Vektorologie ist die Herstellung von AAV-Vektoren frei von durch den Produktionsprozess anfallenden Unreinheiten. Zu diesen Unreinheiten gehören AAV-Kapside, die prokaryotische Sequenzen wie z.B. antibiotische Resistenzgene enthalten, die von den Ausgangsplasmiden stammen.

Das Ziel des ersten Teils dieser Arbeit war die Verbesserung der Sicherheit von AAV-Vektoren. Da es nicht möglich ist, in AAV-Kapside verpackte prokaryotische Sequenzen durch Standard-Reinigungsprotokolle zu entfernen, wurde untersucht, ob die Ausgangsplasmide für die Vektorproduktion durch „Minicircles“ (MCs) ersetzt werden können. MCs sind zirkuläre DNS-Konstrukte die keine funktionalen oder kodierenden prokaryotischen Sequenzen beinhalten; sie bestehen nur aus der TEC und einem kurzen Abschnitt der für ihre Herstellung und Aufreinigung nötig ist. Ein Vektor-MC als Gegenstück für ein Vektorplasmid das für das enhanced green fluorescent (eGFP) Protein kodiert und ein Helfer-MC als Gegenstück für das Helferplasmid welches für die Gene von AAV Serotyp 2 (AAV2) und die Gene des Helfervirus Adenovirus Typ 5 kodiert, wurden von PlasmidFactory (Bielefeld, Germany) entwickelt und produziert. Die vier möglichen Kombinationen von MCs und Plasmiden wurden anschließend verwendet, um einzelsträngige („single-stranded“) AAV2-Vektoren (ssAAV) und self-complementary“ AAV-Vektoren (scAAV) herzustellen. Die Vektorpräparationen wurden gemäß Vektorquantität, –qualität und –funktionalität charakterisiert. Diese Analysen zeigten, dass die Vektor- und Helferplasmide durch MCs ersetzt werden können, ohne die Effizienz der Vektorproduktion oder die Vektorqualität zu verringern. MC-basierte scAAV-Vektorpräparationen wiesen im Vergleich zu Plasmid-basierten Präparationen sogar eine bis zu 30-fach verbesserte Transduktionseffizienz auf. Durch Verwendung der verschiedenen Kombinationen von Plasmiden und MCs konnte das Vektorplasmid als Hauptquelle der falsch in Kapside verpackten prokaryotischen Sequenzen identifiziert werden. Bemerkenswerterweise beinhalteten die Plasmid-basierten scAAV-Vektorpräparationen eine beträchtlich höhere Menge prokaryotischer Sequenzen (bis zu 26,1 %, im Verhältnis zur TEC) als ssAAV-Vektorpräparationen (bis zu 2,9 %). Durch Ersetzen beider Plasmide durch MC wurde die Menge an kodierenden prokaryotischen Sequenzen unter die Nachweisgrenze reduziert. Weitere Analysen zeigten, dass scAAV-Vektoren im Allgemeinen einen höheren Anteil weiterer DNS-Unreinheiten (wie z.B. adenovirale Sequenzen) als ssAAV-Vektoren aufwiesen. So

wohl ssAAV- als auch scAAV-Vektorpräparationen die mit MCs hergestellt wurden tendierten dazu, kleinere Mengen Fremd-DNS zu beinhalten als Vektorpräparationen die mit Plasmiden hergestellt wurden. Keine der getesteten Vektorpräparationen induzierte Immunogenität. Somit lässt sich zusammenfassend sagen, dass die Qualität von AAV-Vektorpräparationen signifikant verbessert wird, wenn statt Plasmiden MCs zur Herstellung verwendet werden.

Nach erfolgreicher Zelltransduktion bilden die AAV-Vektorgenome überwiegend doppelsträngige DNS-Ringe oder DNS-Konkatemere aus. Diese episomalen Moleküle persistieren in post-mitotischen Zellen und vermitteln so langfristige Transgenexpression, gehen jedoch in proliferierenden Zellen mit fortschreitender Zellteilung verloren. Für den zweiten Teil dieser Arbeit wurde, in Kooperation mit Claudia Hagedorn und Hans J. Lipps (Universität Witten/Herdecke), ein AAV-Vektor mit einem autonom replizierenden Element (Scaffold/matrix attachment region (S/MAR)) ausgestattet. Vektor AAV-S/MAR, kodierend für eGFP und ein Blasticidin-Resistenzgen und ein Kontrollvektor mit der gleichen TEC, aber ohne das S/MAR-Element wurden produziert und in schnell proliferierende HeLa-Zellen transduziert. Durch Inkubation mit dem Antibiotikum Blasticidin wurden die Zellen selektioniert die das Vektorgenom stabil bewahrten. AAV-S/MAR-transduzierte Zellen wiesen eine höhere Anzahl an überlebenden Zellkolonien auf als AAV- $\Delta$ S/MAR-transduzierte Zellen. Zellkolonien beider Vektoren wurden isoliert und kultiviert. Sie blieben bis zu 70 Tage (maximaler Kultivierungszeitraum) eGFP-positiv – ohne Selektionsdruck durch Antibiotikagabe. Erstaunlicherweise war die mitotische Stabilität sowohl von AAV-S/MAR als auch des Kontrollvektors AAV- $\Delta$ S/MAR ein Resultat episomaler Persistenz des jeweiligen Vektorgenoms. Diese Ergebnisse lassen die Annahme zu, dass „gewöhnliche“ AAV-Vektorgenome unter spezifischen Bedingungen, wie durch den verwendeten milden Selektionsdruck, episomal persistieren können. Unter diesen Umständen erhöht das S/MAR-Element die Häufigkeit der Etablierung des stabilen Episoms, ist aber keine Grundvoraussetzung.

## Abstract

Adeno-associated viral (AAV) vectors are among the most widely used gene transfer systems in basic and pre-clinical research and have been employed in more than 160 clinical trials. AAV vectors are commonly produced in producer cell lines like HEK293 by co-transfection with a so-called vector plasmid and one (in this work) or two so-called helper plasmids. The vector plasmid contains the transgene cassette of interest (TEC) flanked by AAV's inverted terminal repeats (ITRs) which serve as packaging signals, whereas the helper plasmid provides the required AAV and helper virus functions *in trans*. A pivotal aspect of AAV vectorology is the manufacturing of AAV vectors free from impurities arising during the production process. These impurities include AAV vector preparations that contain capsids containing prokaryotic sequences, e.g. antibiotic resistance genes originating from the producer plasmids.

In the first part of the thesis we aimed at improving the safety of AAV vectors. As we found that encapsidated prokaryotic sequences (using the ampicillin resistance gene as indicator) cannot be removed by standard purification methods we investigated whether the producer plasmids could be replaced by Minicircles (MCs). MCs are circular DNA constructs which contain no functional or coding prokaryotic sequences; they only consist of the TEC and a short sequence required for production and purification. MC counterparts of a vector plasmid encoding for enhanced green fluorescent (eGFP) protein and a helper plasmid encoding for AAV serotype 2 (AAV2) and helper Adenovirus (Ad) genes were designed and produced by PlasmidFactory (Bielefeld, Germany). Using all four possible combinations of plasmid and MCs, single-stranded AAV2 vectors (ssAAV) and self-complementary AAV vectors (scAAV) were produced and characterized for vector quantity, quality and functionality. The analyses showed that plasmids can be replaced by MCs without decreasing the efficiency of vector production and vector quality. MC-derived scAAV vector preparations even exceeded plasmid-derived preparations, as they displayed up to 30-fold improved transduction efficiencies. Using MCs as tools, we found that the vector plasmid is the main source of encapsidated prokaryotic sequences. Remarkably, we found that plasmid-derived scAAV vector preparations contained a much higher relative amount of prokaryotic sequences (up to 26.1 %, relative to TEC) compared to ssAAV vector preparations (up to 2.9 %). By replacing both plasmids by MCs the amount of functional prokaryotic sequences could be decreased to below the limit of quantification. Additional analyses for DNA impurities other than prokaryotic sequences showed that scAAV vectors generally contained a higher amount of non-vector DNA (e.g. adenoviral sequences) than ssAAV vectors. For both, ssAAV and scAAV vector preparations, MC-derived vectors tended to contain lower amounts of foreign DNA. None of the vectors tested could be shown to induce immunogenicity. In summary we could demonstrate that the quality of AAV vector preparations could be significantly improved by replacing producer plasmids by MCs.

Upon transduction of a target tissue, AAV vector genomes predominantly remain in an episomal state, as duplex DNA circles or concatemers. These episomal forms mediate long-term transgene expression in terminally differentiated cells, but are lost in proliferating cells due to cell division. Therefore, in the second part of the thesis, in cooperation with Claudia Hagedorn and Hans J. Lipps (University Witten/Herdecke) an AAV vector genome was equipped with an autonomous replication element (Scaffold/matrix attachment region (S/MAR)). AAV-S/MAR encoding for eGFP and a blasticidin resistance gene and a control vector with the same TEC but lacking the S/MAR element (AAV- $\Delta$ S/MAR) were produced and transduced into highly proliferative HeLa cells. Antibiotic pressure was employed to select for cells stably maintaining the vector genome. AAV-S/MAR transduced cells yielded a higher number of colonies than AAV- $\Delta$ S/MAR-transduced cells. Colonies derived from each vector transduction were picked and cultured further. They remained eGFP-positive (up to 70 days, maximum cultivation period) even in the absence of antibiotic selection pressure. Interestingly, the mitotic stability of both AAV-S/MAR and control vector AAV- $\Delta$ S/MAR was found to be a result of episomal maintenance of the vector genome. This finding indicates that, under specific conditions such as the mild selection pressure we employed, “common” AAV vectors persist episomally. Thus, the S/MAR element increases the establishment frequency of stable episomes, but is not a prerequisite.

# Table of Contents

List of figures .....	IX
List of tables .....	X
List of abbreviations.....	XI
<b>1 Introduction.....</b>	<b>1</b>
1.1 Adeno-associated virus .....	1
1.1.1 Classification .....	1
1.1.2 Genome and proteins.....	2
1.1.3 Life cycle .....	4
1.2 AAV vectorology .....	7
1.2.1 Production.....	8
1.2.1.1 Upstream processing.....	8
1.2.1.2 Downstream processing .....	9
1.2.1.3 Challenges .....	10
1.3 AAV vector transduction and optimization.....	12
1.3.1 Vector tropism and immunogenicity.....	12
1.3.2 Intracellular trafficking .....	13
1.3.3 Vector genome fate in the nucleus .....	13
1.3.3.1 Interaction with DNA damage response proteins .....	13
1.3.3.2 Double strand synthesis .....	14
1.3.3.3 Long-term persistence.....	16
<b>2 Aim of the study.....</b>	<b>17</b>
2.1 Aim of study I: Improving safety of AAV vectors.....	17
2.2 Aim of study II: Establishment of episomal maintenance .....	18
<b>3 Materials.....</b>	<b>19</b>
3.1 Chemicals, reagents and enzymes .....	19
3.2 Commercial kits .....	19
3.3 Cell culture media and supplements .....	19
3.4 Plasmids and MC .....	20
3.5 Primers for qPCR .....	21
3.6 Eukaryotic cell lines .....	21
3.7 Bacteria strain.....	21
3.8 Laboratory equipment.....	22
3.9 Data treating software.....	23

<b>4</b>	<b>Methods</b>	<b>24</b>
4.1	Bacteria Culture	24
4.1.1	Cultivation	24
4.1.2	Preparation of competent bacteria	24
4.1.3	Transformation	24
4.2	Nucleic acid techniques	25
4.2.1	pDNA amplification and extraction	25
4.2.2	DNA extraction from eukaryotic cells	25
4.2.3	RNA extraction from eukaryotic cells	25
4.2.4	Determination of pDNA and RNA concentration	25
4.2.5	Restriction enzyme digest	25
4.2.6	Agarose gel electrophoresis	25
4.2.6.1	Neutral	25
4.2.6.2	Denaturing	26
4.2.7	cDNA synthesis	26
4.2.8	Quantitative real-time PCR	26
4.3	Protein techniques	27
4.3.1	ELISA	27
4.3.2	Western Blot	27
4.4	Eucaryotic cell culture	29
4.4.1	Cultivation conditions	29
4.4.2	Passaging, counting and seeding	29
4.4.3	Freezing and thawing	29
4.5	AAV vector production	30
4.6	AAV vector purification	31
4.6.1	Iodixanol density gradient	31
4.6.2	Affinity chromatography	31
4.6.3	Centrifugal filtration	32
4.6.4	Gel filtration	32
4.7	AAV vector characterization	32
4.7.1	Genomic titer	32
4.7.2	Transducing titer	32
4.7.3	Capsid titer and composition	33
4.7.4	DNA impurity content	33
4.8	Cell transduction by AAV vectors	33
4.8.1	TLR9 activation assays	33
4.8.1.1	Quantification of SEAP protein levels	33
4.8.1.2	Quantification of IL8 transcription levels	33
4.8.2	Colony forming assay	33

4.9	Statistical Analysis .....	34
<b>5</b>	<b>Results</b> .....	<b>35</b>
5.1	Improving the purity of AAV vector preparations using DNA Minicircle (MC) technology.....	35
5.1.1	Encapsidated prokaryotic sequences in AAV vector preparations cannot be removed by standard purification methods.....	35
5.1.2	Evaluation of MC constructs for ssAAV vector production .....	37
5.1.3	Vector plasmids are the main source of encapsidated prokaryotic sequences .....	41
5.1.4	Proximity to ITRs rather than a specific sequence element is decisive for packaging of backbone sequences.....	41
5.1.5	Self-complementary AAV (scAAV) vector preparations produced by MC constructs show improved transduction efficiencies and contain no ampR DNA impurities .....	43
5.1.6	Further characterization of plasmid and MC-derived ssAAV and scAAV vectors .....	46
5.1.7	AAV vectors do not activate Toll-like receptor 9 <i>in vitro</i> .....	48
5.2	Establishment of episomal maintenance of AAV vectors .....	51
5.2.1	Colony forming assay.....	51
5.2.2	Mitotic stability of AAV-S/MAR vector genomes in HeLa cells .....	53
5.2.3	Mitotic stability of AAV- $\Delta$ S/MAR vector genomes in HeLa cells .....	57
<b>6</b>	<b>Discussion</b> .....	<b>60</b>
6.1	MC technology for AAV vector production .....	60
6.1.1	Prokaryotic DNA is encapsidated during AAV vector production .....	60
6.1.2	Comparison of plasmid and MC-derived AAV vector preparations .....	60
6.1.3	Model for packaging of prokaryotic sequences.....	61
6.1.4	DNA impurities in AAV vector preparations .....	64
6.1.5	Interaction of AAV vectors with the innate immune system.....	65
6.1.6	Challenges and chances of using MC for AAV vector production .....	66
6.2	Episomal maintenance of AAV vectors .....	67
6.2.1	S/MAR-based vectors for gene therapy.....	67
6.2.2	Episomal AAV-S/MAR and AAV- $\Delta$ S/MAR vector genomes .....	68
6.2.3	Conditions for establishment of stable AAV vector episomes .....	69
6.2.4	Outlook.....	70
<b>7</b>	<b>References</b> .....	<b>72</b>
	Appendix .....	94
	Danksagung .....	98
	Erklärung .....	99

## List of figures

Figure 1 Genome organization of AAV2.....	2
Figure 2 Capsid of AAV2. ....	4
Figure 3 Schematic model of AAV2 infection. ....	6
Figure 4 AAV vector production by transient transfection. ....	8
Figure 5 AAV genome replication and generation of self-complementary AAV vector genomes. ....	15
Figure 6 Antibiotic resistance gene (ampR) sequences in standard AAV vector preparations. ....	36
Figure 7 ssAAV vector and AAV/Ad helper plasmids and thereof derived MC constructs. ....	37
Figure 8 Western Blot analysis of ssAAV vector preparations.....	39
Figure 9 ampR sequences in ssAAV preparations. ....	41
Figure 10 scAAV vector plasmid and thereof derived MC construct. ....	43
Figure 11 ampR sequences in scAAV preparations. ....	46
Figure 12 Analysis of ssAAV and scAAV vector genomes by denaturing gel electrophoresis. ....	47
Figure 13 SEAP production of HEK blue hTLR9 cells upon transduction. ....	49
Figure 14 IL8 gene expression of HEK blue hTLR9 cells upon transduction. ....	50
Figure 15 Plasmid maps of pAAV-S/MAR and pAAV-ΔS/MAR. ....	51
Figure 16 Cultivation of AAV-S/MAR and AAV-ΔS/MAR-transduced cells in absence of selection. ..	52
Figure 17 Colony count of blasticidin-resistant cells.....	53
Figure 18 Transgene expression of AAV-S/MAR-derived colonies. ....	53
Figure 19 Long-term transgene expression of AAV-S/MAR-derived colonies in absence of selection. .....	54
Figure 20 Episomal maintenance of AAV-S/MAR vector genomes in HeLa cells (I).....	55
Figure 21 Episomal maintenance of AAV-S/MAR vector genomes in HeLa cells (II).....	56
Figure 22 Transgene expression of AAV-ΔS/MAR-derived colonies. ....	57
Figure 23 Long-term transgene expression of AAV-ΔS/MAR-derived colonies in absence of selection. .....	57
Figure 24 Episomal maintenance of AAV-ΔS/MAR vector genomes in HeLa cells (I).....	58
Figure 25 Episomal maintenance of AAV-ΔS/MAR vector genomes in HeLa cells (II).....	59
Figure 26 Model of proposed rescue mechanism.....	63

## List of tables

Table 1 Particle titer and packaging efficiency of ssAAV vector preparations.....	38
Table 2 Transducing titer and transduction efficiency of ssAAV preparations. ....	40
Table 3 Quantification of prokaryotic DNA in the dual plasmid preparations. ....	42
Table 4 Quantification of SCAR sequences in ssAAV vector preparations.....	42
Table 5 Particle titer and packaging efficiency of scAAV vector preparations.....	44
Table 6 Transducing titer and transduction efficiency of scAAV vector preparations.....	45
Table 7 Further DNA impurities in ssAAV and scAAV vector preparations.....	48

## List of abbreviations

°C	Degree celsius	HEPES	(4-(2-hydroxyethyl)-1-piperazineethanesulfonic acid )
μ (g,l,M)	micro (gram, liter, mole/molar)	HP	Hairpin
A	Ampere	HRP	Horseradish peroxidase
Å	Ångström	HSPG	Heparan sulfate proteoglycan
AAP	Assembly-activating protein	HSV	Herpes simplex virus
AAV	Adeno-associated virus	i.e.	lat. Id est, engl. That is
AAVS1	AAV integration site 1	IDGC	Iodixanol density gradient centrifugation
abs.	Absorption	IL	Interleukin
Ad	Adenovirus	IRES	Internal ribosome entry site
ampR	Ampicillin resistance gene	ITR	Inverted terminal repeat
ANOVA	Analysis of variance	IU	International units
AP-1	Activator protein 1	kanR	Kanamycin/neomycin resistance gene
APS	Ammonium persulfate	kb	Kilo bases
bp	Base pair	L	Liter
cDNA	complementary DNA	LB	Lysogeny broth
CMV	Cytomegalovirus	m (g, l, M)	milli-(gram , liter, mole)
DMEM	Dulbecco's modified eagle medium	MC	Minicircle
DMSO	Dimethyl sulfoxide	MFI	Mean fluorescence intensity
DNA	Deoxyribonucleic acid	min	Minutes
DNase	Deoxyribonuclease	n.s.	Not significant
ds	Double-strand	NF-κB	Nuclear factor kappa B
DTT	Dithiothreitol	NPC	Nuclear pore complex
<i>E.coli</i>	<i>Escherichia coli</i>	OD	Optical density
e.g.	lat. Exempli gratia, engl. For example	ORF	Open reading frame
EDTA	Ethylenediaminetetraacetic acid	ori	Origin of replication
eGFP	enhanced green fluorescent protein	p.t.	Post-transduction
ELISA	Enzyme-linked immunosorbent assay	PBS	Phosphate-buffered saline
FACS	fluorescence-activated cell sorting	pDNA	plasmid DNA
FCS	Fetal calf serum	PLA2	Phospholipase A2
FISH	Fluorescence in situ hybridization	PLAT	Tissue plasminogen activator
GAPDH	Glyceraldehyd-3-phosphat-Dehydrogenase	qPCR	quantitative polymerase chain reaction
GOI	Genomic particles per cell	rAAV	recombinant adeno-associated virus
h, hrs	Hour, hours	RFP	Red fluorescent protein
HBS	HEPES-buffered saline	RNA	Ribonucleic acid

rpm	Rounds per minute	Tris	Tris(hydroxymethyl)aminomethane
RT	Room temperature	trs	Terminal resolution site
RT-PCR	Reverse transcriptase polymerase chain reaction	U/ $\mu$ l	Units per $\mu$ l
sc	Self-complementary	UV	Ultraviolet light
SCAR	Sequence for chromatography, affinity and recombination	V	Volt
SDS	Sodium dodecyl sulfate	vg	Vector genomes
SEAP	Secreted embryonic alkaline phosphatase	VP	Viral protein
ss	Single-stranded	wt	Wild type
TAE	Tris-acetate-EDTA	x g	Gravitational force
TEMED	Tetramethylethylenediamine	$\Delta$ , delta	Deletion
TLR	Toll-like receptor		



# 1 Introduction

## 1.1 Adeno-associated virus

### 1.1.1 Classification

Adeno-associated virus (AAV) belongs to the parvovirus family (*Parvoviridae*), which comprises all small, isometric, non-enveloped DNA viruses with a linear single-stranded genome. Parvoviruses are divided into the subfamilies *Parvovirinae*, infecting vertebrates, and *Densovirinae*, infecting arthropods.<sup>1</sup> With capsid diameters of just around 25 nm, *Parvoviridae* contain only a short DNA sequence of about 5 kb. Because of the resulting genetic simplicity *Parvoviridae* are greatly dependent on their host cell to support their life cycle. AAV additionally relies on functions provided by more intricate helper viruses, such as adenovirus (Ad), human papillomavirus (HPV), and members of the herpes virus family, including herpes simplex virus (HSV) -1 and -2, human cytomegalovirus, Epstein-Barr virus and varicella virus to foster its propagation.<sup>2-6</sup> Thus, AAV is classified in the genus *Dependovirus* within the *Parvovirinae*.

Since its discovery in 1965<sup>2, 7</sup> at least twelve AAV serotypes differing in tissue tropism and originating from humans and non-human primates have been described.<sup>8</sup> Moreover, more than 100 AAV genomic variants have been found in human and non-human primate tissues.<sup>9</sup> This reflects the widespread dissemination of AAV: up to 80% of humans (population-to-population variation, region-dependent) possess anti-AAV antibodies to serotypes 1, 2, 3 and 5, with up to 60 % harboring neutralizing antibodies.<sup>10, 11</sup> Given the high prevalence of AAV, reports of AAV-induced pathology are scarce. Except for reports associating early AAV infection in pregnancy with spontaneous abortion,<sup>12</sup> AAV is considered as non-pathogenic.<sup>13</sup> Recently, Nault and colleagues found integrated AAV2 sequences in hepatocellular carcinoma driver genes, which led them to propose that insertional mutagenesis of AAV2 may cause malignant transformation in the liver.<sup>14</sup> Yet, in the meantime, this report has been challenged regarding methodology of the analyses, the conclusions drawn from the data, and the implications of the findings.<sup>15-17</sup> On the other side, researchers have put forward that AAV may actually be beneficial for its host. This hypothesis is based on the finding that AAV inhibits replication of its pathogenic helper viruses.<sup>18, 19</sup> Indeed, possibly due to AAV impeding replication of HPV, serological studies reported a negative correlation of AAV with cervical carcinoma.<sup>13, 20</sup>

### 1.1.2 Genome and proteins

Limited to a genome size of a mere 4.7 kb, AAV2 evolved alternative splicing and alternative open reading frames (ORF) to increase its coding capacity. Structurally, the AAV2 genome contains ORFs *rep*, *cap* and *AAP* in sense orientation, flanked by inverted terminal repeats (ITRs) (Figure 1).

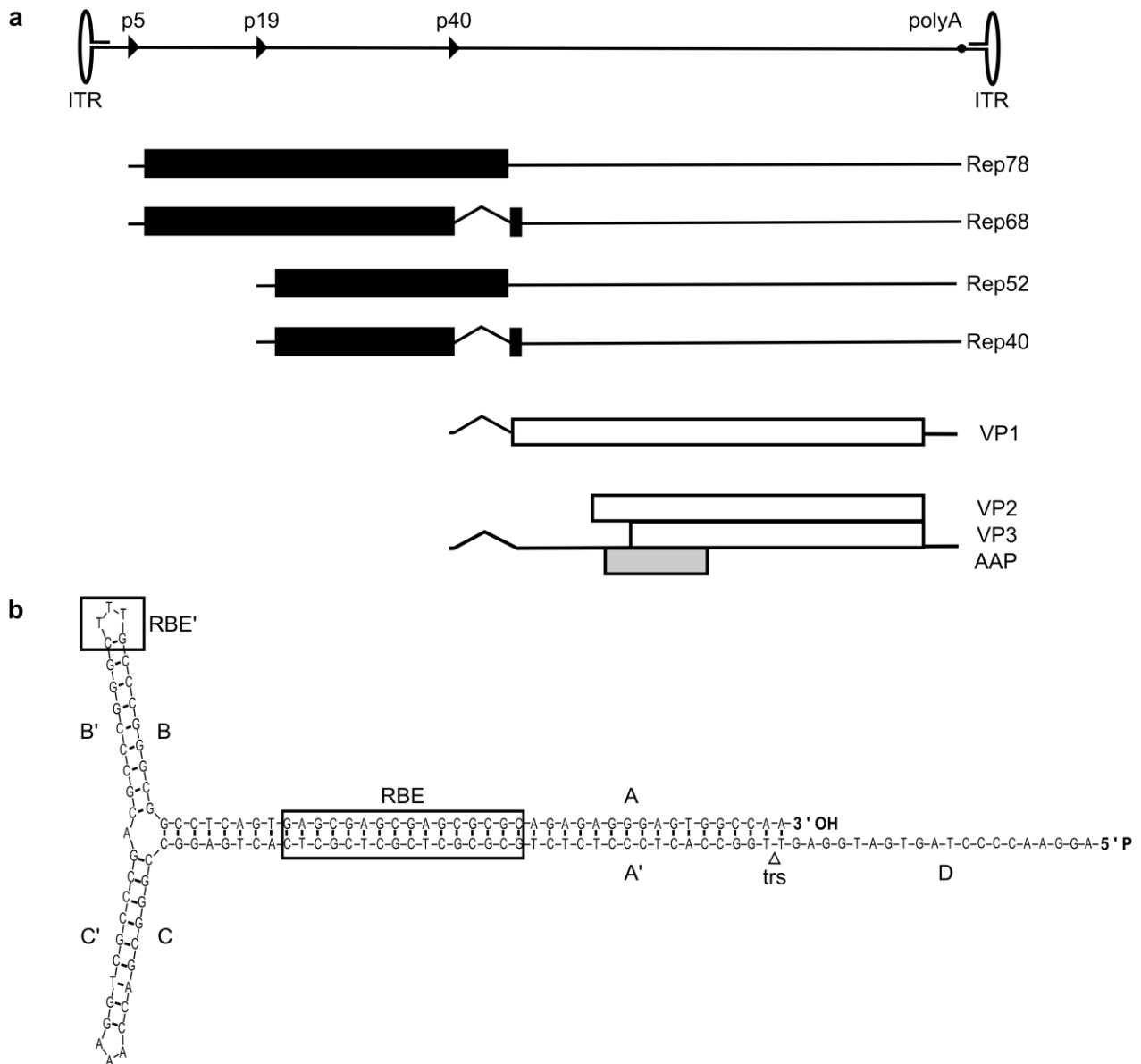


**Figure 1 Genome organization of AAV2.** (a) The single stranded DNA genome of AAV2 has a length of 4.7kb, divided into 100 map units. The positions of promoters p5, p19 and p40 (named according to their map position) are indicated as solid triangles, the polyadenylation signal (polyA) at position 96 is indicated as solid circle. The inverted terminal repeats (ITRs) are represented by ellipses (not to scale). The transcripts from the three promoters are shown below the genome map. Open reading frames (ORF) are depicted by rectangles (in black for *rep* ORF, white for *cap* ORF<sup>21</sup> and light grey for *AAP* ORF<sup>22</sup>), untranslated regions by thin solid lines and introns as nicks. (b) Secondary structure of an AAV2 ITR. The AAV2 ITR is composed of two palindromic regions (B-B' and C-C') within a stem palindrome (A-A'), and a single-stranded D region. The ITR can fold in a flip (depicted here) or flop conformation, with the B-B' or C-C' palindrome closest to the 3' end, respectively. The rectangles mark the binding motif for Rep proteins at the A-A' stem (Rep-binding element, RBE) and the apex of the ITR hairpin (HP) structure (RBE').<sup>23–25</sup> The triangle indicates the terminal resolution site (trs), the specific nicking site of Rep protein. Depiction of the ITR structure is based on Mfold analysis.<sup>26</sup>

The ITRs consist of two 125 nucleotide (nt) palindromes with six segments (A-A', B-B', C-C') forming a T-shaped hairpin (HP) structure, and a 20 nt D sequence (Figure 1b). AAV's origin of replication, the terminal resolution site (*trs*), is located between the A and D sequences.<sup>27, 28</sup> The ITRs act as self-priming HP during genome replication<sup>29</sup> (see Figure 5) and as signals for packaging and integration.<sup>30-32</sup>

The *rep* ORF codes for four non-structural proteins named Rep78, Rep68, Rep52 and Rep40, according to their molecular mass (Figure 1a). Transcription of Rep78 and Rep68 is initiated at promoter site p5, while transcription of Rep52 and Rep40 starts at promoter p19. The smaller Rep proteins of each transcript, Rep68 and Rep40 are generated by splicing of the same intron sequence.<sup>21</sup> The large Rep proteins, Rep78 and Rep68, which possess DNA binding, helicase and site-specific endonuclease activity, are the main protagonists of transcriptional regulation, AAV DNA replication and site-specific integration.<sup>33-38</sup> Rep52 and Rep40 do not seem to be required for DNA replication,<sup>39</sup> but are necessary for generation or accumulation of replicated single-stranded viral DNA in the host cell.<sup>40</sup> Ultimately, Rep52 and Rep40 mediate the packaging of viral DNA into the preformed capsids.<sup>32, 41</sup> The *cap* ORF encodes the capsid structural proteins VP1, VP2 and VP3. They all share a common C-terminus and the complete VP3 sequence of 62kDa. VP1 (87kDa) and VP2 (73kDa) possess additional N-terminal sequences. The N-terminus of VP1 contains motifs which are required for infection (see below); whereas to date, no function of VP2's N-terminus has been determined.<sup>42</sup> Since VP1 is the product of a minor splice transcript and the initiation codon of VP2 is a non-traditional ACG which is frequently skipped, both VP1 and VP2 are translated at lower levels than VP3. Therefore, the AAV capsid consists of 90% VP3, with VP1 and VP2 contributing the remaining 10%.<sup>43, 44</sup> Nested within the *cap* ORF lies an alternative ORF which codes for the assembly activating protein (AAP).<sup>22</sup> AAP targets capsid proteins to the nucleolus and interacts with capsid proteins to provide an assembly scaffold.<sup>45</sup>

The AAV capsid is formed by 60 subunits as an icosahedron,<sup>46</sup> which is characterized by three levels of rotational symmetry, namely fifteen 2-fold axes, ten 3-fold axes and six 5-fold axes (Figure 2). The outward protrusions (red in Figure 2) and adjacent plateau regions at the 3-fold symmetry axes define the interaction of the AAV capsid with cell receptors and represent the capsid's epitope structures.<sup>10, 47-52</sup> At the 5-fold axes, pentameric pores are located (surrounded by elevated rim structures, depicted in yellow in Figure 2). These pores function as channels connecting the capsid inside to the environment and act as portals for externalization of the N-terminal sequences of VP1 and packaging of progeny AAV genomes into the pre-formed capsids.<sup>32, 53</sup>

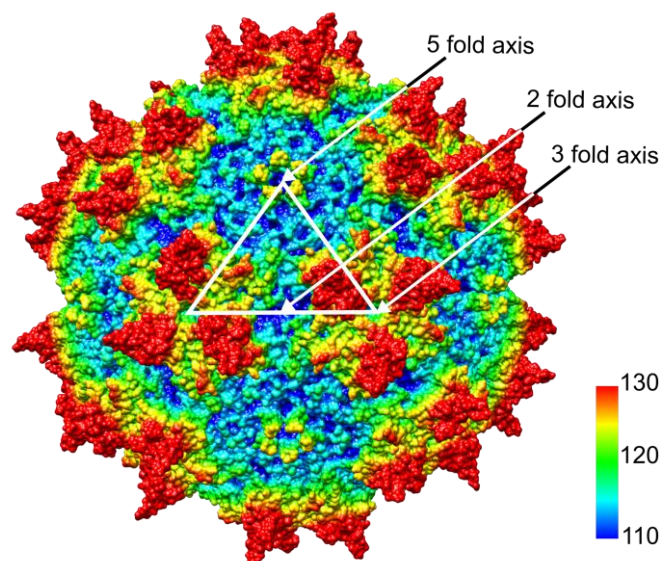


**Figure 2 Capsid of AAV2.** The capsid is shown as space-filling surface representation model with coloring of the amino acids according to the relative distance from the center of the capsid (blue-cyan-green-yellow-red: ~ 110-130 Å). The white triangle indicates the approximate boundary of one viral asymmetric subunit (60 of which compose the capsid). The apex of the triangle touches a pentameric pore at a 5-fold symmetry axis. The outward vertices touch the protrusions (at the right) and plateau regions (at the left) of a 3-fold symmetry axis. The midpoint of the base side touches a 2-fold symmetry axis. This model was generated from the crystal structure of AAV2 (RCSB PDB #1LP3)<sup>46</sup> using Chimera software.<sup>54</sup>

Research into the transcriptome and proteome of AAV is ongoing. Recently, further gene products involved in different stages of AAV's life cycle have been proposed, such as an additional ORF termed *X* under the control of a promoter at map position 81, as well as novel transcripts and splice variants, which are involved in specific stages of viral replication.<sup>19, 55</sup>

### 1.1.3 Life cycle

AAV harnesses different types of glycans as primary receptors for initial attachment to the host cell, followed by interaction with a secondary receptor which facilitates cell entry. AAV2 uses heparan sulfate proteoglycan (HSPG) as attachment receptor.<sup>56</sup> HSPG binding possibly triggers changes in capsid conformation, thus increasing the affinity to a receptor which mediates uptake.<sup>57</sup> As secondary receptors, fibroblast growth factor receptor 1 (FGFR-1),<sup>58</sup> hepatocyte growth factor receptor (HGFR)<sup>59</sup> and laminin receptor,<sup>60</sup> and integrins  $\alpha\beta 5$ <sup>61</sup> and  $\alpha 5\beta 1$ <sup>57</sup> have been proposed, although at least the role of  $\alpha\beta 5$  integrin, FGFR-1 and HGFR in AAV2 cell entry has been challenged.<sup>62, 63</sup> For other AAV serotypes different sets of primary and secondary receptors were described, thus accounting for the differences in tissue tropisms.<sup>8</sup>

Very recently, Pillay et al. identified a previously unknown receptor which is essential for AAV infection in a range of mammalian cell types: transmembrane protein KIAA0319L, which was termed AAV

receptor (AAVR). AAVR is assumed to function as universal receptor for AAV, as infection by serotypes 1-9 is dependent on its presence.<sup>63</sup> It is not clear yet which ubiquitous viral structures partake in the AAV-AAVR interaction or at which stage of infection this interaction takes place. AAVR could act as cell entry receptor, either as monomer, dimer or in a multimeric complex with other receptors, or promote later steps in the virus life cycle.<sup>64</sup>

The major pathway for AAV2 internalization is believed to be clathrin-mediated dynamin-dependent endocytosis.<sup>65, 66</sup> In addition, AAV is capable of exploiting several other entry strategies, such as the clathrin-independent carrier mediated/glycosylphosphatidylinositol-anchored protein- enriched endosomal compartment-associated (CLIC/GEEC) endocytic pathway and macropinocytosis.<sup>67-70</sup> For effective infection AAV processing to an acidified compartment is essential, irrespective of the route of cell entry.<sup>65</sup> In the course of a productive pathway, AAV travels in endosomes toward the nucleus via the cytoskeletal network.<sup>67, 68, 71-73</sup> AAV trafficking to the trans-Golgi network (TGN) and the Golgi apparatus has been proposed,<sup>63, 74, 75</sup> although this also may not be an absolute requirement.<sup>64</sup> Gradual acidification of the endosomal compartment, possibly with assistance of cellular proteases such as cathepsins B and L,<sup>76</sup> induces conformational changes of the AAV capsid. Thus, the N-terminus of VP1 (VP1 unique region, VP1u) is exposed to the capsid outside.<sup>77</sup> VP1u contains a phospholipase A2 (PLA2) domain<sup>78</sup> and nuclear localization signals.<sup>79, 80</sup> The PLA2 domain then mediates virion escape from the endosome into the cytoplasm.<sup>81</sup> Translocation into the nucleus likely occurs through nuclear pore complexes (NPC)<sup>65, 82</sup> in an active transport process supported by cellular karyopherins,<sup>83</sup> although NPC-independent entry mechanisms have been proposed as well.<sup>84</sup> Several studies suggest that AAV2 enters the nucleus as intact particle,<sup>65, 77, 85</sup> while other researchers proposed that uncoating and release of the viral genome already occurs before or during nuclear entry.<sup>86</sup>

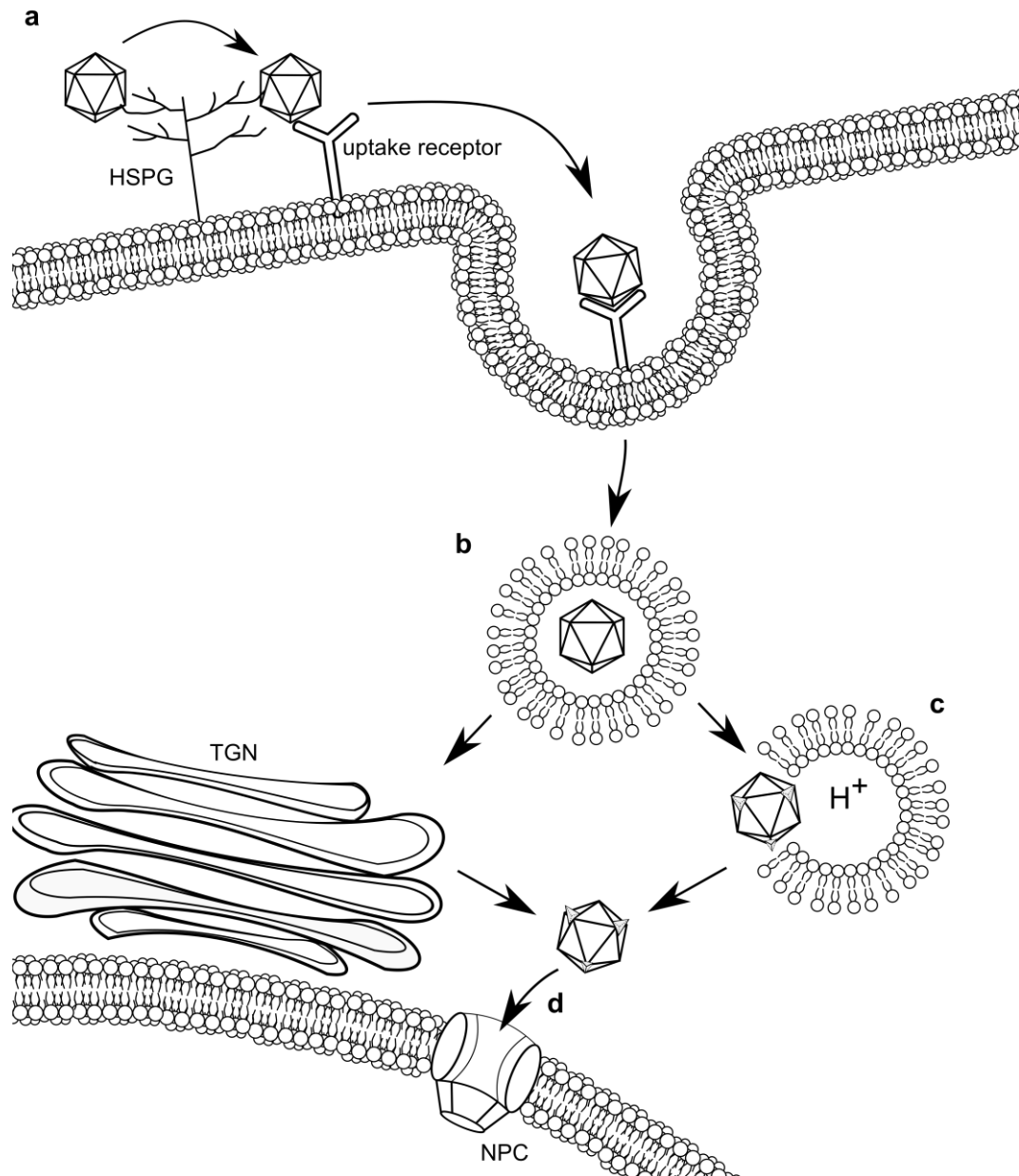


**Figure 3 Schematic model of AAV2 infection.** (a) AAV2 binds to heparan sulfate, a glycan chain of heparan sulfate proteoglycan (HSPG) which serve as AAV2's primary receptor. This binding possibly induces conformational changes to the capsid. Binding to an uptake receptor (see text) initiates endocytosis. The major pathway for AAV2 endocytosis is believed to be clathrin-mediated and dynamin-dependent; but additional other entry mechanisms have been reported. (b) AAV2 traffics toward the nucleus through the endosomal system. Sorting toward the trans-Golgi network (TGN) has been proposed, but may not be an absolute requirement and/or cell-type specific. (c) Acidification of the endosome triggers the externalization of VP1u (VP1 unique region) which contains a phospholipase domain (PLA2) and nuclear localization signals. PLA2 mediates endosomal escape into the cytoplasm. (d) Nuclear localization signals target the virion to the nucleus where entry likely occurs via the nuclear pore complex (NPC). It is not yet clear whether AAV2 uncoats in the nucleus or before or during nuclear entry.

Upon arrival in the nucleus the further fate of AAV depends on whether a helper virus co-infects. In the absence of helper viral functions, only minimal gene expression takes place and Rep gene products negatively regulate further gene expression and viral DNA replication.<sup>37</sup> AAV establishes a latent

infection by persisting episomally<sup>87</sup> or by integration into the host genome. Thereby, AAV2 is unique among eukaryotic viruses as it exhibits a preference for integration in a specific locus, on chromosome 19 (19q13.4)<sup>88</sup> at a site termed AAVS1<sup>89</sup> possessing homology to sequences within the ITR. This process of targeted integration is mediated by Rep78 and Rep68.<sup>31, 90</sup> Super-infection with a helper virus creates a cellular environment which favors AAV replication and propagation. Subsequently AAV enters the productive phase of infection: the suppression of AAV gene expression is relieved, the viral genome is rescued from the integrated state, DNA replication ensues (Figure 5a-f) and progeny viruses are produced.<sup>37, 38, 91</sup>

Even in absence of helper virus infection, however, the factors required for AAV replication can be provided by specific cellular conditions. Such conditions include cellular stress induced by genotoxic treatments, such as UV irradiation<sup>92</sup> or carcinogenic agents.<sup>93, 94</sup> Furthermore, autonomous replication of AAV has been observed in differentiating keratinocytes.<sup>95</sup>

## 1.2 AAV vectorology

AAV's hallmark features of non-pathogenicity and ability to persist in a host cell, in addition to its ability to produce high yields of progeny, prompted interest in exploring AAV as gene delivery platform.<sup>96</sup> By 1982 the complete AAV2 genome had been cloned into a plasmid vector. This enabled production of AAV in Ad-infected cells upon transfection.<sup>97</sup> First experiments with a recombinant AAV (rAAV) in which the *cap/AAP* gene was replaced by a neomycin resistance cassette showed that rAAV could be used to transduce non-AAV DNA into mammalian cells.<sup>98</sup> Subsequently, it was demonstrated that the ITRs are the only viral sequences which are required *in cis* to generate rAAV particles, while *rep* and *cap/AAP* functions can be provided *in trans*.<sup>30</sup> This finding paved the way for the development of "gut-less" AAV vectors containing no coding viral sequences. Instead, a transgene cassette of interest (TEC) of up to 4.9kb could be placed between the ITR sequences and be packaged as genetic payload into the viral vector particle.<sup>99</sup> Today, AAV vectors are considered as one of the most promising delivery systems in human gene therapy, especially for *in vivo* administration into post-mitotic tissues, such as liver, muscle, eye and brain.<sup>100–103</sup> More than 160 clinical trials using AAV vectors have been conducted.<sup>104</sup> In 2012 Glybera® (alipogene tiparvovec) an rAAV1-based therapeutic encoding a hyperactive variant of lipoprotein lipase (LPL<sup>S447X</sup>)<sup>105</sup> for treatment for lipoprotein lipase deficiency was granted marketing authorization by the European Medicines Agency as first gene therapeutic medicine.<sup>106</sup>

## 1.2.1 Production

The production process is a critical aspect of AAV vectorology. To obtain AAV vectors suitable in quality and quantity for gene therapy applications different strategies are employed for production and purification.

### 1.2.1.1 Upstream processing

The upstream process of AAV vector production encompasses the bioprocess, that is, all steps of cell culture work up to harvesting of producer cells. At laboratory scale, transient transfection is the most commonly used method, as it is easily set up and flexible to changes of vector genome and capsid (Figure 4). The vector plasmid containing the TEC flanked by the ITRs serves as template for vector genome replication. AAV genes *rep* and *cap/AAP* are provided *in trans* by co-transfection of an AAV helper plasmid. Earlier in development of AAV vector production, host cells were infected with Ad helper virus to initiate vector replication.<sup>107</sup> This created the need to remove infectious Ad contaminants in AAV vector stocks, in addition to Ad infection diminishing host cell viability. To obviate helper virus infection, plasmids have been constructed, which encode the Ad genes E2A, E4 and VA RNA,<sup>108</sup> or which contain both Ad and AAV helper genes on a single AAV/Ad helper plasmid.<sup>109</sup> For DNA transfer, the most commonly used methods are DNA co-precipitation with calcium phosphate, polycations such as polyethylenimine or cationic lipids.<sup>110</sup> As producer cells, HEK293 are usually used. They have been transformed with Ad5 DNA and stably express E1A and E1B,<sup>111</sup> and thus complete the essential set of Ad functions. Inherently, transfection methods based on adherent HEK293 cells are challenging to scale-up. To generate a more readily scalable production platform Grieger et al. recently adapted HEK293 to grow in suspension.<sup>112</sup>

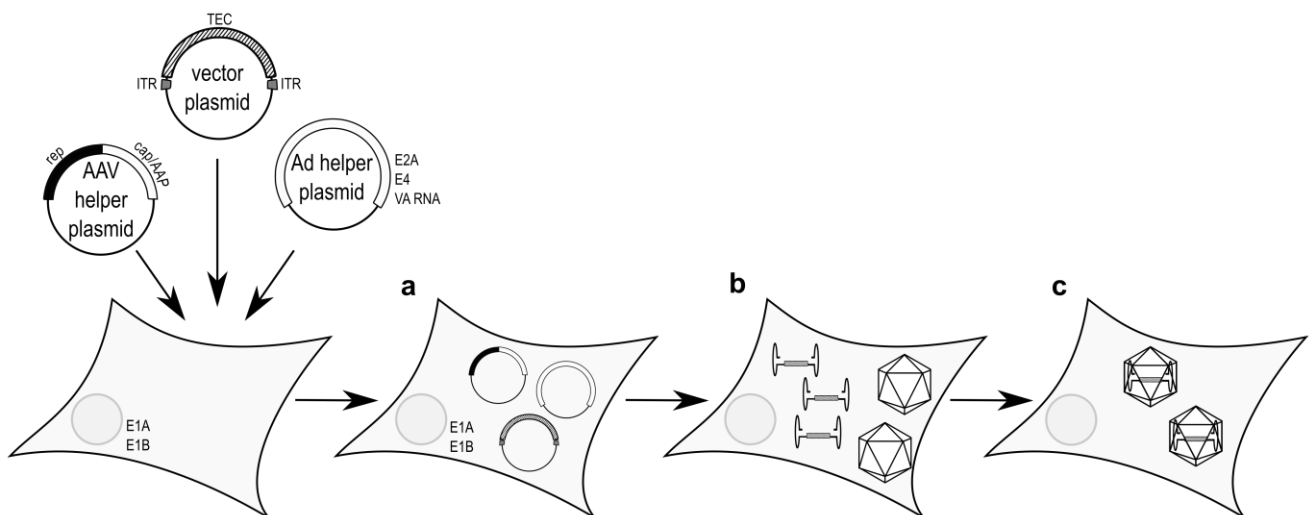


**Figure 4 AAV vector production by transient transfection.** (a) HEK293 cells are transfected with the vector plasmid containing the TEC flanked by ITRs and plasmids providing AAV and Ad helper functions. (b) Upon replication, the AAV vector genome is rescued from the plasmid, and the capsids are assembled. (c) The vector genomes are packaged into the capsids. Cells are harvested and lysed 48 hrs after transfection. Figure shows schematic depiction of a cell with no distinction between cytoplasm and nucleus.

Other production strategies include generation of stable cell lines. So-called packaging cell lines contain *rep* and *cap/AAP* as integrated copies, while so-called producer cell lines further contain the vector genome to be packaged. AAV vector production is initiated by infection with a helper virus, usually Ad, and, in case of packaging cell lines, by co-infection with an additional virus providing the vector genome.<sup>113</sup> Further, HSV's ability to provide helper functions is harnessed for manufacturing of AAV vectors. Commonly, mammalian cells are simultaneously infected with two replication-deficient recombinant HSV, one carrying AAV genes and one transporting the vector genome.<sup>114</sup> As yet another concept, a baculovirus (BV)-based platform in insect cells was implemented. For AAV vector production, one or two BVs encoding the AAV genes under the control of BV-specific promoters and a BV containing the TEC are co-infected, commonly in Sf9 (from *Sodoptera frugiperda*).<sup>113</sup> Alternatively, stable Sf9 cell lines have been developed. They contain integrated copies of AAV genes which are activated upon infection with the BV containing the TEC.<sup>115</sup> A BV-expression vector system has been used for the production of Glybera. All methods relying on helper virus infections, albeit scalable, maintain the risk of contaminating helper virus in the AAV vector preparations.

### 1.2.1.2 Downstream processing

The downstream process encompasses the recovery of AAV vectors from the producer cells and subsequent purification protocols. The specific goal is the removal of process- and product-related impurities. Process-related impurities stem from the materials and components used for manufacture, including host cell nucleic acids and proteins, residue plasmid DNA, components of the cell culture medium and buffers. Product-related impurities are structurally similar to the vector product, but do not meet the specifications for safety and efficacy. Such impurities are empty AAV capsids, AAV capsids containing DNA other than the TEC or replication-competent AAV.<sup>116</sup>

In the first step, upon harvest of producer cells, host cell membranes are disrupted to release the produced AAV vectors into a cell lysate. At laboratory scale, cells are commonly subjected to repetitive freeze thaw cycles or ultrasonication. Next, the vector-containing lysate is incubated with a nuclease to remove contaminating nucleic acids from the production process, followed by removal of cellular debris by centrifugation. In some protocols a precipitation step using polyethylene glycol before or after nuclease treatment is included.<sup>117, 118</sup> Large scale approaches employ chemical agents such as surfactants or mechanical protocols such as microfluidizers or homogenizers and clarify the lysate by microfiltration.<sup>113</sup> Subsequent purification methods harness specific characteristics of AAV particles for their isolation. As the AAV capsid provides high particle stability in temperatures up to 65°C<sup>119</sup> and pH between 2.5 and 8,<sup>120</sup> vector preparations can sustain sophisticated purification protocols.

At laboratory scale, vector-containing cell lysates are commonly purified by density gradient ultracentrifugation: The cleared lysate in a centrifuge tube is mixed with cesium chloride (CsCl) or sub-layered with solutions containing increasing concentrations of iodixanol. While CsCl is a cytotoxic agent and must be removed carefully, iodixanol is a non-toxic contrast agent,<sup>121</sup> which is tolerated by some cell types. After applying high centrifugal force, TEC-containing AAV particles accumulate in specific phases of density and can be harvested. Density gradient ultracentrifugation is applicable to any AAV serotype. Importantly, this method removes a large portion of empty capsids from the vector lysate, as these accumulate in phases of lower density.<sup>118, 121</sup> For further purification, or as alternative approaches, column-based protocols have been implemented, many of which are commercially available. Affinity chromatography utilizes the chemical properties of the capsid surface, such as the heparin binding of AAV2, to enrich vector particles.<sup>121</sup> Further, an immunoaffinity column (AVB column) carrying an anti-AAV single domain antibody specific for a surface-exposed epitope region on the capsid which is common to several serotypes<sup>122</sup> has been developed. Ion-exchange chromatography is based on the isoelectric point (IEP), i.e. the pH at which a particular molecule has a neutral net charge. When the pH is lower than the IEP of a target molecule, it is protonated and binds to a cation exchanger (a negatively charged ion exchange resin, such as sulfonic acid groups). With the buffer pH value approaching the IEP, the target molecule's net charge becomes charge-neutral which allows it to dissociate from the resin and elute from the column. Vice versa, the target molecule carries a negative charge when the pH is higher as its IEP and thus binds to a positively charged anion exchange resin, such as quaternary ammonium groups. By lowering the pH to the specific value of IEP, elution takes place. As empty AAV capsids have an IEP of 6.3, as opposed to the IEP of 5.9 of capsids containing DNA,<sup>123</sup> ion-exchange chromatography is broadly used to specifically enrich the latter. Different protocols using cation exchanger resin, anion exchanger resin, two-step and dual exchange membrane chromatography have been described.<sup>120, 124–128</sup> Another advantage of this method is the broad applicability to different serotypes. Other column-based methods rely on capsid modifications, such as genetic insertion of histidine-tags (his-tags). Capsids with inserted his-tag are purified using immobilized metal affinity chromatography (IMAC) with nickel columns.<sup>129, 130</sup>

As final polishing methods, size-exclusion chromatography (e.g. gel filtration), ultrafiltration or tangential flow filtration are commonly used for buffer exchange or to concentrate the vector suspension. The final AAV vector product can be stored frozen or even lyophilized without losing infectivity.<sup>131</sup>

### 1.2.1.3 Challenges

As mentioned above, vector preparations may contain process- and product-related impurities. In an assessment of type and significance of process-related impurities, J. Fraser Wright concludes that these are similar to those arising in the production of established biologics, and can therefore be re-

solved by appropriate established procedures. Product-related impurities, in contrast, are unique to AAV vector production, pose specific risks to safety and efficacy and so closely resemble the vector product as such, that it becomes challenging to remove them.<sup>116</sup>

Regardless of production method, empty capsids are present in abundance in AAV vector preparations, constituting <50 to > 98 % of total AAV particles.<sup>128, 132, 133</sup> The variation in relative empty capsid content depends on size and sequence of vector genome, cell culture system or transfection efficiency; additionally, since lot-to-lot variability has been observed, other, yet unidentified factors are involved.<sup>126, 132</sup> For most applications, the presence of large numbers of empty capsids is highly undesirable, as they form a source of antigenic material which may induce or contribute to a capsid-triggered anti-AAV immune response.<sup>134, 135</sup> Moreover, they may competitively inhibit transduction and induce capsid particle aggregation.<sup>126</sup> As empty capsids differ from DNA-containing capsids in density and IEP, they can be largely removed by density centrifugation and ion exchange chromatography.

Additionally, capsids containing non-vector DNA are present in vector preparations. Replication-competent AAVs (rcAAV) are capsids containing the wild type (wt) AAV *rep* and *cap/AAP* genes flanked by ITRs. They are generated by recombination events between the ITRs of the vector genome cassette with *rep* and *cap/AAP* sequences provided on helper constructs. Indeed, wtAAV is largely regarded as non-pathogenic (see 1.1.1). Yet, unintended transfer of viral DNA may result in production of AAV proteins, which possess helicase or DNA nickase activity,<sup>33, 34</sup> or induce cytotoxic T lymphocyte reactions.<sup>136</sup> Several strategies to prevent the generation of rcAAV have been reported, including the elimination of sequence homologues within vector and helper plasmids,<sup>137</sup> replacing the p5 promoter which is implicated in recombination events,<sup>109</sup> placing *rep* and *cap/AAP* genes in opposing transcriptional orientations<sup>138</sup> or generating an oversized rep-cap helper plasmid.<sup>139</sup> Further, fragments of host cellular DNA and helper sequences may get packaged into capsids. In Glybera, for example, encapsidated baculovirus DNA stemming from the production system was specified as impurity and as of major concern in the EMEA assessment report.<sup>140</sup>

In vectors derived from plasmid transfection, encapsidated prokaryotic backbone sequences, e.g. antibiotic resistance genes have been reported as substantial impurity, ranging from 1-8 % of packaged genomic particles.<sup>116, 141-143</sup> Although prokaryotic promoter sequences are not functional in mammals, transfer of plasmid backbone sequences should nevertheless be avoided, since they contain motifs that are recognized by the cell-autonomous immune system and are thus prone to induce inflammatory responses or gene silencing.<sup>144, 145</sup> In addition, antibiotic resistance genes have been found to get integrated into the target genome,<sup>141, 146</sup> thus bearing the risk to come under the control of eukaryotic promoters. In an approach to reduce the packaging of prokaryotic sequences Hauck and colleagues inserted a stuffer into the vector plasmid backbone to render it too large to be pack-

aged. This reduced the packaging of plasmid backbone sequences 7.6-fold, but did not completely avoid it.<sup>143</sup>

### 1.3 AAV vector transduction and optimization

The success of AAV vector transduction depends on the target cell type; in some, AAV vector transduction is rather inefficient and requires high particle numbers, while others are altogether refractory. Researchers aim to identify and overcome bottlenecks by modifying both the capsid and the vector genome.

#### 1.3.1 Vector tropism and immunogenicity

AAV2 is the most extensively studied serotype and is widely used for gene transfer applications, but increasingly vectors based on other AAV serotypes are harnessed for their differential tissue tropism and partially lower immunogenicity.<sup>8</sup> Conveniently, it is possible to package a vector genome with ITRs stemming from one serotype into a capsid of another serotype, a process referred to as pseudotyping.<sup>147</sup> For treatment of hemophilia B in a human clinical phase I/II trial<sup>148</sup> for example, a codon-optimized human factor IX (FIX) transgene flanked by AAV2 ITRs was packaged in capsids of AAV8, since the capsid of the latter has a strong tropism for the liver and a lower seroprevalence in humans than the capsid of AAV2.<sup>11</sup> This pseudotyped vector achieved long-term expression of the FIX transgene at therapeutic levels.<sup>148</sup> Moreover, capsid-engineering approaches using rational design or directed evolution aim to increase the efficiency and specificity of AAV vector transduction. Non-genetic approaches target the capsid to a specific receptor by equipping it with a suitable ligand by chemical binding or via bi-specific linkers.<sup>149</sup> In genetic targeting, the ligands are directly incorporated into the capsid structure. Hereby, the ligand DNA sequence is cloned within the *cap* ORF at specific sites where the ligand does not interfere with capsid assembly and vector genome packaging. Insertion of short peptides (up to 34 amino acids) into amino acid position 587 of the VP3 both interrupts the binding motif for HSPG,<sup>49, 51</sup> thereby abolishing the natural tropism of AAV2, and establishes novel ligand-receptor interactions.<sup>150</sup> Larger peptides can be inserted into the N-terminus of VP2.<sup>42, 86</sup> Using this position, Münch and colleagues incorporated designed ankyrin repeat proteins (DARPs) specific for Her2/neu or CD4, thus targeting human Her2/neu-positive tumors or CD4-positive lymphocytes *in vivo*, without off-targeting activity.<sup>151</sup>

Directed evolution strategies were developed to generate targeting vectors, even if a receptor to be targeted or the cell-specific factors hampering transduction are not known. In these approaches, target cells are infected with libraries of capsid mutants carrying random peptide insertions. The mutants achieving successful infection are used for subsequent selection rounds to finally obtain the optimal transducing capsid variant.<sup>149, 152, 153</sup> Employing the directed evolution strategy, Sallach et al.

obtained an AAV2-based capsid variant which efficiently and selectively transduced human keratinocytes, a cell type which is refractory to transduction with AAV2 vectors.<sup>154</sup>

### 1.3.2 Intracellular trafficking

Upon cellular uptake, AAV vectors assumedly follow the same pathway(s) as wtAAV. The acidification required to enable endosomal escape was reported to be cell-type dependent.<sup>68</sup> In the cytoplasm, the AAV capsids may be subjected to phosphorylation which marks them for ubiquitination and proteasome-mediated degradation. Both proteasome inhibiting drugs<sup>68, 155–157</sup> and site-directed mutagenesis of tyrosine residues on the capsid surface, representing the target sites for phosphorylation, significantly increase AAV vector transduction.<sup>158</sup>

SUMOylation is another post-translational modification which participates in regulation of a variety of cellular processes by covalently attaching small ubiquitin-like modifier (SUMO) proteins to target proteins.<sup>159</sup> Recently, Hölscher et al. reported that this mechanism negatively affects AAV vector transduction.<sup>160</sup> Thus, targeting SUMOylation might be an additional strategy to enhance AAV vector transduction.

### 1.3.3 Vector genome fate in the nucleus

#### 1.3.3.1 Interaction with DNA damage response proteins

In the nucleus the DNA damage response (DDR) senses damage to the genome and activates several downstream pathways to induce cell cycle arrest, DNA repair or, ultimately, apoptotic signaling. Players of the cellular DDR also recognize and process incoming AAV vector genomes. The interactions seem to be provoked by AAV's ITRs<sup>161–163</sup> and involve protagonists of the two major pathways for repair of DNA double strand breaks (DSB), homologous recombination (HR) and non-homologous end joining (NHEJ). HR, which requires a sister chromatid to perform repair of DSB, takes place in dividing cells and in S phase, whereas NHEJ functions in both dividing and non-dividing cells independent of cell cycle.<sup>164</sup> Shortly after nuclear entry of AAV vectors, the MRN (Mre11, Rad50 and Nbs1) complex, which acts as sensor of DSB and stalled replication forks,<sup>165</sup> is recruited to the vector genome.<sup>166</sup> Possibly by physical interaction of the DNA binding domain of Mre11,<sup>163</sup> gene expression from AAV vector genomes is suppressed.

A primary responder kinase of the HR pathway, Ataxia telangiectasia mutated (ATM), is recruited by the MRN to sites of DSB.<sup>164</sup> ATM was found to inhibit gene expression from AAV vector genomes in both the native single-stranded and the self-complementary (see chapter 1.3.3.2) conformation. A similar effect is exerted by kinase ATM and RAD3-related (ATR), another enzyme of HR, on single-

stranded, but not self-complementary vector genomes.<sup>167</sup> DNA-PK a serine/threonine kinase consisting of a catalytic subunit (DNA-PKcs) and a heterodimer (Ku70/80) is a crucial player of NHEJ. Somewhat contradictory, DNA-PKcs was reported to enhance transduction of AAV vectors *in vitro*,<sup>167</sup> while another report states that AAV vector transduction is increased in Ku80-defective cells.<sup>168</sup>

In presence of a helper virus, the inhibition imposed by DSB repair proteins is at least partially released. Since Ad is also inhibited by the MRN complex, it has evolved several mechanisms for its inactivation, including degradation of its members.<sup>169</sup> This Ad-mediated abrogation of inhibition increases AAV transduction and replication.<sup>161</sup> HSV, on the other hand, utilizes the MRN complex for its own replication.<sup>170, 171</sup> Currently it is not known how this benefits AAV. It was proposed that the MRN complex has an actual positive effect on AAV replication in presence of HSV-1.<sup>172</sup> Additionally, it is conceivable, that HSV sequesters the MRN complex, thus diverting it from the AAV genome.<sup>163</sup> Interestingly, as is the case with wtAAV replication, (see chapter 1.1.3) in absence of helper virus functions, AAV vectors benefit from specific types of DNA damage. Genotoxic agents, such as UV, DNA synthesis inhibitors aphidicolin and hydroxyurea and topoisomerase inhibitors were found to increase AAV vector transduction.<sup>173–175</sup> In line, Mano and colleagues demonstrated that a high number of siRNAs which induced cellular permissiveness to AAV also directly induced cellular DNA damage and activation of a cell cycle checkpoint.<sup>176</sup> These observations could be explained by diversion of inhibitory DDR proteins away from the AAV vector genome.<sup>166, 176</sup> An *in vivo* study found that exit from the cell cycle, which is connected with downregulation of DDR proteins, particularly the MRN complex, increased permissiveness toward AAV vector transduction.<sup>177</sup> Furthermore, AAV vector transduction was increased *in vitro* upon administration of drugs which induce transient cell-cycle arrest.<sup>178</sup> An earlier study, however, reported that cells in S-phase are 200-fold better transduced than non-dividing cells,<sup>179</sup> which may likely be connected to the higher activity of beneficial DDR proteins at this stage of the cell cycle. All in all, the actual role of the cell cycle for AAV vector transduction is not clear yet.

### 1.3.3.2 Double strand synthesis

From the single-stranded vector genome, the double-stranded template required for transgene expression is generated by second-strand synthesis, or – if higher amounts of vector genomes are available in the nucleus – by annealing of two vector genomes of opposite polarity.<sup>180</sup> In *de novo* second strand synthesis, the 3'ITR provides the 3'OH-primer for the host cell DNA replication machinery (Figure 5 a-c). As second-strand synthesis is hampered in some cell types, thus restricting transduction,<sup>181, 182</sup> self-annealing vector genomes were developed. To generate these so-called self-complementary (sc) genomes, the trs of one ITR sequence is deleted.<sup>183, 184</sup> Thus, Rep cannot process the ITR and the whole vector genome is replicated as inverted dimer (Figure 5 g-l). Upon un-

coating this molecule can fold onto itself to generate a double-stranded vector genome. Although scAAV vectors possess only half the cloning capacity of the ssAAV genome (ca 2.3kb) they are widely used, due to their higher transduction efficiencies.<sup>185, 186</sup>

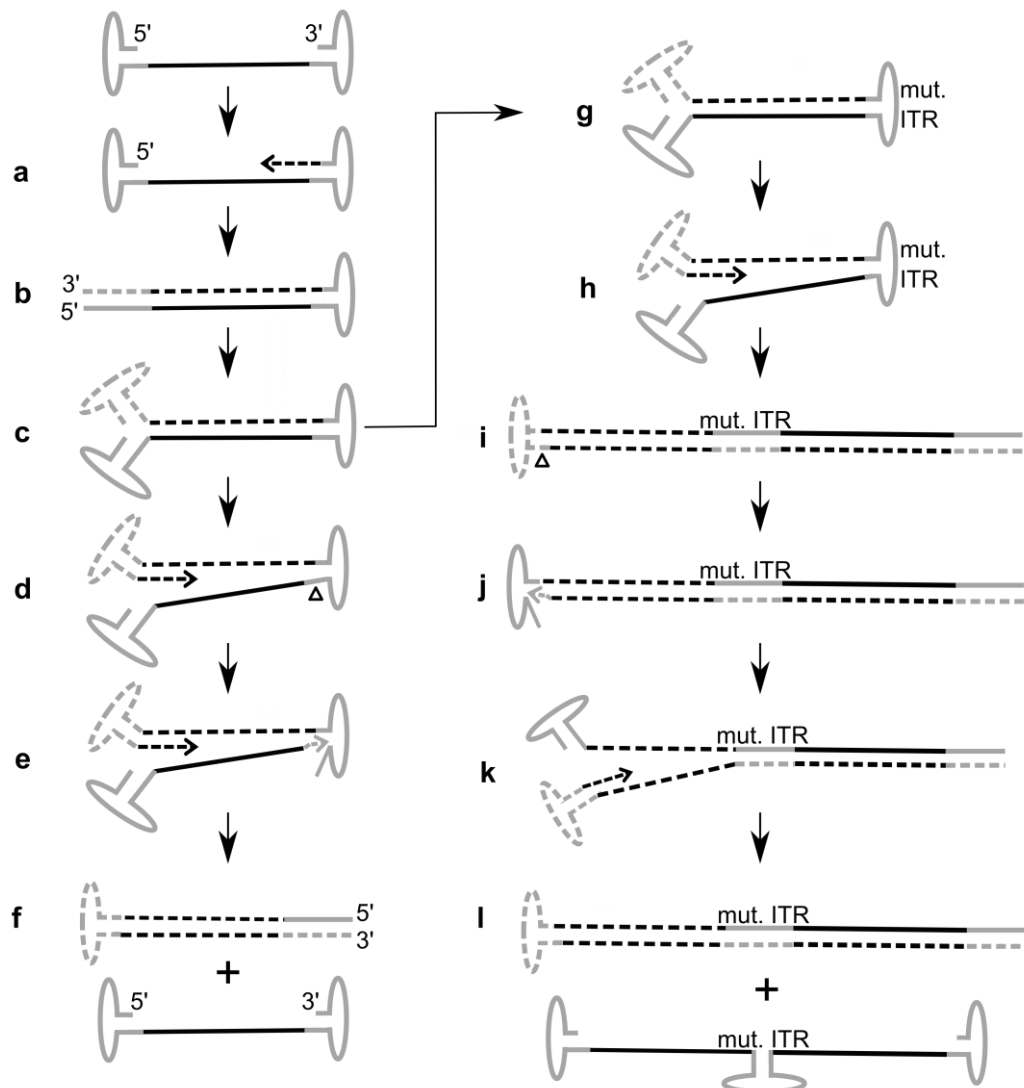


**Figure 5 AAV genome replication and generation of self-complementary AAV vector genomes.** (a) The 3' ITR of the single-stranded AAV genome acts as primer for the host cell DNA replication machinery, including DNA polymerase delta, replication factor C, proliferating cell nuclear antigen, and the minichromosome maintenance complex.<sup>187, 188</sup> (b) The genome is replicated through the 5' ITR, thus displacing the original 5' ITR. This generates a double-stranded intermediate. (c) Both ITRs fold into hairpins (HP) and (d) the newly synthesized ITR functions as new 3' OH primer for DNA synthesis of the AAV genome. At the same time, Rep nicks the terminal resolution site (trs) of the lower strand. (e) At this new 3' OH end, a second DNA replication complex copies the original 3' ITR. (f) One round of replication generates two products: the single-stranded vector genome, ready to be encapsidated, and the double-stranded intermediate as in (b) which serves as template for further replication rounds. (g) To generate a self-complementary vector genome the D sequence, including the trs of one ITR, is deleted. Therefore, Rep cannot nick the lower strand. (h) In this case, replication continues through the mutated ITR (i) and creates a dimeric double-stranded DNA. At the intact ITR, Rep nicks at the trs, creating a new 3' OH end. (j) As in (e), this new 3' OH end serves as primer for the copying of the intact left ITR. (k) The newly synthesized ITR folds into HP conformation and replication continues back into the vector genome. (l) One round of replication generates one self-complementary vector genome and a dimeric double stranded template for further replication

### 1.3.3.3 Long-term persistence

As AAV vectors usually do not contain Rep, no site-specific integration occurs. Yet, as with other transgenic DNA, vector integration in mammalian genomes takes place, albeit at very low levels. In a partial hepatectomy study in mice, between 0.06 and 0.2 integrated vector genomes/cell were estimated.<sup>189</sup> In contrast a study conducted in mouse muscle found no integrated AAV vector genomes at all.<sup>190</sup> Integration has been proposed to occur at pre-existing chromosomal breakage sites, during or caused by repair of DSB by DDR.<sup>191, 192</sup> In line with this hypothesis, DNA-damaging agents increase the rates of vector integration.<sup>175, 193</sup> Regarding the role of individual DDR protagonists, reports are conflicting as to whether DNA-PKcs of the NHEJ pathway would increase<sup>167, 192, 194</sup> or inhibit<sup>195</sup> integration. Likewise it is disputed whether ATM fosters or hampers integration of the AAV vector genome.<sup>167, 193</sup> Several integration studies reported preferred integrational sites such as ribosomal DNA repeats, transcriptionally active genes, DNA palindromes, CpG islands and nearby transcription start sites.<sup>196–198</sup> Kaepfel and colleagues analyzed muscle biopsies of five patients who received intramuscular injections of Glybera (AAV1-LPL<sup>S447X</sup>), the first gene therapy medicine (see chapter 1.2.). They estimated the integration frequency to range from ca.  $1 \times 10^{-4}$  to  $1 \times 10^{-5}$ , and found no preference for specific integration sites.<sup>199</sup>

Chiefly, AAV vector genomes remain in an episomal state. As primary persistent form, duplex vector DNA molecules<sup>200</sup> rapidly circularize via the ITRs. Increasingly with time, circular multimers, so-called concatemers are formed.<sup>180, 201–203</sup> Vector genome circularization seems to be largely mediated by proteins of the NHEJ pathway, specifically DNA-PKcs, in *in vivo* tissues including mouse skeletal muscle, heart and kidney,<sup>201, 204–206</sup> although undefined DNA-PKcs-independent pathways have been proposed in the liver.<sup>204</sup> Interestingly, in dividing cells *in vitro*, players of HR such as members of the MRN complex and ATM are supporting the establishment of circular long-term forms of the vector genome.<sup>201</sup> Regarding the detrimental effects on gene expression exerted by proteins of the HR pathway, interaction with the NHEJ seems to be more beneficial for AAV vector transduction and persistence.<sup>167</sup> This may be one explanation for the success of gene therapy in non-dividing cells (see below). Further exploration of the mechanisms of host nucleus protein interaction with AAV vector genomes may reveal possibilities to circumvent or manipulate the interactions with proteins of DDR to improve AAV vector transduction and maintenance in both non-dividing and dividing cells.

The episomal circles and concatemers formed in non-dividing tissues have been demonstrated to persist and to mediate long-term transgene expression, e.g. in respiratory epithelium,<sup>207, 208</sup> skeletal muscle,<sup>190, 202, 203, 205, 209</sup> brain<sup>210</sup> and liver.<sup>189</sup>

## 2 Aim of the study

### 2.1 Aim of study I: Improving safety of AAV vectors

As described in chapter 1.2.1.3, AAV vectors derived from plasmid transfection were found to contain encapsidated prokaryotic sequences, such as antibiotic resistance genes. While these sequences constitute a minor population (1-8 %) <sup>116, 141-143</sup> in viral vector preparations, non-viral plasmid vectors always transfer prokaryotic backbone sequences upon administration. <sup>211</sup> To circumvent the potential risks mentioned above and to thus improve safety of non-viral vectors, as well as efficiency and duration of cell modification, the minicircle (MC) technology was developed. <sup>212-215</sup> MCs are circular DNA expression cassettes which do not contain functional or coding prokaryotic sequences. They originate from parental plasmids harboring at least the selection marker, an origin of replication and two recombination sites flanking the TEC. Following amplification in *Escherichia coli*, the parental plasmid is split enzymatically by a *cis*-recombination reaction resulting in two circular supercoiled and monomeric molecules: a miniplasmid with all the unwanted bacterial sequences and the MC containing the TEC and a small additional sequence, termed sequence for chromatography, affinity and recombination (SCAR), which represents one recombination sequence and a tag for affinity purification. <sup>211, 216, 217</sup> Given the lack of functional prokaryotic sequences in MCs, we reasoned that the MC technology might be an easy and straightforward strategy for the production of AAV vector preparations devoid of antibiotic resistance genes.

In this study we wanted to investigate whether MC constructs could replace plasmids of a dual plasmid system for AAV2 vector production. MC constructs for substitution of plasmids for production of ssAAV2 were generated and produced by PlasmidFactory. By using all four possible combinations of MCs and plasmids it should be determined if and which plasmids could be replaced by MC without decreasing AAV vector quantity and functionality. Most importantly it was to be determined whether the MC approach decreased encapsidation of prokaryotic sequences. If functional and pure ssAAV vectors could be generated, the system was to be expanded to production and characterization of scAAV2 (see 1.3.3.2) vectors. Further, as AAV vectors were reported to activate Toll-like-receptor 9 (TLR9), <sup>218, 219</sup> a sensor for unmethylated CpG sequences in foreign DNA molecules, <sup>220</sup> both ssAAV and scAAV derived from dual plasmid and dual MC transfection were to be tested on a model cell line expressing TLR9 to measure TLR9 activation.

## 2.2 Aim of study II: Establishment of episomal maintenance

As elaborated in chapter 1.3.3.3, AAV vectors are highly suitable for gene transfer into post-mitotic tissues. In dividing or proliferating cells, however, episomal AAV vector genomes are lost over time and cell divisions.<sup>189, 221, 222</sup> We hypothesized that episomal replication and thus mitotic stability of AAV vector genomes could be achieved by equipping AAV vectors with a scaffold/matrix attachment region (S/MAR). S/MARs are organizational DNA units within eukaryotic genomes. They interact with the nuclear matrix, thus structuring chromosome domains and participating in the regulation of gene expression.<sup>223, 224</sup> In the pioneer S/MAR plasmid vector pEPI, a 2kb S/MAR derived from the 5' region of human  $\beta$ -interferon gene mediates interaction of the nuclear matrix via matrix protein SAF-A, thus mediating episomal gene expression over hundreds of generations.<sup>225, 226</sup> Accordingly it was of interest to apply and investigate this system in an AAV context.

The aim of this study was to develop an AAV vector which would be capable to persist episomally in dividing cells. In cooperation with C. Hagedorn and H.J. Lipps of University Witten/Herdecke an AAV vector plasmid containing the S/MAR sequence and a plasmid containing a control vector genome without the S/MAR were to be produced and packaged into AAV2 capsids. Both vectors were to be transduced in parallel into highly proliferative HeLa cells and examined for maintenance of the AAV vector genome. In colony forming assays, transduced cells were to be selected for cells stably maintaining the vector genome. Upon termination of selection the number of surviving colonies was to be quantified. Additionally, surviving colonies were to be cultivated further in absence of selection to determine the stability of vector genome retention. If the vector genome was mitotically stable it should be determined whether this resulted from episomal maintenance or vector integration.

### 3 Materials

#### 3.1 Chemicals, reagents and enzymes

All common laboratory chemicals and reagents were purchased from Sigma-Aldrich (Taufkirchen, Germany), Carl Roth GmbH & Co. KG (Karlsruhe, Germany), AppliChem (Darmstadt, Germany) or Merck (Darmstadt, Germany).

Optiprep density gradient medium (Iodixanol) was purchased from Sigma-Aldrich (Taufkirchen, Germany). Benzonase endonuclease was purchased from Merck (Darmstadt, Germany). DNA restriction enzymes and MassRuler DNA Ladder Mix were purchased from Thermo Fisher Scientific Fermentas (Braunschweig, Germany).

#### 3.2 Commercial kits

Product	Manufacturer
DNeasy Blood & Tissue Kit	Qiagen, Hilden, Germany
EndoFree Plasmid Kits (Mini, Maxi, Giga)	Qiagen, Hilden, Germany
AAV2 Titration ELISA	Progen, Heidelberg, Germany
LightCycler 480 SYBERGreen Master	Roche, Mannheim, Germany
LightCycler Fast Start DNA Master SYBER Green I	Roche, Mannheim, Germany
RNase-free DNase set	Qiagen, Hilden, Germany
RNeasy Tissue Kit	Qiagen, Hilden, Germany
SuperScript TM III First-Strand Synthesis SuperMix for qRT-PCR	Invitrogen, Karlsruhe, Germany

#### 3.3 Cell culture media and supplements

Product	Manufacturer
Blasticidin – for HEK blue hTLR9 cell culture	Invivogen, San Diego, USA
Blasticidin – for HeLa cell selection	Thermo Fisher, Scientific, Braunschweig, Germany
DMEM+GlutaMAX-I	Invitrogen, Karlsruhe, Germany
FCS	Invitrogen, Karlsruhe, Germany
Normocin	Invivogen, San Diego, USA

Product	Manufacturer
PBS	Invitrogen, Karlsruhe, Germany
Penicillin/Streptomycin	Invitrogen, Karlsruhe, Germany
Trypsin/EDTA	Invitrogen, Karlsruhe, Germany
Zeocin	Invivogen, San Diego, USA

### 3.4 Plasmids and MC

#### Helper plasmids

**pXX6-80:** Helper plasmid encoding Ad proteins VA, E2A and E4. Kindly provided by R.J. Samulski<sup>108</sup>

**pRC:** Helper plasmid containing AAV2 *rep* and *cap/AAP* under the control of wt promoters, but lacking AAV ITRs<sup>150</sup>

**pDP2rs:** Combined AAV and Ad helper plasmid containing Ad E2A, E4 and VA and AAV2 ORFs *rep* and *cap/AAP*. Native p5 promoter of *rep* OFR is exchanged by mouse mammary tumor virus long terminal repeat (MMTV-LTR) promoter. Additionally encodes for red fluorescent protein (RFP) gene.<sup>227</sup>

#### Vector plasmids: encoding TEC(s), flanked by ITRs

**pAAV-S/MAR:** human CMV enhancer/human elongation factor 1 alpha promoter (hCMV/EF1P), encodes eGFP and blasticidin S deaminase gene (*BSD*) from *Aspergillus terreus* separated by an IRES. Contains the 2kb S/MAR element derived from the 5' region of human  $\beta$ -interferon gene

**pAAV- $\Delta$ S/MAR:** as pAAV-S/MAR, but lacking the S/MAR element.

**pAAV-ssGFP:** TEC 1: human cytomegalovirus (CMV) promoter and eGFP cDNA; TEC 2: thymidine kinase promoter and hygromycin resistance gene (pGFP in <sup>228</sup>)

**pAAV-scGFP:** TEC 1 of pAAV-ssGFP, contains a deletion in the D sequence (including the trs) of one ITR, resulting in packaging of a single stranded vector genome with two complementary strands which anneal to form a ds vector genome (pscAAV/EGFP in <sup>229</sup>)

#### MCs

MC are based on the indicated plasmids. Except for a short sequence for chromatography, affinity and recombination (SCAR) no prokaryotic sequences are contained.

**MC.AAV-ssGFP:** MC based on pAAV-ssGFP

**MC.AAV-scGFP:** MC based on pAAV-scGFP

**MC.DP2rs :** MC based on pDP2rs

pDP2rs, pAAV-ssGFP, pAAV-scGFP and all MC used in this work were produced by PlasmidFactory, Bielefeld, Germany.

### 3.5 Primers for qPCR

All primers were purchased from Invitrogen.

Target sequence	forward (5'-3')	reverse (5'-3')
AAV rep	ATTAAGGTCCCCAGCG	GGAAGTAGCTCTCTCCC
Ad E4	GTTACGAGTCCTGGGC	GTGGCGACCCCTCATA
ampR	ATCCCGTATTGACGCC	CGCTCGTCGTTTGGTA
eGFP	CACAACGTCTATATCATGGC	TGTGATCGCGCTTCTC
F1 ori	GCGTGATGGACAGACT	GTCGAGGTGCCGTAAAG
kanR	GCCCTGAATGAACTGC	CCATCCGAGTACGTGC
SCAR	AACCCATAATTGTGAGCG	CATTAAGGTTCGGGAAAATGC
ori	TACCGGGTTGGACTCA	CCCGACAGGACTATAAAG
Human PLAT	ACCTAGACTGGATTCGTG	AGAGGCTAGTGTGCAT
Human GAPDH	GGTATCGTGGAAGGACT	GGGTGTCGCTGTTGAA
Human IL-8	AAGAACTTAGATGTCAGTGC	ACTTCTCCACAACCCT

### 3.6 Eukaryotic cell lines

**HEK293:** human embryonic kidney cell line; transformed with Ad5, contains E1a, E1b; ATCC CRL-1573.<sup>111</sup>

**HeLa:** Human epithelial cervix adenocarcinoma cells; ATCC CCL-2.<sup>230</sup>

**HEK blue hTLR9:** HEK 293 cells, which stably express hTLR9 and secreted embryonic alkaline phosphatase (SEAP) under the control of the interferon (IFN)- $\beta$  minimal promoter fused to five nuclear factor kappa B (NF- $\kappa$ B) and activator protein (AP)-1 binding sites, were purchased from Invivogen (San Diego, USA).

### 3.7 Bacteria strain

*Escherichia coli* (*E.coli*) DH5 $\alpha$ :

F<sup>-</sup>, *lac1*<sup>-</sup>, *recA1*, *endA1*, *hsdR17*,  $\Delta$ (*lacZYA-argF*), U169, F80d/*lacZ* $\Delta$ M15, *supE44*, *thi-1*, *gyrA96*, *relA1*.<sup>231</sup>

### 3.8 Laboratory equipment

#### AAV vector production and purification

Product	Manufacturer
Crimper tube sealing system	Thermo Fisher Scientific Sorvall, Braunschweig, Germany
Silicone tubing, tubing connectors	GE Healthcare, Freiburg, Germany
Peristaltic pump P-1	GE Healthcare, Freiburg, Germany
Syringes and cannulas	B. Braun, Melsungen, Germany
Ultracrimp ultracentrifuge tubes	Thermo Fisher Scientific, Braunschweig, Germany
AVB Sepharose HP column	GE Healthcare, Freiburg, Germany
HiTrap Heparin HP column	GE Healthcare, Freiburg, Germany
Amicon Ultra-15 centrifugal filter units	Merck Millipore, Darmstadt, Germany
Sephadex G50 packed illustra NICK column	GE Healthcare, Freiburg, Germany

#### Analytical instruments and equipment

Product	Manufacturer
BiodocAnalyze live imaging system	Analytik Jena AG, Jena, Germany
FACS Canto I	Becton Dickinson, Heidelberg, Germany
FACS tubes	Becton Dickinson, Heidelberg, Germany
LightCycler 480 II	Roche, Mannheim Germany
LightCycler 96 multiwell plates and foils	Roche, Mannheim Germany
Capillary LightCycler	Roche, Mannheim Germany
LightCycler capillaries	Roche, Mannheim Germany
LightCycler carousel centrifuge	Roche, Mannheim Germany
Mini sub GT gel electrophoresis unit	BioRad, München, Germany
PowerWave 340 microplate reader	BioTek Instruments Inc., Winooski, USA
Mini trans-blot electrophoretic transfer cell	BioRad, München, Germany
Nitrocellulose membrane (Hybond ECL)	GE Healthcare, Freiburg, Germany
Whatman filter paper	Schleicher&Schuell, Dassel, Germany
Amersham Hyperfilm ECL	GE Healthcare, Freiburg, Germany

#### Cell culture equipment and disposables

Product	Manufacturer
Cell culture plastic ware	TPP AG, Trasadingen, Switzerland
Cell scrapers	Corning Incorporated, New York, USA
CO <sub>2</sub> Incubator MCO-20AIC	Sanyo, Munich, Germany
Cryotube vials	Thermo Fisher Scientific, Braunschweig, Germany
Laminar Air Flow BioWizard Golden Line	Kojair, Vilppula, Finland
Laminar Air Flow BioWizard Xtra	Kojair, Vilppula, Finland
Microscope	Olympus, Hamburg, Germany

## Centrifuges

Product	Manufacturer
Beckman Coulter Rotor Type E70Ti	Beckman Coulter GmbH, Krefeld, Germany
Beckman Coulter Optima L-80 XP Ultracentrifuge	Beckman Coulter GmbH, Krefeld, Germany
Centrifuge Avanti J-E	Beckman Coulter GmbH, Krefeld, Germany

## Analytical instruments and equipment

Product	Manufacturer
Balance Adventurer Pro	Ohaus, NJ, USA
Hera -80°C Freezer	Thermo Fisher Scientific, Braunschweig, Germany
Heater/Magnetic stirrer Heidolph MR 3001	Heidolph Instruments, Schwabach, Germany
Incubator Shaker Multitron Standard	Infors HAT, Bottmingen-Basel, Switzerland
NanoDrop™ 1000 spectrophotometer	Thermo Fisher Scientific, Braunschweig, Germany
Parafilm	Pechinery Plastic Packaging, Chicago, USA
pH Meter Seven Easy	Mettler-Toledo, Schwerzenbach, Switzerland
Pipette tips	Sarstedt, Nümbrecht, Germany
Pipettes	Eppendorf, Hamburg, Germany
Reaction tubes (1.5 ml, 2 ml)	Eppendorf, Hamburg, Germany
Serological pipets	Sarstedt, Nümbrecht, Germany
Reaction tubes (15 ml, 50 ml)	Sarstedt, Nümbrecht, Germany
Thermocycler T3000	Biometra, Göttingen, Germany
Thermomixer Comfort	Eppendorf, Hamburg, Germany
Vortex Genie 2	Scientific Industries, NY, USA
Waterbath Medingen W6	Medingen, Freital, Germany
General laboratory ware	VWR, Darmstadt, Germany

## 3.9 Data treating software

Adobe Illustrator, ApE-A plasmid editor, Clone Manager, Inkscape 0.91, Microsoft Excel, R/RStudio, specific software for respective instruments

## 4 Methods

### 4.1 Bacteria Culture

#### 4.1.1 Cultivation

*E.coli* were grown overnight at 37°C in LB medium while shaking. LB medium for culturing of transformed bacteria was supplemented with 100 mg/l ampicillin or 50 mg/l kanamycin.

LB medium:

10 g	Tryptone
5 g	Yeast
5 g	NaCl
15 g	Agar (for plates)
ad 1L	distilled H <sub>2</sub> O

#### 4.1.2 Preparation of competent bacteria

The day before preparation, the CaCl<sub>2</sub> solution was sterilized and cooled to 4°C. *E.coli* were grown overnight at 37°C in 5 ml LB. The next morning, 400 ml LB medium were added to the overnight culture. The culture was grown further to an optical density (OD<sub>590</sub>) of 0.4. The bacteria suspension was chilled for 10 min. All subsequent preparation and incubation steps were conducted on ice and all centrifugation steps were conducted at 4°C. The suspension was centrifuged at 1600 x g for 7 min. The pellet was resuspended in 10 ml CaCl<sub>2</sub> solution, followed by centrifugation for 1100 x g for 5 min. The pellet was resuspended in 8 ml CaCl<sub>2</sub> solution and incubated on ice. The last centrifugation step was conducted at 1100 x g for 5 min. The pellet was again resuspended in 8 ml ice-cold CaCl<sub>2</sub> solution. Aliquots of 100 µl were shock frozen in liquid nitrogen and stored at -80°C.

CaCl<sub>2</sub> solution:

60 mM	CaCl <sub>2</sub>
10 mM	PIPES
10%	Glycerin

#### 4.1.3 Transformation

Competent bacteria were thawed on ice. 100-500 ng transforming plasmid DNA (pDNA) were added to the bacteria and mixed. Following incubation on ice for 10 min, the suspension was subjected to heat shock at 42°C for 90 sec. Thereafter, the bacteria suspension was placed on ice for 2 min. 500 µl of LB medium were added and the suspension was shaken for 1 h at 37°C. Bacteria were plated on a LB agar plate containing the respective selective antibiotic and incubated overnight at 37°C.

## 4.2 Nucleic acid techniques

### 4.2.1 pDNA amplification and extraction

Single clones of successfully transformed bacteria were picked from the plates and amplified overnight in LB medium containing the selective antibiotic. According to the desired yield of pDNA, the protocol of the respective Qiagen plasmid kit was used (“mini”: up to 20 µg, “maxi”: up to 500 µg, “mega”: up to 2.5 mg).

### 4.2.2 DNA extraction from eukaryotic cells

From eukaryotic cells, DNA was extracted using the DNeasy Blood & Tissue Kit, according to the provided “Purification of Total DNA from Animal Blood or Cell” protocol. Deviating from manufacturer’s instructions, DNA was eluted in 10 mM Tris/HCl pH 8.5.

### 4.2.3 RNA extraction from eukaryotic cells

RNA was extracted using the RNeasy Mini Kit, according to the provided “Purification of Total RNA from Animal Cell” protocol. A DNA digestion step was included in the RNA extraction protocol, using the RNase-free DNase set according to the manufacturer’s instructions.

### 4.2.4 Determination of pDNA and RNA concentration

pDNA and RNA concentration was determined using a spectrophotometer and a wavelength of 260 nm or 280 nm, respectively. Purity of DNA preparations was assessed by the ratio  $\text{abs. } 260\text{nm}/\text{abs. } 280\text{nm}$  ( $A_{260/280}$ , absorbance of protein impurities), with a ratio of 1.8 indicating high purity. Lower values for  $A_{260/280}$  point to protein contaminations, higher values point to contamination with RNA.

### 4.2.5 Restriction enzyme digest

pDNA digestion with restriction enzymes was performed according to the manufacturer’s protocol using 1-10 units of restriction enzyme per 1 µg DNA.

### 4.2.6 Agarose gel electrophoresis

#### 4.2.6.1 Neutral

Analytic agarose electrophoreses were performed in 1xTAE buffer with agarose concentrations of between 0.8 and 1.2 %. The agarose was added to 1xTAE and boiled until dissolved. Ethidium bromide was added (0.5 µg/1 ml gel volume) to the gel solution before pouring onto the casting plate. Approximately 500 ng DNA or DNA fragments from restriction digest were used. Commercial DNA ladders were used for size reference.

50x TAE electrophoresis buffer:

2 M	Tris base
1 M	Glacial acetic acid
50mM	EDTA solution, pH 8.0

#### 4.2.6.2 Denaturing

Denaturing conditions for gel electrophoresis were established by alkalinity. In neutral gel buffer, 0.8% agarose was boiled until dissolved and cast. After solidifying for 30 min, the gel was immersed in alkaline electrophoresis buffer for 1 to 1.5 hrs. Samples and ladder were mixed with 6x alkaline loading buffer, heated at 70°C for 5 min and quickly chilled on ice for 3 min before loading. Electrophoresis was performed at low voltage (30-40 volt) for 3-6 hrs. After electrophoresis, the gel was immersed in 300 ml of 0.5 M Tris-HCl, pH 7.5. Thereafter the gel was stained in a 0.5 µg/ml ethidium bromide solution for 30 min and visualized under UV light.

Neutral gel buffer:

30 mM	NaCl
2 mM	EDTA, pH 7.5

Alkaline electrophoresis buffer:

30 mM	NaOH
2 mM	EDTA

6x alkaline loading buffer:

180 mM	NaOH
6 mM	EDTA
18 %	Ficoll 400
0.05 %	Bromcresol green

#### 4.2.7 cDNA synthesis

cDNA was synthesized from RNA in a maximum volume of 8 µL using the SuperScript™ III First-Strand Synthesis SuperMix for qRT-PCR according to manufacturer's instructions.

#### 4.2.8 Quantitative real-time PCR

qPCR was employed to determine the concentration of vector genomes and DNA impurities in AAV vector preparations. Samples were prepared with LightCycler 480 SYBR Green Master kit for measurement on a 96 multwell plate for LightCycler 480 II, or with LightCycler FastStart DNA Master SYBR Green I kit for measurement on the Capillary LightCycler. Concentrations were calculated from a standard curve generated by serial dilutions of a plasmid or a MC containing the gene of interest.

Commonly, particle concentrations in the range of  $2 \times 10^2$  to  $2 \times 10^8$  per 2  $\mu\text{L}$  sample preparation were quantified. Specificity of the quantified product was confirmed by melting peak analysis.

Pipetting scheme:

	Per well of 96-well plate	Per Capillary
Template DNA	2 $\mu\text{l}$	2 $\mu\text{l}$
20 $\mu\text{M}$ forward primer	1 $\mu\text{l}$	1 $\mu\text{l}$
20 $\mu\text{M}$ reverse primer	1 $\mu\text{l}$	1 $\mu\text{l}$
Reaction mix (including FastStart Taq DNA polymerase, reaction buffer, dNTPs, SYBRGreen I dye, $\text{MgCl}_2$ )	10 $\mu\text{l}$	4 $\mu\text{l}$
$\text{H}_2\text{O}$	6 $\mu\text{l}$	12 $\mu\text{l}$

qPCR program

Program	Cycles	Analysis Mode	Target ( $^{\circ}\text{C}$ )	Acquisition mode	Duration	Ramp Rate ( $^{\circ}\text{C}/\text{s}$ )	Acquisitions (per $^{\circ}\text{C}$ )
Denaturation	1	None	95	None	00:05:00	4.4	
Amplification	40	Quantification	95	None	00:00:15	4.4	
			60	None	00:00:10	2.2	
			72	Single	00:00:15	4.4	
Melting	1	Melting Curve	95	None	00:00:01	4.4	
			68	None	00:00:15	2.2	
			95	Continuous			5
Cooling	1		40?	None	00:00:30	2.2	

## 4.3 Protein techniques

### 4.3.1 ELISA

To determine the capsid titers of AAV vector preparations, the AAV 2 Titration ELISA kit was used according to the manufacturer's protocol. The color reaction was quantified on a microplate reader.

### 4.3.2 Western Blot

Western Blot was performed to investigate the composition of the VP proteins. To samples containing approximately  $5 \times 10^{10}$  vector capsids, Laemmli buffer was added. After incubation at  $95^{\circ}\text{C}$  for 7 min, the samples were loaded onto a gel, consisting of a 5 % stacking and an 8 % resolving gel. Electrophoresis was performed in Running Buffer at 80 V for 30 min, then at 100 V for approximately

2-3 hrs, to separate the proteins by size. The proteins were transferred from the gel to a nitrocellulose membrane using an electrophoretic transfer cell in Blotting Buffer for 1 h at 400 mA. After blotting, the membrane was incubated in blocking buffer overnight at 4°C while shaking. The next day the membrane was incubated with B1 primary antibody solution (recognizes C-terminus of VP1, VP2 and VP3, kindly provided by Martin Müller, DKFZ Heidelberg, Germany; dilution of 1:10) for 1 h at RT. The membrane was washed three times with 0.1 % Tween20 in PBS before incubation with secondary antibody (donkey anti-mouse IgG-HRP, Jackson ImmunoResearch Ltd., Suffolk, UK; dilution of 1:2500) for 1 h. After removal of the secondary antibody the washing procedure was repeated. Western Lightning Chemiluminescence Reagent Plus (PerkinElmer, Waltham, USA), the substrate solution for the peroxidase-conjugated secondary antibody was pipetted onto the membrane and incubated at RT for 1 min. Finally a radiographic film was exposed to the membrane and subsequently developed.

6x Laemmli buffer:	60 mM	Tris, pH 6.8
	9.3 mg/ml	DTT
	12 %	SDS
	47 %	Glycerol
	0.6 mg/ml	Bromophenol Blue

Running Buffer:	25 mM	Tris Base
	192 mM	Glycin
	0.1 %	SDS

Blotting Buffer, pH 8.3:	0.3 %	Tris Base
	1.44 %	Glycin
	0.02 %	SDS

Blocking Buffer:	5 %	Milk powder
	0.1 %	Tween20
		in PBS

## Electrophoresis gel

	5 % stacking gel	8 % resolving gel
distilled H <sub>2</sub> O	4.1 ml	6.9 ml
acrylamide stock solution, 30%	1 ml	4.0 ml
1 M Tris (pH 6.8)	0.75 ml	-
1.5 M Tris (pH 8.8)	-	3.8 ml
10% SDS	60 µl	150 µl
10% APS	60 µl	150 µl
TEMED	6 µl	9 µl

## 4.4 Eukaryotic cell culture

### 4.4.1 Cultivation conditions

HeLa and HEK293 cells were cultivated in Dulbecco's modified Eagle's medium (DMEM) with Gluta-MAX-I supplemented with 10 % FCS, 100 IU/ml of penicillin and 100 µg/ml of streptomycin. HEK-Blue-hTLR9 were subcultured in DMEM supplemented with 10 % FCS, 50 IU/ml of penicillin, 50 µg/ml of streptomycin, 100 µg/ml normocin, 10 µg/ml blasticidin and 100 µg/ml zeocin. All cell lines were maintained in cell culture flasks or plates in a humidified incubator at 37°C and 5 % CO<sub>2</sub>.

### 4.4.2 Passaging, counting and seeding

All cell lines used were grown in adherent cultures. Prior to detachment, cells were washed with PBS. HeLa and HEK293 were incubated with trypsin (0.05 %). HEK-BLUE-TLR9 cells were shortly incubated in PBS at 37°C and then detached by tapping. For further cultivation, cells were diluted to a suitable concentration and transferred into a cell culture vessel. For counting, 10 µl of cell suspension were pipetted into a hemocytometer. A minimum of four squares was counted. The concentration of cells per ml was calculated from the mean value of cell counts, multiplied by 10<sup>4</sup>. Cells were seeded at the desired density in plates or dishes.

### 4.4.3 Freezing and thawing

Cells were detached, suspended in medium and pelleted at 1000 rpm for 5 min. The cell pellet was resuspended in the respective freezing medium (standard: 90 % FCS, 10 % DMSO; HEK blue hTLR9: 70 % DMEM, 20 % FCS, 10 % DMSO) and aliquoted into cryovials. The cryovials were stored overnight at -80°C in a freezing container. After 24 hrs, the frozen cells could be transferred to liquid nitrogen for long-term storage. For thawing, the frozen cell suspension was briefly incubated at

37°C and transferred into pre-warmed medium. To remove DMSO the cell suspension was pelleted as described above. Cells were resuspended in fresh medium and plated in cell culture dishes.

#### 4.5 AAV vector production

$7.5 \times 10^6$  HEK293 producer cells were seeded in 15 cm<sup>2</sup> cell culture plates. 24 hrs later, at cell confluency of approximately 80 %, medium was exchanged. Two hours thereafter, cells were transfected using the calcium phosphate method (see below).

##### Transfection scheme for 1 plate:

##### Triple plasmid transfection (equimolar ratio):

7.5 µg vector plasmid

7.5 µg pRC

22.5 µg pXX6-80

##### Dual transfections:

single-stranded (molar ratio of 1:1.3)

30 µg pDPs OR 27.6 µg MC.DP2rs

7.5 µg pAAV-ssGFP OR 4.3 µg MC.AAV-ssGFP

Self-complementary (molar ration of 1:1.3)

38.7 µg pDP2rs OR 35.8 µg MC.DP2rs

7.5 µg pAAV-scGFP OR 3.2 µg MC.AAV-scGFP

For one plate, DNA constructs were pipetted into 1 ml 250 mM CaCl<sub>2</sub>. 1 ml HBS puffer was added dropwise. The suspension was mixed, incubated for 2 min and then pipetted onto the plate. Transfected cells were incubated at 37°C and 5% CO<sub>2</sub>. 24 hrs after transfection, medium was exchanged for DMEM containing only 2 % FCS to reduce cell proliferation. 48 hrs after transfection, cells were harvested by scraping and pelleted by centrifugation at 1200 rpm for 20 min at 4°C. The cell pellet was resuspended in Lysis buffer. Cells were lysed by three freeze/thaw cycles using liquid nitrogen and a water bath at 37°C. To remove cellular nucleic acids as well as non-packaged pDNA the cell suspension was treated with 50 U/ml Benzonase for 30 min at 37°C. Subsequently, the suspension was centrifuged for 1 h at 4000 rpm at 4°C. The supernatant contained the vector particles.

HBS buffer, pH 7.2:

50 mM	HEPES
280 mM	NaCl
1.5 mM	Na <sub>2</sub> HPO <sub>4</sub> 2H <sub>2</sub> O

Lysis buffer, pH 8.5

150 mM	NaCl
50 mM	Tris-HCl

## 4.6 AAV vector purification

### 4.6.1 Iodixanol density gradient

The supernatant of lysed cells (see chapter 4.5) was transferred into an ultracentrifugation tube. A peristaltic pump was used to underlay the vector suspension, via a cannula connected to a tube system, with the different iodixanol phases in the following order: 9 ml 15 % phase, 6 ml 25 % phase, 5 ml 40 % phase, 5 ml 60 % phase. The ultracentrifugation tube was filled up with PBS supplemented with 1 mM MgCl<sub>2</sub> and 2.5 mM KCl (PBS-MK), sealed and centrifuged at 60,000 rpm for 2 hrs at 4°C. Upon centrifugation, the 40% phase containing the vector particles was harvested using a cannula and a syringe.

	15 %	25 %	40 %	60 %
10xPBS	5 ml	5 ml	5 ml	-
1M MgCl <sub>2</sub>	50 µl	50 µl	50 µl	50 µl
2.5M KCl	50 µl	50 µl	50 µl	50 µl
5M NaCl	10 ml	-	-	-
Optiprep	12.5 ml	20 ml	33.3 ml	50 ml
0.5 % phenol red	50 µL	80 µL	-	25 µl
H <sub>2</sub> O	ad 50 ml	ad 50 ml	ad 50 ml	ad 50 ml

### 4.6.2 Affinity chromatography

The affinity chromatography column was equilibrated with the appropriate binding buffer (hiTrap Heparin column: PBS-MK, AVB column: PBS). AAV vector preparations isolated from iodixanol density gradient were diluted approximately 1:10 with binding buffer and applied to the column twice. The

column was washed with 10 column volumes binding buffer. The bound vector particles were eluted using the appropriate elution buffer (hiTrap Heparin column: PBS-MK + 1 M NaCl, AVB column: PBS + 2.5 M MgCl<sub>2</sub>). AVB columns were performed by Elke Barczak, Hannover Medical School.

#### **4.6.3 Centrifugal filtration**

PBS-MK was added to the vector suspension to a total volume of 15 ml and ultrafiltered using Amicon Ultra-15 centrifugal filter units (MWCO 100 kDa). The Amicon tube was centrifuged until the vector suspension was concentrated to approximately 1 ml. The retentate was filled up to 15 ml with PBS-MK and centrifuged again. This step was repeated twice (total of three cycles). In the last centrifugation step, the vector suspension was concentrated to 200 to 500 µl.

#### **4.6.4 Gel filtration**

The Sephadex G50 packed illustra NICK column was equilibrated with 5 ml PBS-MK. 200 µl of the vector preparation was applied to the column. The vector was eluted using PBS-MK in fractions of 100 µl. From each fraction, vector DNA was extracted and quantified. The fractions containing the highest vector concentrations were pooled.

### **4.7 AAV vector characterization**

#### **4.7.1 Genomic titer**

From an aliquot of a vector preparation (usually 10 µl) vector DNA was extracted as described in chapter 4.2.2. The genomic titer, i.e., the concentration of TEC-containing particles was determined by qPCR using TEC-specific primers (see chapter 4.2.8).

#### **4.7.2 Transducing titer**

HeLa cells were transduced with a serial dilution (1:3 steps) of a vector preparation. 48 hrs post-transduction (p.t.), the number of cells per well was determined and the number of eGFP<sup>+</sup> cells was measured by flow cytometry. The vector serial dilution was used to determine the linear range, i.e. the range in which the dilution factor of the vector preparation correlates to the respective fold-decrease in eGFP expression. Using the total cell number per well and the dilution factors and corresponding percentages of eGFP-positive cells within the linear range, the transducing titer was calculated. Alternatively, the transducing titer was determined from the vector dilution which resulted in a single transduction event (approximately 10 % eGFP<sup>+</sup> cells).<sup>232</sup>

### 4.7.3 Capsid titer and composition

The concentration of AAV2 capsids of a vector preparation was determined by ELISA as described in 4.3.1. The composition of capsid proteins VP1, VP2 and VP3 was determined by Western Blot as described in 4.3.2.

### 4.7.4 DNA impurity content

Vector genome DNA (see chapter 4.7.1), was examined for content of DNA other than the TEC by qPCR, using primers as specified in 3.5.

## 4.8 Cell transduction by AAV vectors

### 4.8.1 TLR9 activation assays

Activation of HEK blue hTLR9 was monitored by two different methods.

#### 4.8.1.1 Quantification of SEAP protein levels

For production of mock inoculum pXX6-80 and pAAV-scGFP were transfected into HEK293 cells. Cells were harvested and the lysate purified using IDGC as described above (chapter 4.6.1). The mock inoculum harvested from the 40 % phase served as negative control. As positive control TLR9 agonist ODN2006 (Invivogen) at a concentration of 5  $\mu$ M was used. 20  $\mu$ L of sample (vector preparation, mock negative control or positive control) was added to the bottom of a flat-bottomed 96-well plate. HEK blue hTLR9 cells were detached and suspended in HEK-Blue detection medium.  $4 \times 10^4$  cells in 180  $\mu$ l volume were added to the samples and the plates were incubated at 37°C in 5 % CO<sub>2</sub> for 20 hrs.

#### 4.8.1.2 Quantification of IL8 transcription levels

$7.5 \times 10^4$  were seeded in a 48-Well plate. The following day, cells were incubated with AAV vectors at a genomic particle per cell ratio (GOI) of  $10^5$ . As negative control, cells were incubated with mock-inoculum using a volume equal to the highest volume applied for the AAV vectors. 5  $\mu$ M ODN 2006 served as positive control. 3 hrs p.t. RNA was extracted and reverse-transcribed as described above (chapters 4.2.3, 4.2.7). Gene expression levels of IL8 vs. reference gene GAPDH were determined by qPCR using specific primers (chapters 4.2.8, 3.5).

### 4.8.2 Colony forming assay

$1 \times 10^5$  HeLa cells were seeded in a 6-well plate. 24 hrs later cells were transduced with AAV-S/MAR or AAV- $\Delta$ S/MAR at a GOI of 5000. 24 hrs p.t., the percentage of eGFP-positive (eGFP<sup>+</sup>) cells was determined by flow cytometry. A minimum of 10,000 cells was counted, with the background fluores-

cence set to 1 %. For a standard experiment, the cell suspension containing a mixture of eGFP<sup>+</sup> and eGFP<sup>-</sup> cells was seeded to yield 10<sup>5</sup> eGFP<sup>+</sup> cells per 15 cm<sup>2</sup> dish or 150 cm<sup>2</sup> flask. For Experiment 3 described in Figure 17 the cell suspension was sorted for eGFP expressing cells by the CMMC FACS facility service using a FACS ARIA III (Becton Dickinson) to seed only eGFP<sup>+</sup> cells at a density of 10<sup>5</sup> cells per plate. 24 hrs after seeding 2 µg/ml blasticidin was added. With the next medium exchange the blasticidin concentration was increased to a concentration of 2.5 µg/ml. Cells were selected for 3 to 4 weeks. This time span was chosen to guarantee that cell survival was due to stable establishment of vector genomes. Thereafter the blasticidin-resistant colonies were either picked and cultured further without blasticidin, or the plates were stained for colony count. Before the staining procedure cells were washed twice with ice-cold PBS. Cells were incubated in fixing solution (1% formaldehyde in PBS) for 15 min at room temperature while agitating gently. The fixing solution was removed and cells were incubated with staining solution (0.5 % crystal violet, 25 % methanol in PBS) for 10 min at room temperature. The dishes were rinsed carefully with H<sub>2</sub>O to remove staining solution and dried. The colonies were quantified by C. Hagedorn (University Witten/Herdecke) using Fiji ImageJ software setting the threshold for colony size to 200 pixel<sup>2</sup>.

#### 4.9 Statistical Analysis

Data are presented as mean ± standard deviation (SD). Quantitative data was log<sub>2</sub>-transformed and tested with t-test or ANOVA, followed by Tukey Test. Calculated p-values below 0.05 were considered statistically significant.

Statistical analyses shown in Tables 1-6 and Figures 9 and 11 were conducted by B. Kracher (MPI for Plant Breeding Research, Cologne, Germany). Statistical analysis shown in Figure 17 was conducted by C. Hagedorn (University Witten/Herdecke).

## 5 Results

### 5.1 Improving the purity of AAV vector preparations using DNA Minicircle (MC) technology

#### 5.1.1 Encapsidated prokaryotic sequences in AAV vector preparations cannot be removed by standard purification methods

Several laboratories using different production methods reported nuclease-resistant DNA impurities in AAV vector preparations.<sup>141–143</sup> We examined single-stranded AAV (ssAAV) vector preparations, which were produced and purified by standard protocols, for the presence of nuclease-resistant plasmid backbone sequences. Thereby, the ampicillin resistance gene (*ampR*) *bla*, encoding for TEM-1  $\beta$ -lactamase was used as marker, as it is contained in all used vector and helper plasmids. For vector production, HEK293 producer cells were transfected using the triple plasmid method. 48 hrs after transfection, cells were harvested and lysed. The cell lysate was treated with Benzonase to remove all non-encapsidated nucleic acids and loaded onto a discontinuous iodixanol density gradient (IDGC). Thereafter, vector preparations #1 and #2 were purified by affinity chromatography utilizing an anti-AAV single-domain antibody (AVB column), followed by centrifugal filtration. Vector preparation #3 was instead purified by affinity chromatography harnessing the heparin binding ability of AAV2, followed by gel filtration. For each step in the process, vector DNA was extracted from the vector preparations and analyzed by qPCR. The quantity of vector genomes was determined by primers specific for enhanced green fluorescent (eGFP) protein, the TEC intended to be packaged, while primers specific for *ampR* were employed to indicate the presence of plasmid backbone sequences. The majority of encapsidated sequences (> 98 % for all preparations) matched the intended transgene (Figure 6a). However, *ampR* sequences were detected in each IDGC-purified vector preparation, ranging from 0.5 % (vector preparations #3) to 1.8 % (vector preparation #2) relative to TEC (eGFP) sequences. None of the employed purification methods succeeded in removing the plasmid backbone sequences from the vector preparations (*ampR* concentrations relative to TEC: vector preparation #1: IDGC 1.3 % vs. AC-AVB 1.1 %, vector preparation #2: IDGC 1.8 % vs. AC-AVB 1.7 %, vector preparation #3: IDGC 0.5 % vs. AC-Heparin 0.6 %).

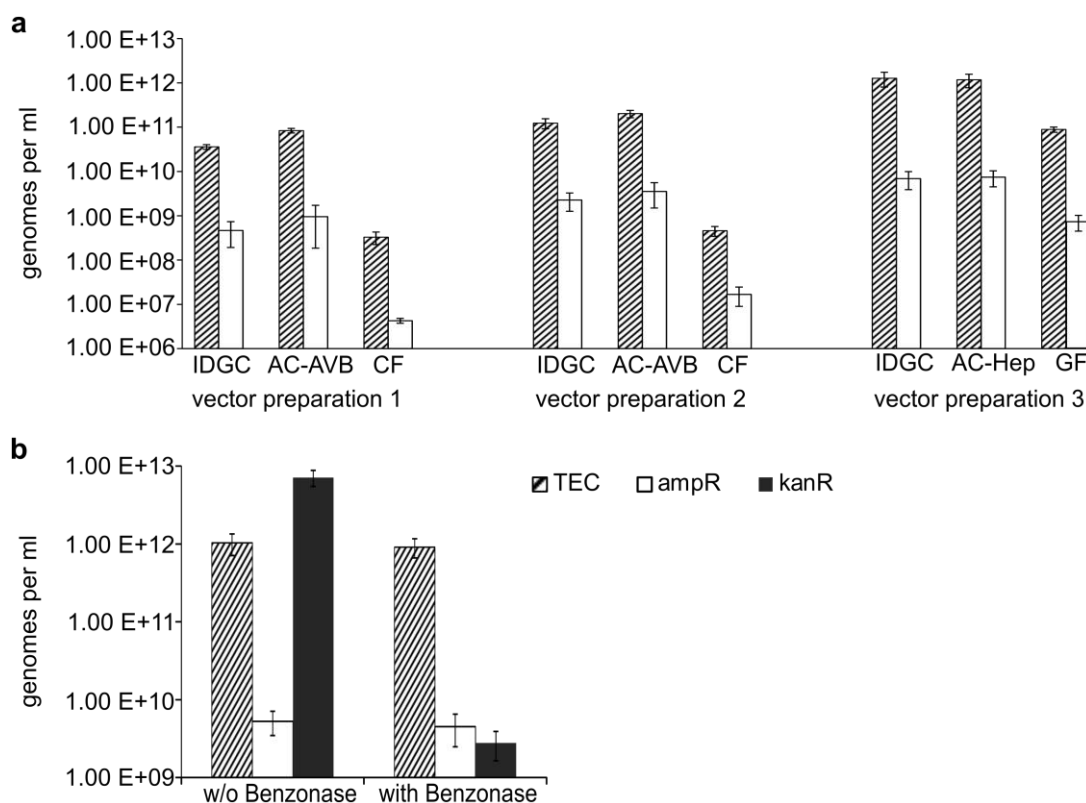


**Figure 6 Antibiotic resistance gene (*ampR*) sequences in standard AAV vector preparations. (a)** Quantification of DNA sequences contained in AAV vector preparations. Lysates of vector producing cells were purified by discontinuous iodixanol density gradient centrifugation (IDGC). AAV vector particles were harvested from the 40 %-phase and further purified by either affinity chromatography using AVB column (AC-AVB) or Heparin column (AC-Hep), followed by centrifugal filtration (CF) or gel filtration (GF). At each step of purification, total DNA from aliquots was isolated and analyzed by qPCR using indicated primers. **(b)** Benzonase protection assay. Two aliquots of AAV vector preparation #3 encoding for eGFP were spiked with 400 ng of a plasmid encoding for the kanamycin/neomycin resistance gene (*kanR*). One aliquot was treated with Benzonase. Total DNA of the treated and an untreated second aliquot was isolated and analyzed by qPCR using indicated primers. qPCR analyses described in (a) and (b) were performed three times independently. Figure was published in (Schnödt et al.).<sup>233</sup>

To determine whether these DNA impurities are protected by the viral capsid and thus tightly associated or encapsidated, a Benzonase protection assay was performed. Two aliquots of vector preparation #3 were spiked with 400 ng of a plasmid containing the kanamycin/neomycin resistance gene cassette (*kanR*) instead of *ampR*. One aliquot was treated with Benzonase. Total DNA was extracted from both aliquots and analyzed by qPCR (Figure 6b) Benzonase treatment did not affect the quantity of TEC nor *ampR*-specific sequences, but removed > 99.9% of input control plasmid sequences. Accordingly, it can be assumed that both TEC and *ampR* sequences are contained within or at least closely associated to the viral capsid and thus protected from enzymatic digestion. Therefore, the prokaryotic DNA contained in AAV vector preparations is Benzonase-resistant and cannot be removed by standard purification methods.

### 5.1.2 Evaluation of MC constructs for ssAAV vector production

In order to develop a strategy to decrease or even avoid packaging of prokaryotic sequences into AAV vectors, we tested whether the plasmids for AAV2 vector production can be replaced by MC constructs. MCs are circular DNA expression cassettes devoid of coding prokaryotic sequences. They are generated from a parental plasmid which contains, in addition to all necessary elements for plasmid propagation, the TEC(s) flanked by recombination sites and the *parA* resolvase gene under the control of an inducible promoter. Upon induction of cis-recombination the MC is separated from the functional prokaryotic sequences. The only prokaryotic remainder is a small sequence for chromatography, affinity and recombination (SCAR), which represents one recombination sequence and a tag for affinity purification.<sup>211, 216, 217</sup> In AAV vector production by dual transfection, one plasmid provides the TEC flanked by ITRs (pAAV-ssGFP, Figure 7a), while a second plasmid provides all required helper functions (pDP2rs, Figure 7b). The corresponding MC constructs (MC.ssGFP and MC DP2rs, Figure 7c and d) were designed, generated and produced by PlasmidFactory (Bielefeld, Germany).

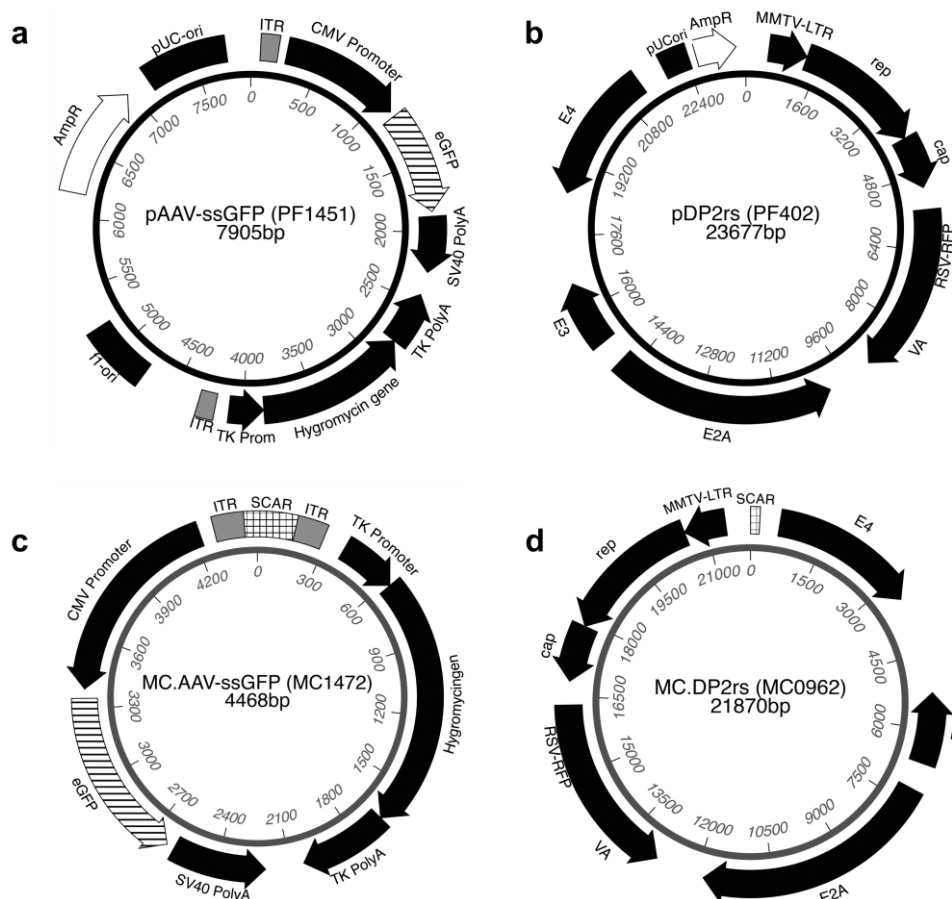


**Figure 7 ssAAV vector and AAV/Ad helper plasmids and thereof derived MC constructs.** (a) pAAV-ssGFP contains two TECs flanked by ITRs and the plasmid backbone including *ampR*, bacterial ori (pUC-ori) and *f1* ori. (b) pDP2rs is a combined AAV and Ad helper plasmid providing *rep*, *cap*/AAP and Ad E2A, E4 and VA functions, plus a red fluorescent protein (RFP). (c) MC.AAV-ssGFP consists of the TECs of pAAV-ssGFP, plus a residual SCAR sequence (213 bp). (d) MC.DP2rs contains all helper genes and RFP of pDP2rs, plus a residual SCAR sequence. All constructs shown were provided by PlasmidFactory. Figure was published in (Schnödt et al.).<sup>233</sup>

We performed a side-by-side comparison of the four possible combinations of MCs and plasmids for packaging of ssAAV vectors. After production and IDGC-purification, vector preparations were characterized by qPCR, Western Blotting and ELISA. With all four combinations AAV vector preparations of comparable yield could be obtained (Table 1). Comparable physical particle titers (capsids per ml) (analysis of variance (ANOVA), not significant (n.s.)) and an identical capsid composition (Figure 8) was determined for all preparations. qPCR analyses showed that the capsids contained vector genomes (TEC) and that MC-based vector preparations yielded a genomic particle titer, i.e. Benzonase-resistant TEC-containing particles per ml, which did not differ negatively from those obtained by the dual plasmid packaging system (ANOVA; Tukey *post hoc* tests vs. dual plasmid, n.s.). On the contrary, the highest genomic particle titers were measured for those preparations that were produced using MC.AAV-ssGFP. Thus, MC.AAV-ssGFP served as efficient template for vector genome replication, although the ITRs are separated by only 213 bp (Figure 7c).

Vector construct	Helper construct	Duplicate	Physical particles (vp)*	TEC (vg)*	Tukey groups: TEC	Ratio vp:vg	Tukey groups: vp:gv
plasmid	plasmid	1	637.2 ± 213.5	153.0 ± 86.6	<b>A. B</b>	4.2	<b>A. B</b>
		2	500.8 ± 34.7	130.6 ± 43.0		3.8	
plasmid	MC	1	698.8 ± 353.7	93.5 ± 43.2	<b>A</b>	7.5	<b>B</b>
		2	788.5 ± 343.2	101.4 ± 53.6		7.8	
MC	plasmid	1	934.8 ± 258.6	295.5 ± 265.0	<b>B</b>	3.2	<b>A</b>
		2	604.4 ± 343.2	269.4 ± 146.4		2.2	
MC	MC	1	628.0 ± 330.2	309.6 ± 117.2	<b>B</b>	2	<b>A</b>
		2	612.2 ± 387.3	210.3 ± 60.1		2.9	

\* x 10<sup>9</sup> ml<sup>-1</sup>

**Table 1 Particle titer and packaging efficiency of ssAAV vector preparations.** ssAAV vectors were produced side-by-side using all four possible combinations of plasmids and MCs as technical duplicates in a 4 x 15 cm<sup>2</sup> format. Preparations were purified by IDGC of Benzonase-treated cell lysate. The amount of physical particles (empty and DNA-containing capsids = capsid titer, vp) per ml was determined by ELISA. TEC-containing vector genomes (vg) were quantified by qPCR. The ratio vp:vg represents the packaging efficiency. All analyses were performed in parallel for all vector preparations. All analyses were performed three times independently. The effect of the different MC and plasmid combinations on physical and TEC genomic particles (per ml) and ratio vp:vg was assessed using analysis of variance (ANOVA) (physical particles: p=0.7288; TEC genomes: p=0.0249; ratio vp:vg: p=0.0098; transducing units: p<0.0001; ratio vp:tu: p=0.0731) and subsequent Tukey *post hoc* tests (Appendix A). Preparations that were not significantly different in the Tukey tests are marked with a common letter, while groups that were significantly different (p<0.05) do not contain a common letter in the Tukey groups column. Table content was published in (Schnödt et al.).<sup>233</sup>

As volume independent measure, the packaging efficiency, which is defined as the ratio of capsid titer to genomic (=TEC) particle titer (vp:vg), was calculated. A ratio of 50 and below is judged as a wild type phenotype,<sup>49</sup> while higher values indicate that either replication of vector genomes and/or the packaging process itself occurred inefficiently. In none of the cases in which plasmids were exchanged by MCs, a significant negative impact on the packaging efficiency was observed (ANOVA; Tukey *post hoc* tests vs. dual plasmid, n.s.). On the contrary, the lowest value, i.e. the highest packaging efficiency, was determined for preparations in which MC.AAV-ssGFP was used (Table 1).

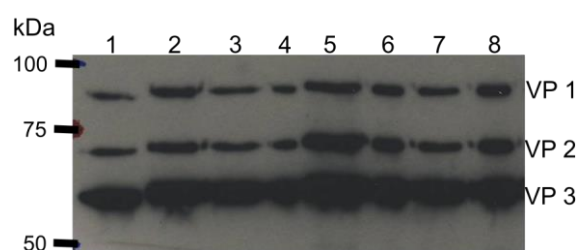


**Figure 8 Western Blot analysis of ssAAV vector preparations.**  $5 \times 10^{10}$  capsids were applied for each preparation and separated by SDS-PAGE. After Western blotting, the membrane was incubated with antibody B1 detecting the C-terminus of all three AAV capsid proteins. The figure shows the technical duplicates of vector preparations derived from transfection using the dual plasmid system (lanes 1,2), plasmid-helper: MC-vector constructs (lanes 3,4), MC-helper: plasmid-vector constructs (lanes 5,6) and dual MC system (lanes 7,8).

Next, the cervix carcinoma cell line HeLa, which is highly permissive for AAV2, was incubated with a serial dilution of the ssAAV vector preparations, followed by assessment of eGFP-expressing cells by flow cytometric measurements 48 hrs post-transduction (p.t.) to determine the transducing titers (Table 2).

Vector construct	Helper construct	Duplicate	Physical particles (vp)*	Transducing units (tu)*	Tukey groups: tu	Ratio vp:tu
plasmid	plasmid	1	637.2 ± 213.5	1.7 ± 0.2	<b>A. B</b>	365.5
		2	500.8 ± 34.7	1.2 ± 0.2		405.1
plasmid	MC	1	698.8 ± 353.7	1.5 ± 0.6	<b>A</b>	474.0
		2	788.5 ± 343.2	0.9 ± 0.4		856.2
MC	plasmid	1	934.8 ± 258.6	6.2 ± 2.6	<b>C</b>	149.9
		2	604.4 ± 343.2	2.9 ± 0.4		208.2
MC	MC	1	628.0 ± 330.2	2.7 ± 0.2	<b>B</b>	233.7
		2	612.2 ± 387.3	1.4 ± 0.1		439.7

\* x 10<sup>9</sup> ml<sup>-1</sup>

**Table 2 Transducing titer and transduction efficiency of ssAAV preparations.** The amount of physical particles was determined by ELISA (Table 1). Transducing particle titers (tu) were determined by FACS analysis measuring transgene-expressing cells after transduction of HeLa cells with a serial dilution of indicated preparations. The ratio vp:tu represents the transduction efficiency, e.g. the number of physical particles that need to be applied to successfully transduce HeLa cells. All analyses were performed in parallel for all vector preparations. All analyses were performed three times independently. The effect of the different MC and plasmid combinations on transducing units (per ml), and vp:tu ratios was assessed using ANOVA (transducing units:  $p < 0.0001$ ; ratio vp:tu:  $p = 0.0731$ ) and subsequent Tukey *post hoc* tests (Appendix A). Preparations that were not significantly different in the Tukey tests are marked with a common letter, while groups that were significantly different ( $p < 0.05$ ) do not contain a common letter in the Tukey groups column. Table content was published in (Schnödt et al.).<sup>233</sup>

No significant negative impact on AAV vector production was observed when either or both packaging plasmids were exchanged for MCs (ANOVA; Tukey *post hoc* tests). MC-based preparations tended to show a higher transducing titer, with preparations produced by combining pDP2rs and MC.AAV-ssGFP being superior to the dual MC system (ANOVA; Tukey *post hoc* tests,  $p < 0.001$ ). However, in a subsequently performed repetition experiment in which specifically ssAAV vector preparations produced by MC.AAV-ssGFP either in combination with pDP2rs or with MC.DP2rs were compared, transducing titers did not differ significantly (MC.AAV-ssGFP+ pDP2rs:  $6.2 \times 10^8 \pm 2.3 \times 10^8$  per ml; MC.AAV-ssGFP+MC.DP2rs:  $5.3 \times 10^8 \pm 2.1 \times 10^8$  per ml, t-test: n.s.). As volume-independent measure the transduction efficiency, which indicates the number of particles per cell required to obtain an infectious unit, was calculated. A ratio below  $10^4$  is defined as wild type phenotype,<sup>49</sup> and was reached by all preparations (Table 2). Thus, ssAAV vector preparations produced by transfection of MCs demonstrated an at least comparable overall yield, packaging and transduction efficiency compared to ssAAV vector preparations produced by transfection of vector and AAV/Ad helper plasmids.

### 5.1.3 Vector plasmids are the main source of encapsidated prokaryotic sequences

Using qPCR analysis we determined  $3.2$  and  $4.6 \times 10^9$  ampR-specific sequences per ml in the preparations produced by the dual plasmid strategy (Figure 9). This corresponds to approximately one ampR sequence per 150 particles, or an approximate 1:40 ratio of ampR- to TEC-containing particles. Replacing the helper plasmid by MC.DPRs had no beneficial effect (ANOVA; Tukey *post hoc* test vs. dual plasmid, n.s.). In contrast, replacing the vector plasmid by MC.AAV-ssGFP reduced the number of ampR-containing and thus falsely packaged particles, by more than two orders of magnitude. Under these conditions, the ratio of ampR to TEC-containing particles was reduced to less than 1:6000 (ANOVA; Tukey *post hoc* test vs. dual plasmid,  $p=0.0021$ ). A further decrease in the frequency of ampR sequences was observed in preparations produced by the dual MC approach, for which the frequency of ampR particles was lowered to 0.004 % or less relative to TEC (ANOVA; Tukey *post hoc* test vs. dual plasmid,  $p<0.001$ ). Thus, by replacing packaging plasmids for respective MC constructs, ampR DNA impurities can be reduced to background levels.

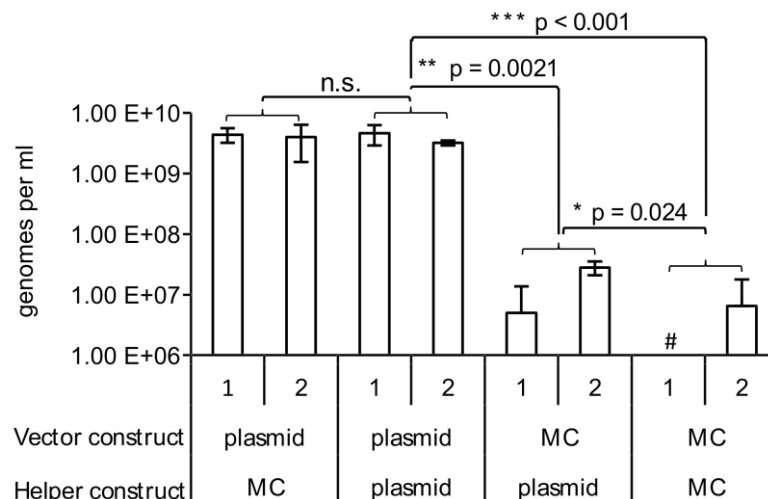


**Figure 9 ampR sequences in ssAAV preparations.** DNA isolated from vector preparations was quantified for ampR sequences by qPCR. All analyses were performed in parallel for all vector preparations. All analyses were performed three times independently. Differences in ampR content between preparations were assessed using ANOVA ( $p < 0.0001$ ) and subsequent Tukey *post hoc* tests. # < Limit of quantification (LOQ). Figure was published in (Schnödt et al.).<sup>233</sup>

### 5.1.4 Proximity to ITRs rather than a specific sequence element is decisive for packaging of backbone sequences

As cause for ampR DNA impurities, the presence of a weak packaging signal was proposed.<sup>234</sup> To test this hypothesis and to gain insight into the mechanism of false packaging, the dual plasmid-based preparations were analyzed for the presence of further plasmid backbone sequences. Specifically, we chose the bacterial origin of replication (ori) and the f1 origin (f1 ori) of replication, which are neighboring the left and the right ITR, respectively (Figure 7a) for qPCR analyses. Both sequences

were present with a frequency that correlated with the findings for ampR: we detected 2.0 to 2.3 % and 2.5 to 3.0 % of ori- and f1 ori-containing relative to TEC-containing particles, respectively (Table 3). Thus, prokaryotic sequences located *in cis* to the ITRs are packaged independent of a specific sequence element.

Duplicate	ampR particles*	f1 ori particles*	ori particles*
1	4.6 ± 1.7 (2.9 %)	4.7 ± 0.6 (3.0%)	3.2 ± 1.1 (2.0%)
2	3.2 ± 0.3 (2.3%)	3.3 ± 0.8 (2.5%)	3.1 ± 0.7 (2.3%)

\* x 10<sup>9</sup> ml<sup>-1</sup>

**Table 3 Quantification of prokaryotic DNA in the dual plasmid preparations.** DNA isolated from vector preparations produced by the dual plasmid strategy was quantified for the presence of ampR, f1 origin (f1 ori) of replication and pUC ori (ori) sequences by qPCR. All analyses were performed three times independently. The values in parentheses show the percentage of indicated prokaryotic sequences relative to summated TEC and indicated prokaryotic sequences. Table was published in (Schnödt et al.).<sup>233</sup>

Based on this result, we next evaluated whether the short prokaryotic non-coding SCAR sequence which remains present in MC constructs becomes encapsidated as well (Figure 7c). qPCR quantification showed that this DNA sequence is indeed being packaged into viral capsids when MC.AAV-ssGFP, containing this sequence *in cis*, was used for vector production. Up to 1.3 % of SCAR relative to TEC-containing particles were found, with no significant difference in content between vectors produced with either MC.DP2rs or pDP2rs (Table 4, t-test n.s.) further confirming that backbone sequences are packaged independent of a specific motif.

Vector construct	Helper construct	Duplicate	SCAR particles*
MC	plasmid	1	3.1 ± 1.3 (1.0 %)
		2	3.7 ± 2.4 (1.3 %)
MC	MC	1	1.5 ± 1.1 (0.5 %)
		2	2.5 ± 1.1 (1.2 %)

\* x 10<sup>9</sup> ml<sup>-1</sup>

**Table 4 Quantification of SCAR sequences in ssAAV vector preparations.** DNA isolated from indicated vector preparations were quantified for the presence of SCAR sequence by qPCR. All analyses were performed three times independently. Differences in SCAR content between vector preparations produced with either MC.DP2rs or helper plasmids were analyzed using t-test (p=0.1361, n.s.). The values in parentheses indicate the percentage of SCAR sequences relative to summated TEC and SCAR containing particles. Table was published in (Schnödt et al.).<sup>233</sup>

### 5.1.5 Self-complementary AAV (scAAV) vector preparations produced by MC constructs show improved transduction efficiencies and contain no ampR DNA impurities

Given the preferred use of scAAV vectors for *in vivo* applications, an easy to implement strategy to avoid unintended transfer of functional prokaryotic sequence is needed for this vector type as well.

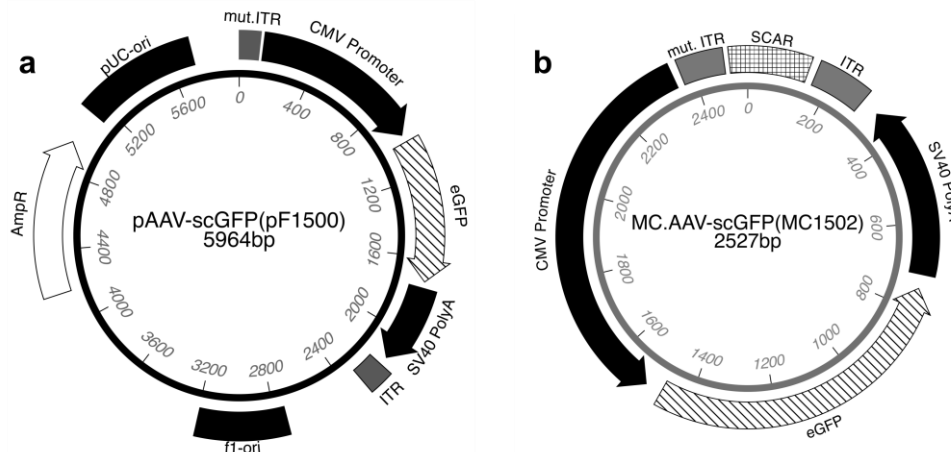


**Figure 10 scAAV vector plasmid and thereof derived MC construct. (a)** Plasmid pAAV-scGFP contains one TEC. One ITR has been mutated to generate a self-complementary vector genome. **(b)** Minicircle MC.AAV-scGFP consists of the TEC of pAAV-scGFP plus a residual SCAR sequence (213 bp). Both constructs were provided by PlasmidFactory. Figure was published in (Schnödt et al.).<sup>233</sup>

As source, we decided for pAAV-scGFP, which encodes for eGFP and results in production of self-complementary vector genomes due to the deletion of the trs of the left ITR sequence (Figure 10, for mechanism, see Figure 5). The corresponding MC.scGFP was designed, cloned and produced by PlasmidFactory.

As with the ssAAV vector preparations, all four possible combinations of vector (pAAV-scGFP, MC.AAV-scGFP) and helper constructs (pDP2rs and MC.DP2rs) were packaged and analyzed side-by-side. In line with the results for the ssAAV vector preparations (see Table 1), MC constructs were as efficient as plasmids in physical particle production (vp per ml) (ANOVA, n.s.). Replacing plasmids by MC constructs, however, beneficially impacted on genomic (TEC) particle titer and packaging efficiency, although here, statistical significance was not reached (ANOVA, Tukey *post hoc* tests) (Table 5).

Vector construct	Helper construct	Triplicate	Physical particles (vp) *	TEC (vg) *	Tukey Groups TEC	Ratio vp:vg
plasmid	plasmid	1	367.9	13.6	<b>A,B</b>	27.1
		2	1320.2	34.4		38.4
		3	603.2	20.5		29.4
plasmid	MC	1	409.0	10.6	<b>A</b>	38.6
		2	167.1	4.5		37.2
		3	1153.7	18.1		63.7
MC	plasmid	1	587.4	87.4	<b>C</b>	6.7
		2	1140.9	95.8		11.9
		3	1986.5	84.7		23.5
MC	MC	1	785.7	52.0	<b>B,C</b>	15.1
		2	395.8	51.8		7.6
		3	2306.4	71.0		32.5

\* x 10<sup>9</sup> ml<sup>-1</sup>

**Table 5 Particle titer and packaging efficiency of scAAV vector preparations.** scAAV vector preparations were produced side-by-side employing all four possible combinations of MCs and plasmids in a 3x15 cm<sup>2</sup> format three times independently. Preparations were purified by IDGC of Benzonase-treated cell lysate. Capsid titers (physical particles, vp) and genomic titers (TEC vector genomes, vg) were determined as described above (**Table 1**) The ratio vp:vg represents the packaging efficiency. All analyses were performed in parallel for all vector preparations. The effect of the different MC and plasmid combinations on particle numbers, genomic titer and ratio vp:vg was assessed using ANOVA (physical particles: p=0.5269; eGFP genomes: p<0.0001; ratio vp:vg: p=0.04725) and subsequent Tukey *post hoc* tests (Appendix B). Preparations that were not significantly different in the Tukey tests are marked with a common letter, while groups that were significantly different (p < 0.05) do not contain a common letter in the Tukey groups column. Table content was published in (Schnödt et al.).<sup>233</sup>

The most remarkable difference between MC-based and plasmid-based scAAV vector preparations was observed in the biological activity of the preparations: up to 30-fold improved transducing titers on HeLa (ANOVA, Tukey *post hoc* tests vs. dual plasmid, p<0.001) and as a consequence a significantly higher transduction efficiency (vp:tu) were determined for vector preparations generated using MC.scGFP (Table 6).

Vector construct	Helper construct	Tripllicate	Physical particles (vp) *	Transducing units (tu) *	Tukey Groups tu	Ratio vp:tu	Tukey Groups Ratio vp:tu
plasmid	plasmid	1	367.9	0.7		558.8	
		2	1320.2	0.8	<b>A</b>	1617.0	<b>B</b>
		3	603.2	0.6		1068.5	
plasmid	MC	1	409.0	0.8		491.0	
		2	167.1	0.3	<b>A</b>	562.7	<b>B</b>
		3	1153.7	0.7		1709.9	
MC	plasmid	1	587.4	9.5		62.0	
		2	1140.9	23.7	<b>B</b>	48.2	<b>A</b>
		3	1986.5	32.5		61.1	
MC	MC	1	785.7	5.8		136.0	
		2	395.8	13.9	<b>B</b>	28.4	<b>A</b>
		3	2306.4	8.9		259.2	

\* x 10<sup>9</sup> ml<sup>-1</sup>

**Table 6 Transducing titer and transduction efficiency of scAAV vector preparations.** The amount of physical particles was determined by ELISA (Table 4). Transducing particle titers (tu) were determined by FACS analysis measuring transgene-expressing cells after transduction of HeLa cells with a serial dilution of indicated preparations. The ratio vp:tu represents the transduction efficiency. All analyses were performed in parallel for all vector preparations. The effect of the different MC and plasmid combinations on transducing units (per ml), and vp:tu ratios was assessed using ANOVA (transducing units:  $p < 0.0001$ ; ratio vp:tu:  $p = 0.002471$ ) and subsequent Tukey *post hoc* tests (Appendix B). Preparations that were not significantly different in the Tukey tests are marked with a common letter, while groups that were significantly different ( $p < 0.05$ ) do not contain a common letter in the Tukey groups column. Table content was published in (Schnödt et al.).<sup>233</sup>

Again using ampR as marker, the amount of prokaryotic DNA contaminations was determined. Surprisingly, scAAV vector preparations were found to contain significantly higher amounts of ampR sequences than ssAAV vector preparations, relative to TEC. Specifically,  $4.8 \times 10^9$  –  $1.1 \times 10^{10}$  ampR-specific sequences per ml were measured (Figure 11). This corresponds to approximately one ampR sequence per 100 particles or an approximate 1:3 ratio of ampR- to TEC-containing particles. Replacing just the helper plasmid by the helper MC had, again, no beneficial effect (ANOVA; Tukey *post hoc* test vs. dual plasmid, n.s.), while, solely by replacing the vector construct, ampR-containing particles were decreased to 0.2 % or less relative to TEC (ANOVA; Tukey *post hoc* test vs. dual plasmid,  $p < 0.001$ ). Replacing both vector and helper plasmid by MCs resulted in scAAV vector preparation free of ampR-containing particles (Figure 11, below limit of quantification) providing further proof that firstly, packaging of functional prokaryotic sequences can be avoided by employing the MC technolo-

gy, and secondly, that the helper plasmid contributes to packaging of DNA impurities in AAV vector preparations.

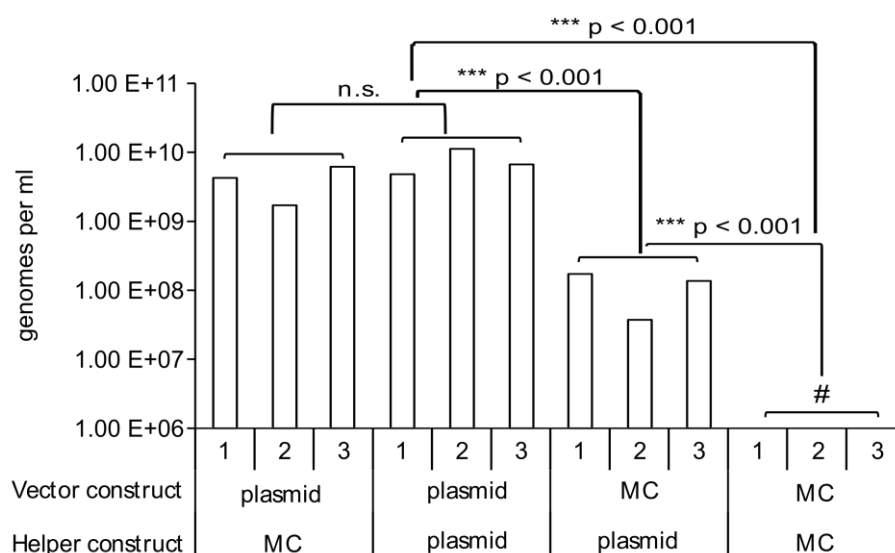


**Figure 11 ampR sequences in scAAV preparations.** DNA isolated from vector preparations was quantified for ampR sequences by qPCR. Analysis was performed in parallel for all vector preparations. Differences in ampR content between preparations were assessed using ANOVA ( $p < 0.0001$ ) and subsequent Tukey *post hoc* tests. # < Limit of quantification (LOQ). Figure was published in (Schnödt et al.).<sup>233</sup>

### 5.1.6 Further characterization of plasmid and MC-derived ssAAV and scAAV vectors

For further analyses new batches of ssAAV and scAAV vectors were produced, using the dual plasmid (pDP2rs or pAAV-ssGFP or pAAV-scGFP) and the dual MC (MC.DP2rs and MC.AAV-ssGFP or MC.AAV-scGFP) system side-by-side, and applying the same conditions and protocols as before. Vector DNA was isolated and analyzed by denaturing gel electrophoresis. Under denaturing conditions, any secondary DNA structure is disrupted and the vector genome unfolds into a linear single-stranded sequence. For both ssAAV and scAAV, MC-based and plasmid-based vector preparations showed a comparable appearance (Figure 12). Thus, agarose gel electrophoresis confirmed homogeneity of genomes contained in our preparations, as well as the correct size.

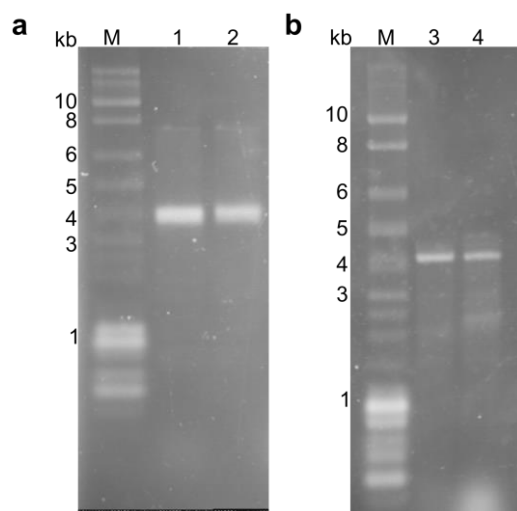


**Figure 12 Analysis of ssAAV and scAAV vector genomes by denaturing gel electrophoresis.**(a) ssAAV vector preparations. Lane 1 dual plasmid preparation, lane 2 dual MC preparation. (b) scAAV vector preparations. Lane 3 dual plasmid preparation, lane 4 dual MC preparation. M standard DNA marker.

Further, these vector preparations were analyzed for DNA impurities other than prokaryotic sequences ampR, ori and f1ori. qPCR analyses were performed for cellular genomic DNA (Tissue plasminogen activator, *PLAT*), adenoviral gene sequences (Ad *E4*) and AAV helper gene sequences (AAV2 *rep*). All preparations were free of cellular genomic DNA (below quantification limit, LOQ), while adenoviral and AAV viral sequences were detected (Table 7a,b).

a

Reference sequence	ssAAV	
	Dual plasmid vector	Dual MC vector
TEC ( <i>eGFP</i> )	2873.33 ± 181.48*	2260.00 ± 140.00*
<i>ampR</i>	150.32 ± 5.16* (5.0 %)	0.03 ± 0.01* (< 0.002 %)
AAV2 <i>Rep</i>	1.14 ± 0.06* (0.04 %)	0.54 ± 0.08* (0.02 %)
Ad <i>E4</i>	1.47 ± 0.03* (0.05 %)	0.69 ± 0.05* (0.03 %)
<i>PLAT</i>	< LOQ	< LOQ

b

Reference sequence	scAAV	
	Dual plasmid vector	Dual MC vector
TEC ( <i>eGFP</i> )	317.00 ± 14.11 *	188.67 ± 44.84 *
<i>ampR</i>	197.33 ± 17.79* (38.4 %)	< LOQ
<i>AAV2 Rep</i>	0.76 ± 0.04* (0.24 %)	0.18 ± 0.08* (0.10 %)
Ad <i>E4</i>	1.00 ± 0.09* (0.31 %)	0.21 ± 0.12* (0.11 %)
<i>PLAT</i>	< LOQ	< LOQ

\* x 10<sup>9</sup> ml<sup>-1</sup>

**Table 7 Further DNA impurities in ssAAV and scAAV vector preparations.** (a) ssAAV and (b) scAAV vectors were produced using the dual plasmid or the dual MC strategy. Vector genomes were isolated three times independently and quantified by qPCR for vector genomic titers (TEC, eGFP), and encapsidated ampR, AAV2 rep, Ad E4 and PLAT sequences. All analyses were performed in parallel for dual plasmid and dual MC-derived vector preparations. < LOQ = below limit of quantification.

Overall, scAAV vectors produced by dual plasmid transfection contained, besides ampR, higher levels of other non-TEC DNA. For both ssAAV and scAAV vectors, MC-based vector preparations tended to contain lower amounts of DNA impurities compared to plasmid-based preparations.

### 5.1.7 AAV vectors do not activate Toll-like receptor 9 *in vitro*

Researchers aiming to identify and characterize the interactions of AAV vectors with the host immune system proposed that the AAV vector genome is recognized by Toll-like receptor 9 (TLR9), a pathogen recognition receptor (PRR) of the innate immune system which senses unmethylated CpG sequences in DNA molecules.<sup>218</sup> Moreover, activation of TLR9 was reported to be enhanced with scAAV vector genomes.<sup>219</sup> As we detected a significantly higher content of prokaryotic sequences in scAAV compared to ssAAV vector preparations, we wondered whether this may be the reason for the higher immunogenicity of the former and, furthermore, whether MC-derived AAV vectors might activate TLR9 to a lesser degree than vectors produced by the standard plasmid transfection.

We used HEK blue hTLR9 cells to assay our ssAAV and scAAV vector preparations for TLR9 activation. This commercially available HEK293-derived cell line stably expresses human TLR9 and the reporter gene secreted embryonic alkaline phosphatase (SEAP). The SEAP reporter gene is under

the control of an interferon (IFN)- $\beta$  minimal promoter fused to binding sites for transcription factors nuclear factor kappa B (NF- $\kappa$ B) and activator protein (AP-)1. Stimulation with a TLR9 ligand activates NF- $\kappa$ B and AP1, which induces the production of SEAP. During stimulation, the cells are maintained in a cell culture medium which contains a SEAP color substrate. Thus, the magnitude of TLR9 activation can be detected colorimetrically. The ssAAV and scAAV vector preparations characterized in Table 7 were incubated on HEK blue hTLR9 cells for 20 hrs using a GOI of  $10^5$ . The scAAV vector produced by dual plasmid transfection contained a high amount of prokaryotic sequences (38.4 % ampR, relative to TEC) compared to the ssAAV vectors produced by either method (dual plasmid: 5.0 %, dual MC < 0.002 %). In the scAAV vector produced by dual MC transfection, no ampR-specific sequences were detected. Yet, neither tested vector preparation induced a SEAP gene expression above background (mock-treated cells), whereas incubation of cells with a CpG oligonucleotide positive control (ODN2006) induced a strong color reaction (Figure 13).

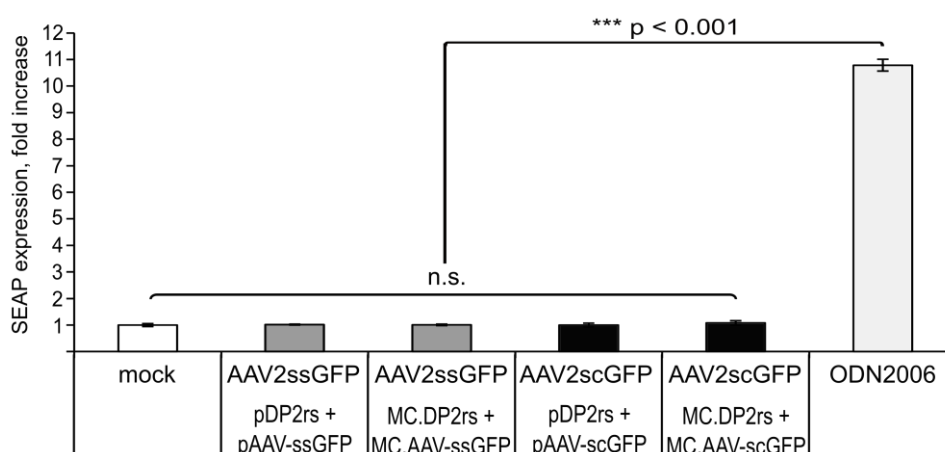


**Figure 13 SEAP production of HEK blue hTLR9 cells upon transduction.**  $4 \times 10^4$  HEK blue hTLR9 cells were incubated with AAV2ssGFP and AAV2scGFP produced by dual transfection of indicated constructs at GOI  $10^5$ , or challenged with  $5\mu$ M ODN2006 (TLR9 agonist). As negative control, cells were incubated with mock inoculum using a volume equal to the highest volume used for the AAV vectors. SEAP gene expression was determined at 20 hrs p.t. using a spectrophotometer at 620 nm. The results are expressed as fold-increase over mock-treated cells. Each sample was applied in triplicate. Differences in SEAP levels between samples were assessed using ANOVA ( $p < 0.0001$ ) and subsequent Tukey *post hoc* test.

As we speculated that the SEAP assay might not be sensitive enough, we repeated the transduction experiments and, instead of measuring SEAP after 20 hrs, we evaluated the gene expression levels of pro-inflammatory chemokine interleukin 8 (IL8) 3 hrs p.t. in HEK blue hTLR9 cells, as established previously in HEK293-TLR9 cells.<sup>134</sup> New batches of AAVscGFP were produced using either the dual plasmid method or the combination pDP2rs+MC.scGFP and concentrated in PBS-MK using centrifugal filtration. AAV2scGFP (dual plasmid) contained 27.5 % ampR-specific sequences, whereas AAV2scGFP (pDP2rs+MC.AAV-scGFP) contained 0.02 % ampR-specific sequences. In parallel,

cells were transduced with standard eGFP-encoding vectors ssAAV (2.8 % ampR) and scAAV (20.5 % ampR), produced by triple plasmid transfection. In cells treated with the positive control ODN2006 a robust elevation in IL8 gene expression was observed (Figure 14). In contrast, no increase of IL8 gene expression over background (PBS-MK or mock-transduced cells) was detected upon transduction with either vector preparation. Therefore, using two different assays, TLR9 activation by AAV vectors of either single-stranded or self-complementary genome conformation could not be confirmed.

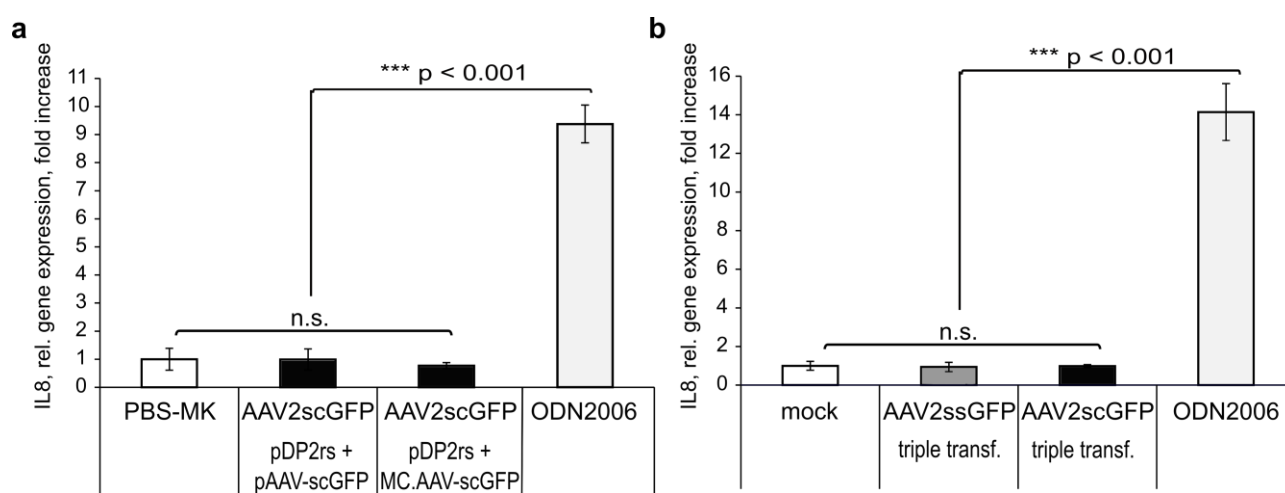


**Figure 14 IL8 gene expression of HEK blue hTLR9 cells upon transduction.**  $7.5 \times 10^4$  HEK blue hTLR9 cells were incubated with AAV vectors produced by **(a)** dual transfection or **(b)** triple transfection (triple transf.) at GOI  $10^5$  or challenged with  $5 \mu\text{M}$  TLR9 agonist ODN2006. As negative control, cells were incubated with **(a)** PBS-MK or **(b)** mock inoculum, using a volume equal to the highest volume used for the AAV vectors. IL8 gene expression was determined by RT-qPCR at 3 hrs p.t. and normalized to glyceraldehyde-3-phosphate dehydrogenase (GAPDH) reference gene. The results are expressed as fold-increase over **(a)** PBS-MK- or **(b)** mock-treated cells. Each sample was applied in triplicate. One representative experiment out of three independent experiments is shown. Differences in relative IL8 levels between samples were assessed using ANOVA ( $p < 0.0001$ ) and subsequent Tukey *post hoc* test.

## 5.2 Establishment of episomal maintenance of AAV vectors

### 5.2.1 Colony forming assay

In this study we aimed at developing an AAV vector which is able to persist in proliferating cells as a replicating episome. For that purpose, the AAV vector genome was equipped with a 2 kb S/MAR element derived from the 5' region of the human  $\beta$ -interferon gene.<sup>225</sup> Therefore, a bicistronic AAV vector plasmid pAAV-S/MAR encoding eGFP and a blasticidin resistance gene (BSD) containing the S/MAR element flanked by AAV2 ITRs, (Figure 15a) was constructed by Claudia Hagedorn (University Witten/Herdecke) and used for producing AAV-S/MAR. As a control vector genome, plasmid pAAV- $\Delta$ S/MAR containing the same TEC as pAAV-S/MAR but lacking the S/MAR sequence (Figure 15 b) was packaged as AAV- $\Delta$ S/MAR.

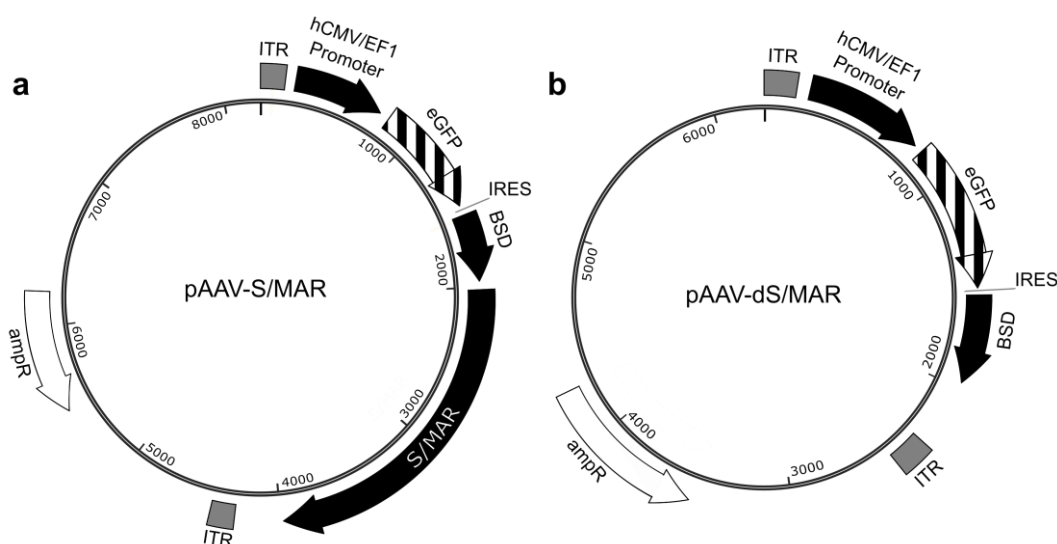


**Figure 15 Plasmid maps of pAAV-S/MAR and pAAV- $\Delta$ S/MAR.** (a) vector plasmid pAAV-S/MAR containing a TEC encoding for eGFP and blasticidin resistance gene (BSD), separated by an internal ribosomal entry site (IRES) and the S/MAR element derived from the human  $\beta$ -interferon gene. (b) vector plasmid pAAV- $\Delta$ S/MAR containing all elements of pAAV-S/MAR but the S/MAR sequence. Both plasmids were cloned by Claudia Hagedorn, University Witten/Herdecke.

HeLa cells were transduced with AAV-S/MAR or AAV- $\Delta$ S/MAR at a GOI of 1000. Twenty-four hrs p.t. transduced cells were sorted for transgene expression and  $10^5$  eGFP-expressing cells of the respective vector were seeded into cell culture flasks. The cells were cultured further and split regularly. Soon after initiation of the experiment, the eGFP gene expression of cells declined to the level of non-transduced cells ( $\leq 1\%$ , Figure 16)

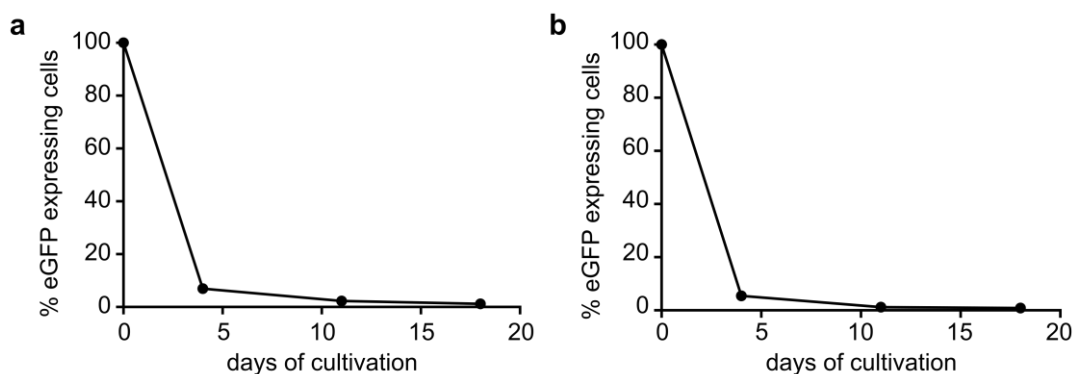


**Figure 16 Cultivation of AAV-S/MAR and AAV-ΔS/MAR-transduced cells in absence of selection.** HeLa cells were transduced with (a) AAV-S/MAR and (b) AAV-ΔS/MAR at a GOI of 1000. 24 hrs p.t. cells were sorted and  $10^5$  eGFP-positive cells were seeded in 25 cm<sup>2</sup> flasks. Cells were cultured in normal cell culture medium without adding the selection antibiotic blasticidin and measured for eGFP gene expression at indicated time points. Data points represent mean of triplicates.

Therefore we performed colony forming assays in which we employed selection pressure to select for cells stably maintaining the vector genome. HeLa cells were transduced with either AAV-S/MAR or AAV-ΔS/MAR at a GOI of 5000. Twenty-four hrs p.t. the percentage of transduced cells was determined by measuring eGFP by flow cytometry. Subsequently, the cell suspension consisting of a mixture of eGFP<sup>+</sup> and eGFP<sup>-</sup> cells was seeded to contain  $10^5$  eGFP<sup>+</sup> cells per dish. Selection for cells which maintained the vector genome was initiated 24 hrs after re-seeding, by addition of blasticidin to the culture medium. An optimized blasticidin concentration of 2 μg per ml cell medium, to be raised to 2.5 μg/ml with the next medium exchange, was determined in preliminary experiments. Using these concentrations, non-transduced HeLa cells were killed within one week. After three to four weeks of selection, the surviving colonies were quantified by C. Hagedorn using imaging software. We found that HeLa cells transduced with AAV-S/MAR resulted in a significantly higher number of blasticidin-resistant colonies compared to cells treated with control AAV-ΔS/MAR (Figure 17; Experiment 1: AAV-S/MAR  $66 \pm 25$ , AAV-ΔS/MAR  $12 \pm 6$ ,  $p=0.0013$ ,  $n=5$ ; Experiment 2: AAV-S/MAR  $291 \pm 82$ , AAV-ΔS/MAR  $114 \pm 89$ ,  $p=0.011$ ,  $n=5$ ). However, when cells were sorted for eGFP expression prior to selection, to seed only those cells which were successfully transduced by the respective AAV vector, no significant difference in colony formation could be observed after selection (Figure 17; Experiment 3: AAV-S/MAR  $27 \pm 28$ , AAV-ΔS/MAR  $23 \pm 22$   $p=0.75$ ).

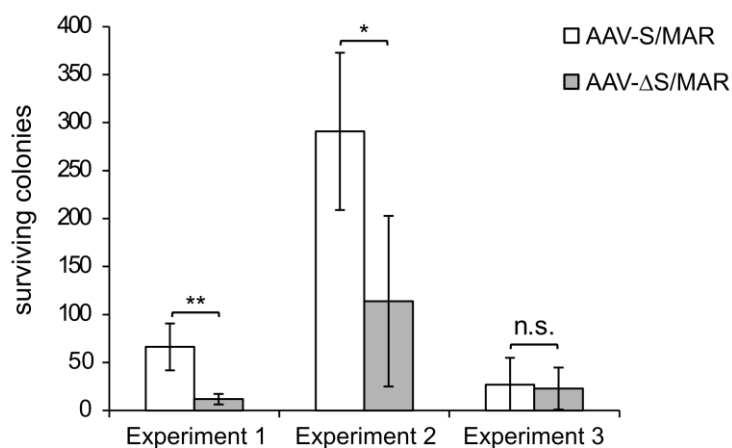


**Figure 17 Colony count of blasticidin-resistant cells.** HeLa cells were transduced with AAV2-SMAR or AAV-ΔS/MAR at a GOI of 5000. 24h p.t.  $10^5$  eGFP<sup>+</sup> cells were seeded into 15cm<sup>2</sup> dishes or 150 cm<sup>2</sup> flasks. For Experiment 1 and 2 a mixed suspension of eGFP<sup>+</sup> and eGFP<sup>-</sup> was seeded to contain  $10^5$  eGFP<sup>+</sup> cells per dish. For Experiment 3, cells expressing high levels and low levels of eGFP expression were sorted separately in 15 cm<sup>2</sup> dishes. 24 hrs after seeding, blasticidin was added at a concentration of 2 μg/mL and, with the next medium change, increased to 2.5 μg/ml. After 3 to 4 weeks of selection, the cells on plates or flasks were fixed and stained with crystal violet. Cell colonies were quantified and analyzed by C. Hagedorn. Experiment 1: \*\* p = 0.0013, Experiment 2: \* p = 0.011.

## 5.2.2 Mitotic stability of AAV-S/MAR vector genomes in HeLa cells

AAV-S/MAR-derived HeLa cell colonies from two independent experiments were picked and analyzed for eGFP expression. Of a total of 18 colonies, 14 were highly positive for eGFP (> 96 % eGFP gene expression, mean fluorescence intensity (MFI) > 841, Figure 18).

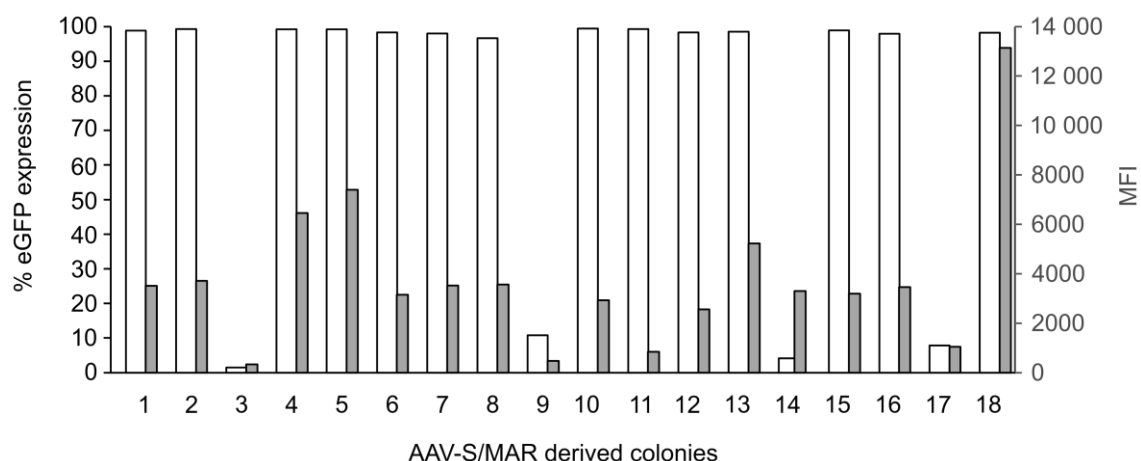


**Figure 18 Transgene expression of AAV-S/MAR-derived colonies.** After performing colony forming assays as described in chapter 5.2.1, colonies were picked from the dishes. At the same day or up to 10 days after picking, colonies were analyzed by flow cytometry for eGFP expression (white bars) and mean fluorescence intensity (MFI) (grey bars).

Seven eGFP<sup>+</sup> colonies were cultivated further in absence of selection pressure. Over a time span of up to 70 days the eGFP expression remained stable at high levels (Figure 19).

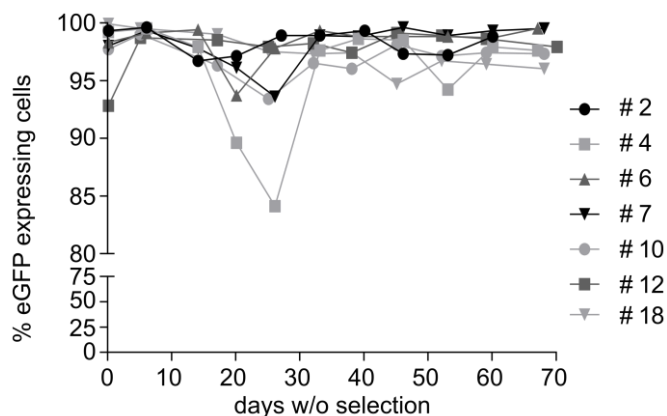


**Figure 19 Long-term transgene expression of AAV-S/MAR-derived colonies in absence of selection.** Picked colonies were cultivated further without addition of blasticidin. eGFP expression was measured by FACS analysis at indicated time points.

To determine whether this mitotic stability was a result of episomal maintenance or integration of vector genomes, Southern blot analyses were then performed by C. Hagedorn. For that purpose cellular DNA was isolated, digested with a single-cut restriction enzyme and probed for the presence of the CMV-eGFP-IRES-BSD cassette. For colonies #2, #4, #6 and #12 a 4.6 kb band was detected (Figure 20), indicative for either a single circular episome, or a head-to-tail concatemer (see scheme in Figure 20). The colonies #7, #10 and #18 showed bands at 7.9 kb, indicative for tail-to-tail or head-to-head-concatemers. Integration of vector genomes, which would be expected to result in multiple bands on the Southern Blot<sup>235</sup> was not observed.

To investigate the vector genome status of eGFP-negative colonies, colony #3 (see Figure 18) was included in the Southern Blot analysis and showed no signal for the vector genome (Figure 20). In line, qPCR analysis of cells of colony #3 did not show an eGFP-specific signal. Thus, some HeLa cells which were not transduced or had lost the vector genome were capable of spontaneously developing a resistance toward the selection antibiotic blasticidin.

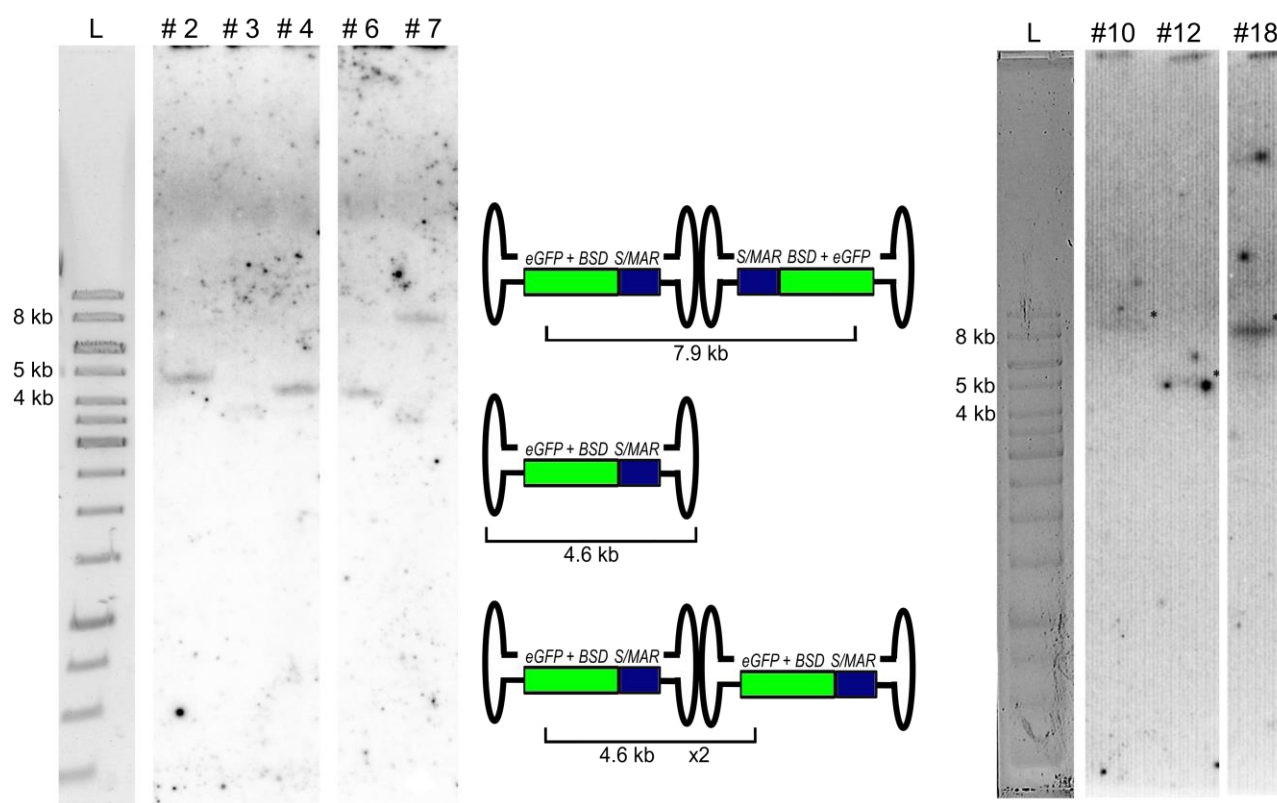


**Figure 20 Episomal maintenance of AAV-S/MAR vector genomes in HeLa cells (I).** Southern blot analyses of colonies of Figure 19. Asterisks indicate the positions of bands. Schematic depiction shows the expected bands of a single vector genome and head-to-tail and head-to-head/tail-to-tail concatemers. Southern Blot analyses were conducted by C. Hagedorn. Images were kindly provided by C. Hagedorn.

The episomal status of AAV-S/MAR vector genomes was confirmed by fluorescence *in situ* hybridization (FISH) on metaphase spreads of these colonies, conducted by C. Hagedorn. This method enables detection of even rare integration signals on both sister chromatids, whereas a signal on only one of the sister chromatid indicates an episomal association with the host chromosome.<sup>236</sup> For each clone, at least three different metaphase plates were analyzed. FISH analyzes confirmed the episomal status of AAV-S/MAR vector genomes in the analyzed colonies (Figure 21) and enabled estimation of an average of 1-2 vector genomes per cell, (C. Hagedorn, personal communication) which was confirmed by qPCR analysis of colonies #4, #6 and #7 (eGFP vector genomes vs. PLAT reference gene).

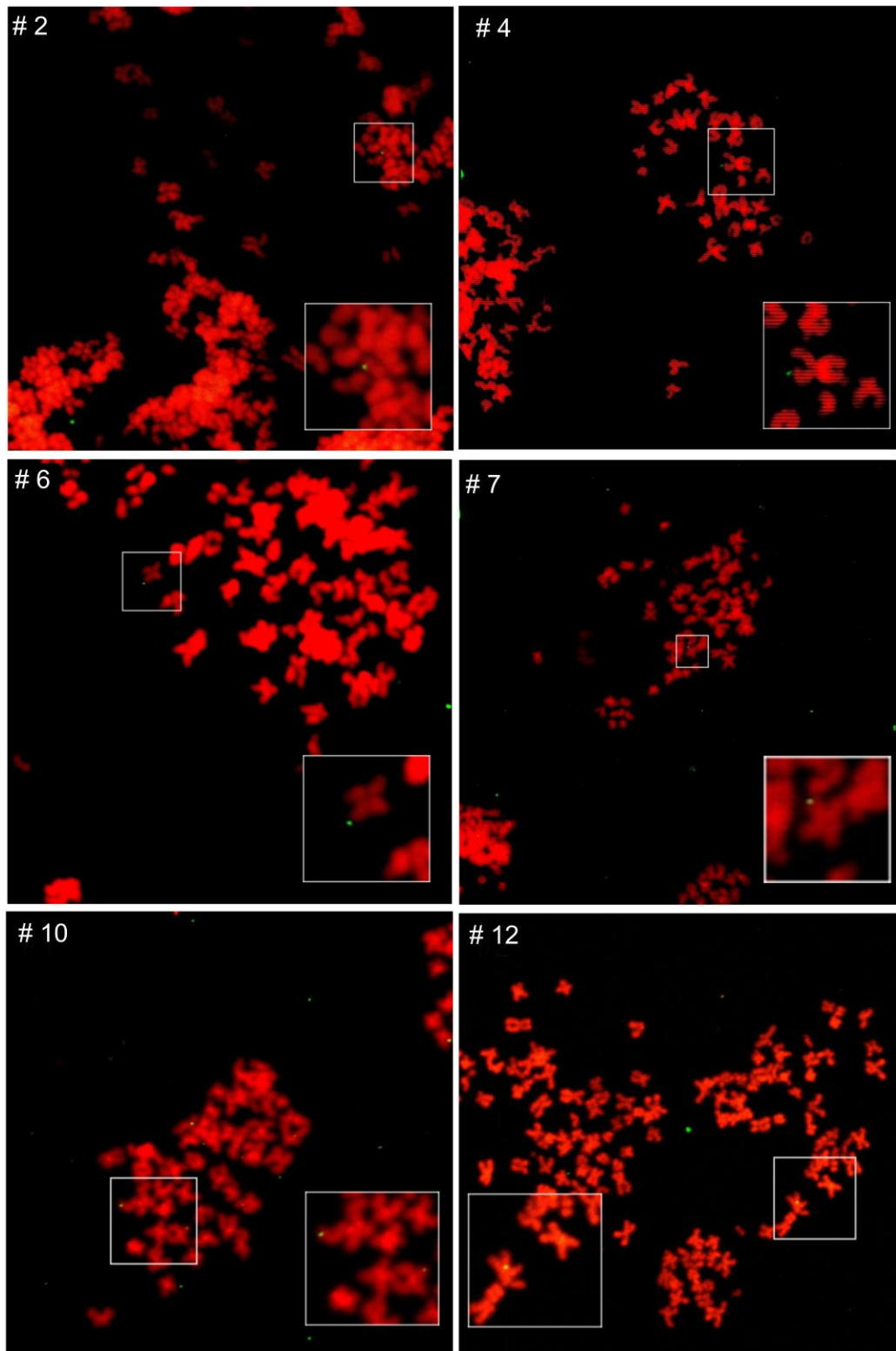


**Figure 21 Episomal maintenance of AAV-S/MAR vector genomes in HeLa cells (II).** FISH analyses on metaphase chromosomes of colonies of Figure 19. Green dots represent AAV-S/MAR vector genomes. White boxes show an image enlargement. Representative images are shown. FISH analyses were conducted by C. Hagedorn. Images were kindly provided by C. Hagedorn.

### 5.2.3 Mitotic stability of AAV- $\Delta$ S/MAR vector genomes in HeLa cells

As described for AAV-S/MAR, we also picked blasticidin-resistant cell colonies derived from cells transduced with control vector AAV- $\Delta$ S/MAR and measured their eGFP expression. Of 14 colonies from two independent experiments, cells of 7 colonies were eGFP-positive, with 6 colonies being highly positive for eGFP (> 94 % eGFP gene expression, MFI > 3262, Figure 22)

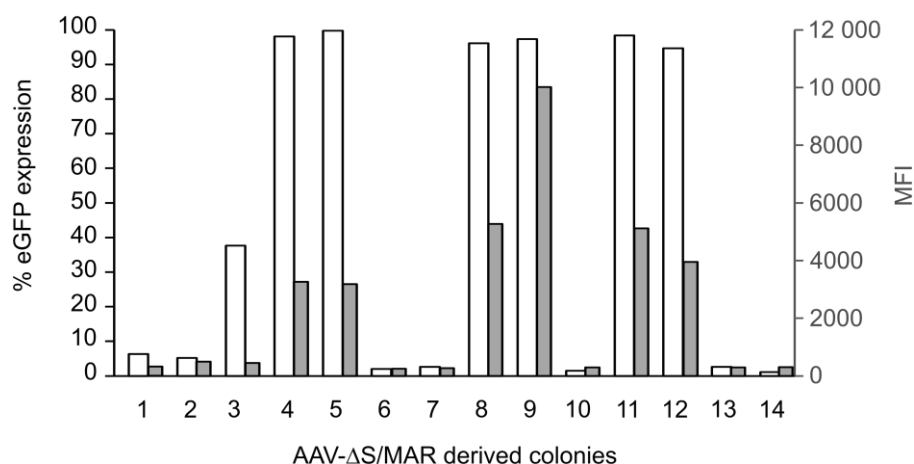


**Figure 22 Transgene expression of AAV- $\Delta$ S/MAR-derived colonies.** After performing colony forming assays as described in chapter 5.2.1, colonies were picked from the dishes. At the same day or 5 days after picking colonies were analyzed by flow cytometry for eGFP expression (white bars) and MFI (grey bars).

Similar to AAV-S/MAR-derived colonies, eGFP-positive AAV- $\Delta$ S/MAR-derived colonies also maintained long-term high-level eGFP expression after further cultivation in absence of selection pressure (Figure 23).

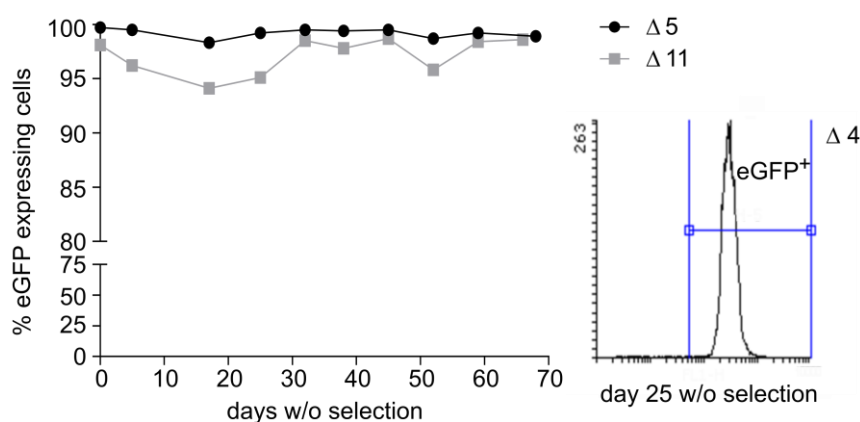


**Figure 23 Long-term transgene expression of AAV- $\Delta$ S/MAR-derived colonies in absence of selection.** Picked colonies of colony forming experiments were cultivated further in absence of selection pressure. eGFP expression was measured by FACS analysis at indicated time points.

Accordingly, the same analyses for vector genome status as described above were then conducted by C. Hagedorn. Southern Blot analyses showed episomal signals for eGFP<sup>+</sup> colonies as single circular episomes or head-to-tail concatemers (2.6 kb, colonies  $\Delta 4$  and  $\Delta 11$ , Figure 24) or head-to-head/tail-to-tail concatemers (4.8 kb, colony  $\Delta 5$ ). As was the case with the AAV-S/MAR colony #3 described above, one eGFP-negative colony which was analyzed in parallel gave no signal in the Southern Blot analysis ( $\Delta 1$ , Figure 24) and qPCR, although surviving blasticidin selection.

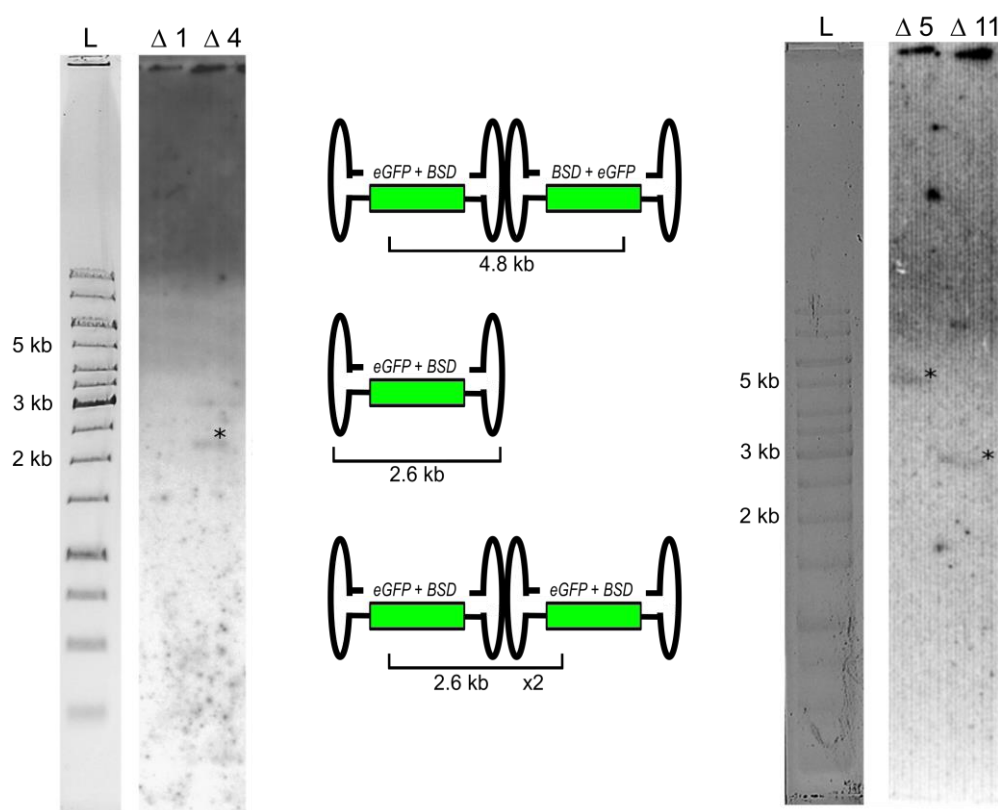


**Figure 24 Episomal maintenance of AAV- $\Delta$ S/MAR vector genomes in HeLa cells (I).** Southern blot analyses of colonies of Figure 23. Asterisks indicate the positions of bands. Schematic depiction shows the expected bands of a single vector genome and head-to-tail and head-to-head/tail-to-tail concatemers. Southern Blot analyses were conducted by C. Hagedorn. Images were kindly provided by C. Hagedorn.

Additionally, the cells were analyzed by FISH on metaphase spreads. This time, FISH on colony  $\Delta 11$  revealed rare integration signals (Figure 25, indicated by a white bracket) in addition to episomal signals, indicating that rare integration events occur in absence of S/MAR. For the other colonies, hybridization signals concur with solely episomal maintenance of vector genomes (Figure 25). Based on FISH analyses, an average of 3 AAV- $\Delta$ S/MAR genomes per cell was estimated (C. Hagedorn, personal communication). Summing up, we demonstrated that a standard AAV vector genome is maintained episomally in proliferating cells after an initial selection phase. By including an S/MAR element in the TEC cassette, the establishment frequency of stable episomes is increased.

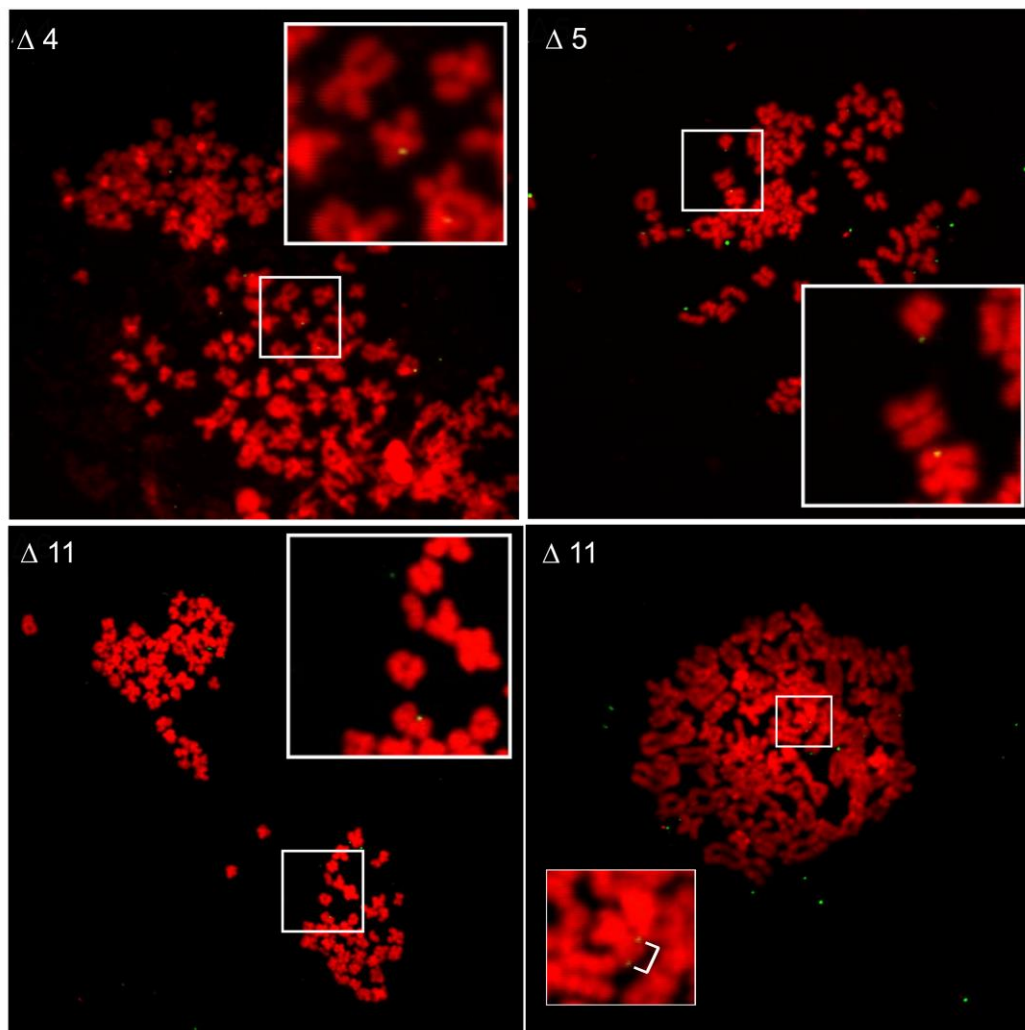


**Figure 25 Episomal maintenance of AAV- $\Delta$ S/MAR vector genomes in HeLa cells (II).** FISH analyses on metaphase chromosomes of colonies of Figure 23. Green dots represent AAV- $\Delta$ S/MAR vector genomes. White bracket indicates integrated vector genomes. White boxes show image enlargement. Representative images are shown. FISH analyses were conducted by C. Hagedorn. Images were kindly provided by C. Hagedorn.

## 6 Discussion

### 6.1 MC technology for AAV vector production

#### 6.1.1 Prokaryotic DNA is encapsidated during AAV vector production

AAV vectors are developed for *ex vivo* or *in vivo* gene therapy or to contribute to answering basic biological questions. In line with previous reports, we observed that AAV vector preparations produced by transient plasmid transfection of HEK293 cells contained DNA other than the intended TEC as genetic payload (Figure 6, <sup>116, 128, 141–143, 234</sup>). Benzonase protection assays conducted on purified vector preparations indicated that these DNA impurities are protected from nuclease digestion, pointing toward their encapsidation, or at least to a close enough association with the viral capsid to protect them from degradation. We detected up to 1.8 % of plasmid backbone sequences in our ssAAV vector preparations, which could not be removed by standard purification protocols (Figure 6). These values for prokaryotic DNA impurities, as well as those determined in the plasmid-derived vectors of the side-by-side comparison (up to 3.0 %, Table 3; 5.0 %, Table 7a) are within the range of those which have been reported (1-8 %) elsewhere for ssAAV.<sup>116, 141–143</sup> In contrast, we found that scAAV vector preparations, which are preferentially used for *in vivo* gene transfer and modification of primary cells,<sup>185</sup> contain a much higher amount of encapsidated prokaryotic sequences (up to 26.1 %, Figure 11; 38.4 %, Table 7). These plasmid backbone sequences are transferred *in vivo* upon administration of the vector preparations and are delivered into the target tissue, presumably with half-lives comparable to AAV vectors delivering the intended TEC.<sup>141</sup> Although Hauck and colleagues provided evidence that these sequences are not being transcribed,<sup>143</sup> it cannot be excluded that they trigger immune responses. The latter have been reported to limit long-term expression of TEC delivered by non-viral vectors.<sup>237, 238</sup> Furthermore, the long-term consequences of co-delivered antibiotic resistance genes cannot be predicted. Accordingly, it is highly desirable to remove or at least extensively reduce these elements in vector preparations. As removal of prokaryotic DNA impurities from a vector preparation appears impossible once the packaging has occurred, we employed vector production by MCs as a strategy that precludes packaging of these sequences in the first place.

#### 6.1.2 Comparison of plasmid and MC-derived AAV vector preparations

The MC technology was implemented to remove antibiotic resistance genes and other functional prokaryotic sequences from therapeutic non-viral vectors.<sup>212–215</sup> Due to their significantly reduced size compared to plasmids and the absence of CpG motifs, MCs achieve an increased transgene expression level.<sup>211</sup> As they are considered as substantial improvement in non-viral vector technology they are currently employed in a number of *in vivo* studies.<sup>239</sup> Both the vector plasmids for ssAAV and

scAAV vector genomes and the combined AAV/Ad helper plasmid (Figure 7, Figure 10) were generated as MCs by PlasmidFactory. A side-by-side comparison revealed that MC constructs are at least as potent as plasmids in AAV vector production: for both ssAAV and scAAV vector production, each component of the standard dual plasmid system could be replaced by a MC without impairing total genomic particle yield, capsid titer and composition and genomic titer (Table 1, Figure 8, Table 2, Table 5, Table 6). Further, both MC- and plasmid-based ssAAV and scAAV vector preparations contained packaged vector DNA of comparable size and homogeneity (Figure 12). Vectors produced by transfection of MC.AAV-ssGFP or MC.AAVscGFP and either helper (MC.DP2rs or pDP2rs) yielded preparations in which packaging of functional prokaryotic sequences was significantly reduced or even avoided, and thus in preparations with improved packaging efficiency compared to the dual plasmid system (Table 1, Table 5). Furthermore, regarding transducing titers and transduction efficiency, MC.AAV-ssGFP-based vector preparations did not differ for the worse (Table 2), while MC.AAV-scGFP-based vector preparations significantly outperformed the vector preparations produced by standard dual plasmid transfection system (Table 6).

### 6.1.3 Model for packaging of prokaryotic sequences

Using the MC constructs as tools (Figure 9, Figure 11), we obtained data supporting Chadeuf and coworkers, who provided evidence for the vector plasmid being the main source of antibiotic resistance gene sequences found in AAV vector preparations, while the helper plasmid contributes only to a minor extent.<sup>141</sup> To better understand what causes the packaging of plasmid backbone sequence, we quantified our ssAAV preparations produced by the dual plasmid strategy for the presence of *ori* and *f1 ori* located in the plasmid backbone neighboring either ITR (Figure 7a). We found that *f1 ori* and *pUC ori* are present in AAV vector preparations to a similar extent as *ampR* (Table 3). Thus, it is unlikely that a specific sequence contained in *ampR* fosters its encapsidation. The more intriguing explanation would be that sequences of the plasmid backbone are being packaged by virtue of location in *cis* to the ITRs, as a side product during vector genome rescue/replication from a circular plasmid (see below). In line with this assumption, we observed that the SCAR also becomes encapsidated (Table 4). This sequence is the sole non-vector genome element in MC.AAV-ssGFP (Figure 7c). It does not contain a *Rep* binding site or functional element, but is surrounded by the two ITR sequences.

The ITR consists of palindromic sequences A-A', B-B', C-C' forming a HP structure and a single-stranded D sequence (Figure 26a, see Figure 1b for detailed sequence). Between the A segment and the D sequence resides AAV's origin of replication, the terminal resolution site (*trs*), which is recognized by the viral *Rep* proteins.<sup>240</sup> In order to replicate integrated AAV proviruses or – in case of vector production – to replicate AAV vector genomes provided on vector plasmids, viral/vector ge-

nome templates have to be rescued. The rescue process is postulated to be initiated by Rep-mediated nicking of one strand of the duplex DNA at the trs (Figure 26b).<sup>33, 36</sup> The partially single-stranded GC-rich palindromic sequence of the ITR then forms a T-shaped HP (Figure 26c) - stabilized by Rep binding to a Rep binding element (RBE') at the apex of the HP structure<sup>25</sup> - and serves as primer for genome replication. Replication initially ensues along the displaced strand. Upon reaching the 3'-end, Rep helicase activity resolves the duplex, which allows the newly synthesized ITR to fold upon itself and serve as primer for replication back into the AAV vector genome (Figure 26d). At the second ITR, the same event takes place, thus generating a single-stranded vector genome with intact ITRs that can serve as further template for viral/vector genome replication (Figure 26e).<sup>241</sup> If the trs of the second ITR is not nicked prior to arrival of the replication complex, replication continues beyond the ITR structures, thus producing a large vector genome-plasmid backbone molecule (Figure 26f). This duplex DNA molecule can be processed - again Rep-dependent - into two single-stranded DNA molecules,<sup>241</sup> none of which containing two fully intact ITRs. Specifically, the vector genome containing the TEC possesses one intact ITR and the D sequence of the second ITR, while the plasmid backbone sequence contains one ITR or, if replication covers the entire plasmid backbone, two ITRs, both without the D sequence (Figure 26g). The defective ITR of the vector genome can be repaired through a panhandle intermediate involving base pairing of the two D sequences flanking the vector genome by using the intact ITR as template (Figure 26h).<sup>242</sup>

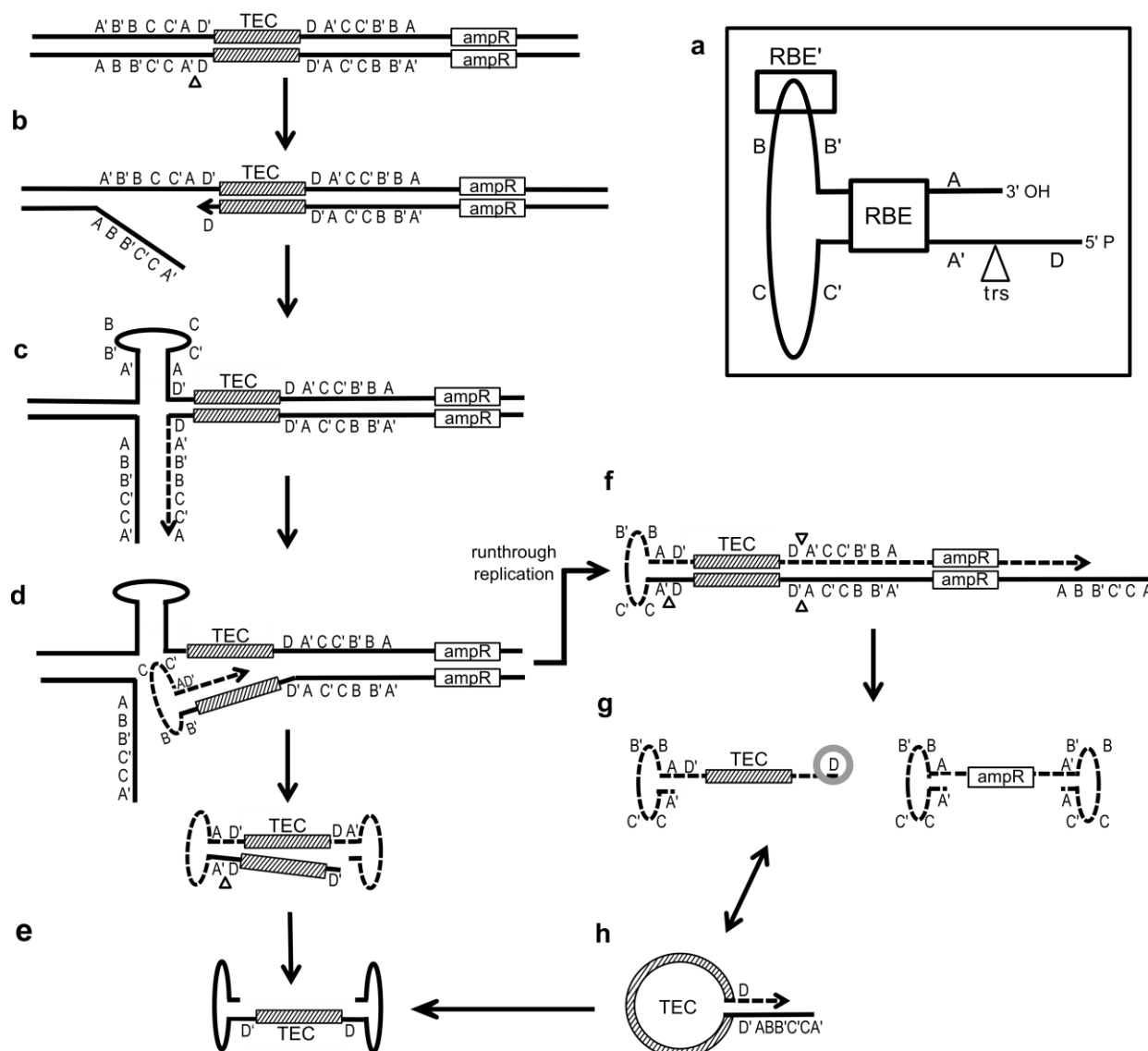


**Figure 26 Model of proposed rescue mechanism.** Circular plasmid genome is represented as linearized. **(a)** Schematic representation of AAV2 ITR. The triangle represents the nicking activity of Rep at the trs. **(b)** Rep nicks at trs and creates a single-strand break. **(c)** The template strand folds into a hairpin (HP) conformation thus enabling replication along the displaced strand. **(d)** The newly generated ITR folds into the HP conformation which allows for replication into the vector genome sequence. **(e)** Upon the nicking event at the trs of the second ITR, the single-stranded AAV vector genome is created. **(f)** If the second ITR is not nicked before the arrival of the replication machinery a large replicon encompassing TEC and backbone sequences is generated. **(g)** The TEC genome can be rescued by Rep nickase activity which then creates the TEC with one intact ITR and an additional D sequence and the prokaryotic backbone sequences with two ITRs lacking the D sequence. **(h)** The defect ITR of the TEC genome can be repaired by a panhandle mechanism, thus generating an intact AAV vector genome. RBE: Rep protein binding element, trs: terminal resolution site. Figure adapted from Ward et al.<sup>241</sup> and published in (Schnödt et al.).<sup>233</sup>

While the presence of one HP structure is sufficient to rescue AAV vector genomes and to induce replication, the efficiency of vector genome replication, and in particular, the packaging of vector genomes into viral capsids depends on the presence of the D sequence in *cis*.<sup>243, 244</sup> Based on the latter observation Wang and coworkers postulated the D sequence to function as actual packaging signal for AAV.<sup>244</sup> Thus, the presence of the D sequence - independent of the pathway followed for its pro-

duction (Figure 26) – is the likely reason for the so obviously preferred packaging of the TEC-containing vector genomes.<sup>243–245</sup>

To generate vector plasmids harboring scAAV vector genomes, the *trs*, including the D sequence, of the left ITR is deleted (Figure 5, Figure 10). Our data demonstrates that this modification of the ITR structure in pAAV-scGFP considerably increases the encapsidation of prokaryotic sequences (Figure 11). According to our model, this increase is the product of a run-through replication that occurs more frequently in scAAV compared to ssAAV vector production, as specific nicking of Rep at the *trs* of the mutated ITR cannot occur (Figure 26 f-h).

#### 6.1.4 DNA impurities in AAV vector preparations

Lecomte and coworkers quantified DNA impurities in a ssAAV vector preparation with next generation sequencing (NGS) and reported a clear ranking with vector plasmid backbone being the most frequent one (0.84–5.97 %), followed by the helper plasmid (0.01–0.08 %) and human genome sequences (0.04–0.30 %).<sup>142</sup> In line, we (Figure 9, Figure 11 and Table 3, Table 4) and others<sup>141</sup> observed a striking preference for backbone sequences derived from the vector plasmid or the corresponding MC construct. Yet, we also found specific DNA impurities stemming from the helper plasmid in our vector preparations (Table 7). Values for ssAAV vector preparations were comparable to those reported by Lecomte et al.<sup>142</sup> (dual plasmid preparation: 0.04–0.05 %, dual MC preparation: 0.02–0.03 %). Remarkably, scAAV vectors were found to contain, in addition to vector plasmid-derived sequences, more helper plasmid-specific sequences than ssAAV vectors (dual plasmid preparation: 0.24–0.31 %, dual MC preparation: 0.10–0.11 %). For ssAAV and even more so for scAAV vector preparations, MC-based vector preparations tended to contain lower amounts of DNA impurities compared to plasmid-based preparations, which may be another possible effect of an improved vector genome packaging when the vector plasmid is replaced by a vector MC. However, in contrast to Lecomte et al., we did not detect human genome sequences in our vector preparations (PLAT < LOQ for all tested vector preparations). This discrepancy may be accounted for by the differences in vector production and purification (IDGC vs. CsCl gradient ultracentrifugation or affinity chromatography) and analytical methodology (qPCR vs. NGS).<sup>142</sup>

According to the rescue model proposed above, plasmid backbone sequences of vector plasmids could become rescued and equipped with HP structures (Figure 26g). As Rep proteins bind to RBE' at the apex of the HP structure<sup>25</sup> as well as to the pores at the 5-fold symmetry axis of the capsid through which newly produced genomes are channeled,<sup>32, 53</sup> HP-flanked plasmid backbone containing sequences may become connected and eventually packaged. In support of this model Chadeuf and coworkers isolated ITR-plasmid junctions from AAV vector stocks and AAV-transduced tissue

that showed a preferential retention of the A region containing the RBS within the otherwise damaged ITRs. However, they also observed partially retained D-sequences, including the trs,<sup>141</sup> which argues for mechanisms other than those postulated in Figure 26 through which undesired DNA sequences additionally become equipped with signals that foster packaging.<sup>242, 246</sup> Such events may explain how DNA sequences other than those contained in the vector plasmid, such as helper plasmid sequences, become targets for encapsidation. Additionally, it is possible that the DNA binding and helicase activity of Rep leads to unspecific packaging events, even in absence of DNA replication.

### 6.1.5 Interaction of AAV vectors with the innate immune system

When confronted with foreign structure or pathogens, host organisms evoke various immune responses for protection. Recognition of evolutionary conserved pathogen-associated molecular patterns (PAMPs) by pathogen recognition receptors (PRRs) activates the innate immune system. In its course of action, secretion of cytokines and chemokines is induced, immune cells are recruited to the site of infection, the complement cascade is initiated and the highly specific adaptive immune system is activated and modulated. For AAV vectors, two members of the TLR family, TLR2 and TLR9, have been described as PRRs. TLR2 senses the AAV capsid in primary human liver cells (sinusoidal endothelial cells and Kupffer cells) and activated macrovascular endothelial cells from human umbilical veins.<sup>134</sup> TLR9, a sensor of unmethylated CpG motifs,<sup>220</sup> was reported to be activated by AAV vector genomes in murine and human plasmacytoid dendritic cells (pDC). *In vivo*, the TLR9-MyD88 pathway was found to be crucial for activation of CD8<sup>+</sup> T cell responses against both transgene and AAV capsid, which ultimately led to loss of transgene expression and generation of neutralizing antibodies against AAV vectors.<sup>218</sup> Remarkably, TLR9-dependent activation of innate immunity was reported to be increased if scAAV vectors were used.<sup>219</sup> To explain this phenomenon, two hypotheses were put forward. Firstly it was proposed that the capsids of scAAV vectors are less stable in the endosome, and thus prone to release the vector genome more readily, which exposes the latter to TLR9 sensing.<sup>219</sup> Secondly, the additional ITR sequence present in scAAV vector genomes (see Figure 5I) has been implicated.<sup>247</sup> This hypothesis is supported by the finding that adaptive immune responses are reduced when AAV vectors in which the TEC was depleted from CpG sequences were used.<sup>248</sup>

We wondered whether the reason for the higher immunogenicity of scAAV vectors may lie in their significantly increased content of prokaryotic DNA sequences. However, using two different assays *in vitro*, no TLR9 activation at all was observed upon transduction of a TLR9-expressing cell line with both ssAAV and scAAV vectors at a high GOI of 10<sup>5</sup> (Figure 13, Figure 14). While a TLR9 agonist showed strong and reproducible induction of TLR9-mediated SEAP and IL8 gene expression, AAV vectors with high or low content of prokaryotic sequences in plasmid- or MC-derived vector preparations, respectively, showed no increase over non- or mock-transduced cells. Previously our group

has shown a small (2-3-fold) but significant increase in TLR9 activation by scAAV vectors over mock-transduced cells *in vitro*, with TLR9 activation by a scAAV vector being in the range of activation by a TLR9 agonist.<sup>134</sup> In addition to differences in experimental setup (model cell lines HEK blue TLR9 vs. 293/TLR9, possible differences in vector dosage, different TLR9 agonists), the reason for the divergent findings regarding TLR9 activation may be the only very short and transient nature of TLR9 activation by AAV vectors,<sup>249, 250</sup> which might make detection and quantification *in vitro* very difficult. Possibly, a longer incubation time or a kinetic study spanning a range from 1 h to 20 hrs might elucidate this question. Interestingly, *in vivo* interaction of AAV vectors with TLR9 seems to be context-dependent, e.g. genetic background of mouse model, or i.v. vs. i.m. vector administration.<sup>218, 251</sup>

In the future, evaluation of MC- versus plasmid-derived AAV vectors in an animal model using established conditions may show more conclusively whether MC-derived AAV vectors, specifically those containing a self-complementary genome, are of lesser immunogenicity than plasmid-derived AAV vectors.

### 6.1.6 Challenges and chances of using MC for AAV vector production

As ampR signals in a low range remained detectable in some dual MC vector preparations (technical duplicate #2 in Figure 9: < 1000 particles over background; ssAAV vector in Table 7: < 2100 particles over background), we analyzed the MC preparations which were used for packaging using ampR-specific primers. While MC.ssGFP contained only marginal amounts of ampR-specific sequences (<0.0005 %, relative to TEC), we found ampR particles ranging from 0.03-5.35 % (relative to AAV *rep*) in different batches of MC.DP2rs. With exception of the SCAR sequence, which contains significantly less CpG and has been shown to be safe for *in vivo* applications<sup>211, 252</sup> MC constructs contain neither an antibiotic resistance gene sequence nor any other sequence that is not intended to be transferred. The identification of contaminating ampR sequences highlights the requirement of sophisticated production procedures including single-use material and preferably a dedicated facility to generate MC preparations free of any kind of contamination.

The second issue concerns the elaborate production process itself. Up-scaling of the MC production and purification to produce large batches of AAV vectors may present a challenge for the combined AAV/Ad helper constructs owing to their size and the high quantities required for vector production. This limitation, however, could be overcome by shifting to the triple transfection strategy, where AAV and Ad helper functions are provided on separate and thus smaller plasmids. MCs from these plasmids are smaller in size and, at least at present, easier to produce.

In overcoming these limitations, the MC technology offers an elegant and potent strategy to avoid unintended transfer of functional prokaryotic plasmid backbone sequences and may represent a key step in the development of safe AAV vectors for gene therapy in human patients.

## 6.2 Episomal maintenance of AAV vectors

Upon successful transduction of a target tissue, AAV vector genomes remain predominantly in an episomal state, as duplex DNA circles or concatemers.<sup>180, 200–203</sup> These episomal DNA forms mediate long-term transgene expression in post-mitotic tissues,<sup>189, 190, 202, 203, 205, 207–210</sup> but are diluted out by cell division in proliferating cells.<sup>189, 221, 222</sup> We therefore aimed at finding a strategy which would enable AAV vector genomes to persist episomally in dividing cells, i.e. an approach other than integration which establishes persistence of the vector genome and its distribution to the daughter cells during mitosis. For this purpose we incorporated an S/MAR sequences into the TEC cassette.

### 6.2.1 S/MAR-based vectors for gene therapy

S/MARs are specific genomic DNA segments which hook onto the nuclear matrix.<sup>223</sup> This attachment contributes to the spatial organization of the chromatin and the functional regulation of gene expression and replication. Due to these important structural and functional roles in the nucleus and the association of S/MARs with chromosomal origins of replication, researchers aimed to explore these sequences as auxiliary elements in plasmid vectors.<sup>253–255</sup>

Pioneer S/MAR plasmid vector pEPI combined a transcription unit containing GFP and a kanamycin resistance gene with a 2kb S/MAR derived from the 5' region of human  $\beta$ -interferon gene. After an initial antibiotic selection phase pEPI established itself as stable episome, mediated by the S/MAR sequence. Episomal pEPI was retained *in vitro* over hundreds of generations in the absence of selection.<sup>225</sup> Subsequently, second generation plasmid vector pEPito was developed as promoter-optimized and CpG-depleted improved version of pEPI, and achieved higher transgene expression *in vitro* and more prolonged gene expression *in vivo*.<sup>256</sup> Due to the success of pEPI and its derivatives, S/MAR elements are routinely included in plasmid vectors for gene therapeutic applications.<sup>254, 255</sup>

Aiming to combine the nuclear persistence mediated by S/MARs with the efficiency of viral delivery, hybrid vector systems were developed. Voigtlander and colleagues designed a two-vector system based on high capacity adenoviral vectors (HCAAdV): HCAAdV-pEPito-FRT<sup>2</sup> contained the pEPito plasmid sequence whereas HCAAdV-FLPe delivered the FLPe recombinase. Upon co-transduction, the FLPe recombinase excises and circularizes the pEPito-based replicon. Using this co-delivery strategy, episomal maintenance of the replicon for six months *in vivo* could be achieved.<sup>257</sup> Further-

more, Verghese and colleagues inserted the pEPI/pEPito S/MAR sequence into a non-integrating lentiviral vector to stabilize the episomal DNA circles formed via the vector's long terminal repeats. The thus generated anchored non-integrating lentiviral vector (aniLV) established episomes in HEK293T cells which were stable for more than a hundred cell divisions without the requirement of an initial selection. Additionally, aniLV was able to modify murine hematopoietic progenitor cells *in vitro* and *in vivo* for up to 10 weeks.<sup>258</sup>

### 6.2.2 Episomal AAV-S/MAR and AAV- $\Delta$ S/MAR vector genomes

The aim of this study was to investigate whether the S/MAR technology, which has been successfully applied for plasmid vectors and other viral vectors, could be harnessed to generate episomally persistent AAV vector genomes in dividing cells. For that purpose an AAV vector was packaged with the gene expression cassette of pEPito (eGFP-IRES-BSD-S/MAR),<sup>256</sup> in parallel with an AAV vector containing the same TEC but without the S/MAR sequence (Figure 15).

Both vectors were transduced into highly proliferative HeLa cells. Antibiotic selection pressure was applied to select for cells which stably maintained the AAV vector genome. When cells of a mixed population, that is, in a mixture of transduced and non-transduced cells were seeded and selected, AAV-S/MAR-transduced cells yielded higher colony forming numbers than AAV- $\Delta$ S/MAR-transduced cells (Figure 17). However, when cells were sorted using flow cytometry so that only successfully transduced cells underwent the selection process, no difference in colony forming numbers between the two vectors was observed. This finding suggests an establishment advantage of AAV-S/MAR in a competing environment with non-transduced cells over the control vector.

Colonies surviving the selection were picked and cultivated further in the absence of selection. For both vectors, cells derived from colonies which were highly eGFP-positive after ending selection maintained high transgene expression levels over a time span of up to 70 days, even in absence of selection pressure (Figure 19, Figure 23). Some colonies, however, which had survived antibiotic selection did not contain the vector genome at the end of the selection phase (Figure 18, Figure 22) pointing to development of spontaneous resistance toward the selection antibiotic. While this phenomenon has been observed before in HeLa cells treated with other selection antibiotics,<sup>259</sup> it is remarkable that colonies derived from AAV-S/MAR transduction seemed to have a higher likelihood of actually maintaining the vector genome, compared to colonies derived from AAV- $\Delta$ S/MAR: Only 4 out of 18 S/MAR-derived colonies surviving selection were negative for eGFP expression (approximately one fourth of colonies, Figure 18), while half of the picked  $\Delta$ S/MAR-derived colonies were eGFP-negative (7 out of 14, Figure 22). Taking this into account, the colony forming assay might be slightly

biased against AAV-S/MAR-derived colonies, with the true colony forming ability being more in favor of AAV-S/MAR-transduced cells.

For eGFP<sup>+</sup> colonies derived from AAV-S/MAR transduction, both Southern Blot and FISH analyses demonstrated episomal maintenance of the vector genome (Figure 20, Figure 21). Surprisingly, we found that the mitotic stability of eGFP<sup>+</sup> colonies derived from the control vector AAV-ΔS/MAR was also predominantly a result of episomal maintenance (Figure 24, Figure 25), with only one of the AAV-ΔS/MAR-derived colonies containing integrated vector genomes. This finding is all the more surprising as previous studies commonly employed antibiotic selection to induce AAV vector genome integration *in vitro*.<sup>30, 179, 260</sup> The protocols employed by the former studies differ from our approach as they used a rather high selection pressure, while we used only moderate concentrations of antibiotic (up to 2.5 μg/mL blasticidin, 4-fold less than the manufacturer recommends for selection of HeLa cells). Under these conditions, AAV vector genomes were capable to establish stable episomes, with the S/MAR sequence increasing the frequency of the event.

### 6.2.3 Conditions for establishment of stable AAV vector episomes

Kymäläinen and colleagues have tried before to combine AAV vectors and S/MAR, using a truncated version of the β-interferon S/MAR sequence. Yet, neither this AAV-S/MAR hybrid nor an AAV vector lacking the S/MAR achieved stable establishment *in vitro*, and rAAV-transduced cells were lost with cell proliferation.<sup>261</sup> As a key difference to our work, no antibiotic selection was employed in the former study.

In our setting the selection pressure can potentially serve two purposes. Firstly, the initial antibiotic selection conveys the survival advantage to transduced cells in a competing environment with non-transduced cells. This survival advantage is crucial in the context of plasmid-based S/MAR vectors where antibiotic selection compensates for the low establishment efficiencies of the plasmid episomes.<sup>262, 263</sup> Likewise, when transduced HeLa cells were cultured in absence of selection pressure, non-transduced cells and/or cells which had lost the vector genome rapidly overgrew cells which maintained the vector genome (Figure 16). Once established both plasmid-based S/MAR vectors and AAV-S/MAR are stably maintained in the absence of selection. Episomal maintenance in dividing cells requires constant replication and distribution during mitosis. To date, pEPI is the only S/MAR-based vector system which was examined regarding the mechanisms behind these processes. Upon establishment pEPI is associated with highly transcribed nuclear domains and early replicating chromatin.<sup>262</sup> Replication of pEPI occurs in synchrony with these foci,<sup>262</sup> once per cell cycle in a semiconservative fashion, with the origin recognition complex assembling at various regions of the vector.<sup>226</sup> By interacting with the nuclear matrix protein scaffold attachment factor A (SAF-A) the plasmid episome is able to co-segregate with the chromosomes during mitotic division.<sup>262, 264</sup> Although it remains

to be shown whether these processes also occur when the S/MAR sequence is combined with an AAV vector, it is possible that the S/MAR element mediates replication and segregation of episomal AAV-S/MAR vector genomes in the same manner.

Surprisingly, we observed long-term episomal maintenance not only for AAV-S/MAR but also for AAV- $\Delta$ S/MAR vector genomes. Most likely this is mediated by the ITRs, the only viral elements remaining in the vector genome. The ITRs serve as origins of replication, but usually require AAV Rep proteins and helper viral functions.<sup>265–268</sup> Under specific conditions, however, no viral gene products are required. Thus, Yalkinoglu and colleagues reported on replication of isolated ITR sequences in carcinogen-treated mammalian cells in absence of AAV Rep and helper virus proteins.<sup>269</sup> Mild selection pressure, as employed in our study, might create similar cellular conditions as treatment with genotoxic agents.

Therefore, antibiotic selection pressure may serve the additional or alternative purpose of altering the cellular environment to facilitate episomal maintenance of AAV vectors independent of an S/MAR unit.

Further another explanation for episomal maintenance of “common” AAV vectors is conceivable; as described in chapter 1.1.3, genotoxic treatment supports wtAAV replication in absence of a helper virus. Moreover, in absence of both helper virus functions and genotoxic agents Yakobson and colleagues detected wtDNA synthesis in 0.1 % of cells which were synchronized by mitotic detachment.<sup>93</sup> Based on this observation, Peter Ward hypothesized that a small fraction of a cell population, which is for example in a specific transient state such as repairing DNA, is able to synthesize AAV DNA. If this is the case, genotoxic treatment might support AAV replication by increasing the percentage of cells in this specific state.<sup>270</sup> The notion that the antibiotic treatment, in analogy to the process proposed above for genotoxic treatment, might have enriched a sub-species of cells which are capable of low but constant replication of AAV vector genomes, is quite fascinating. However, as the described study by Yakobson et al. was conducted with wtAAV not with AAV vectors, the findings thereof cannot be readily extrapolated.

#### 6.2.4 Outlook

Further work should firstly aim to elucidate the mechanisms underlying episomal maintenance of AAV vectors with and without the S/MAR sequence and secondly advance the development and optimization of S/MAR-based AAV vectors.

In investigating the mechanisms one essential question is whether antibiotic selection assures the survival advantage of the small number of cells which are capable of replicating the AAV vector genome (with or without S/MAR), or whether antibiotic treatment actually creates the conditions for

AAV's episomal maintenance. To examine this question, transduced cells could be cultivated for longer time periods without selection pressure. Using flow cytometric sorting, cells expressing the vector genome could be enriched repeatedly. If this approach ultimately leads to the isolation of a cell population which maintains constant transgene expression, the hypothesis that selection pressure compensates for the low establishment efficiency of the AAV vector episome would be supported. To identify cellular factors contributing to the occurring processes AAV-S/MAR and AAV- $\Delta$ S/MAR could be tested in cell lines containing knockouts in DDR enzymes which were implicated in AAV vector genome circularization which is essential for episome formation, such as DNA-PKcs, members of the MRN complex or ATM (see chapter 1.3.3.3).

As next step toward developing AAV-S/MAR as a gene therapy vector, a self-complementary AAV-S/MAR could be generated and tested. Since the S/MAR used in this study is too large for packaging in a self-complementary vector genome cassette (coding capacity ca. 2.3 kb), a smaller S/MAR element<sup>271</sup> would have to be incorporated and tested.

## 7 References

1. Tijssen P, Agbandje-McKenna M, Almendral JM, Bergoin M, Flegel TW, Hedman K *et al.* (2011) in *Virus taxonomy. Ninth report of the International Committee on Taxonomy of Viruses*, ed King A. (Elsevier, Oxford), p. 405–425.
2. Atchison RW, Casto BC and Hammon WM (1965). Adenovirus-Associated Defective Virus Particles. *Science* **149**: 754–755.
3. Buller RM, Janik JE, Sebring ED and Rose JA (1981). Herpes simplex virus types 1 and 2 completely help adenovirus-associated virus replication. *J Virol* **40**: 241–247.
4. Richardson WD and Westphal H (1981). A cascade of adenovirus early functions is required for expression of adeno-associated virus. *Cell* **27**: 133–141.
5. Georg-Fries B, Biederlack S, Wolf J and Zur Hausen H (1984). Analysis of proteins, helper dependence, and seroepidemiology of a new human parvovirus. *Virology* **134**: 64–71.
6. Walz C, Deprez A, Dupressoir T, Dürst M, Rabreau M and Schlehofer JR (1997). Interaction of human papillomavirus type 16 and adeno-associated virus type 2 co-infecting human cervical epithelium. *J Gen Virol* **78 ( Pt 6)**: 1441–1452.
7. Mayor HD, Jamison RM, Jordan LE and Melnick JL (1965). Structure and Composition of a Small Particle Prepared from a Simian Adenovirus. *J Bacteriol* **90**: 235–242.
8. Asokan A, Schaffer DV and Samulski RJ (2012). The AAV vector toolkit: poised at the clinical crossroads. *Mol Ther* **20**: 699–708.
9. Gao G, Vandenberghe LH, Alvira MR, Lu Y, Calcedo R, Zhou X *et al.* (2004). Clades of Adeno-associated viruses are widely disseminated in human tissues. *J Virol* **78**: 6381–6388.
10. Moskalkenko M, Chen L, van Roey M, Donahue BA, Snyder RO, McArthur JG *et al.* (2000). Epitope mapping of human anti-adeno-associated virus type 2 neutralizing antibodies: implications for gene therapy and virus structure. *J Virol* **74**: 1761–1766.
11. Boutin S, Monteilhet V, Veron P, Leborgne C, Benveniste O, Montus MF *et al.* (2010). Prevalence of serum IgG and neutralizing factors against adeno-associated virus (AAV) types 1, 2, 5, 6, 8, and 9 in the healthy population: implications for gene therapy using AAV vectors. *Hum Gene Ther* **21**: 704–712.
12. Pereira CC, de Freitas, Luciana Bueno, de Vargas, Paulo Roberto Merçon, de Azevedo, Maria Luiza Borges, do Nascimento, Jussara Pereira and Spano LC (2010). Molecular detection of

- adeno-associated virus in cases of spontaneous and intentional human abortion. *J Med Virol* **82**: 1689–1693.
13. Kerr JR and Linden RM (2006) in *Parvoviruses*, ed Kerr JR. (Hodder Arnold; Distributed in the U.S.A. by Oxford University Press, London, New York), p. 381–385.
  14. Nault J-C, Datta S, Imbeaud S, Franconi A, Mallet M, Couchy G *et al.* (2015). Recurrent AAV2-related insertional mutagenesis in human hepatocellular carcinomas. *Nat Genet* **47**: 1187–1193.
  15. Berns KI, Byrne BJ, Flotte TR, Gao G, Hauswirth WW, Herzog RW *et al.* (2015). Adeno-Associated Virus Type 2 and Hepatocellular Carcinoma? *Hum Gene Ther* **26**: 779–781.
  16. Büning H and Schmidt M (2015). Adeno-associated Vector Toxicity-To Be or Not to Be? *Mol Ther* **23**: 1673–1675.
  17. Schmidt M, Gil-Farina I and Büning H (2016). Reply to "Wild-type AAV Insertions in Hepatocellular Carcinoma Do Not Inform Debate Over Genotoxicity Risk of Vectorized AAV". *Mol Ther* **24**: 661–662.
  18. Timpe JM, Verrill KC and Trempe JP (2006). Effects of adeno-associated virus on adenovirus replication and gene expression during coinfection. *J Virol* **80**: 7807–7815.
  19. Stutika C, Gogol-Döring A, Botschen L, Mietzsch M, Weger S, Feldkamp M *et al.* (2015). A Comprehensive RNA Sequencing Analysis of the Adeno-Associated Virus (AAV) Type 2 Transcriptome Reveals Novel AAV Transcripts, Splice Variants, and Derived Proteins. *J Virol* **90**: 1278–1289.
  20. Bowles DE, Rabinowitz JE and Samulski RJ (2006) in *Parvoviruses*, ed Kerr JR. (Hodder Arnold; Distributed in the U.S.A. by Oxford University Press, London, New York), p. 15 - 23.
  21. Srivastava A, Lusby EW and Berns KI (1983). Nucleotide sequence and organization of the adeno-associated virus 2 genome. *J Virol* **45**: 555–564.
  22. Sonntag F, Schmidt K and Kleinschmidt JA (2010). A viral assembly factor promotes AAV2 capsid formation in the nucleolus. *Proc Natl Acad Sci U S A* **107**: 10220–10225.
  23. McCarty DM, Ryan JH, Zolotukhin S, Zhou X and Muzyczka N (1994). Interaction of the adeno-associated virus Rep protein with a sequence within the A palindrome of the viral terminal repeat. *Journal of Virology* **68**: 4998–5006.
  24. Chiorini JA, Wiener SM, Owens RA, Kyostio SR, Kotin RM and Safer B (1994). Sequence requirements for stable binding and function of Rep68 on the adeno-associated virus type 2 inverted terminal repeats. *Journal of Virology* **68**: 7448–7457.

25. Ryan JH, Zolotukhin S and Muzyczka N (1996). Sequence requirements for binding of Rep68 to the adeno-associated virus terminal repeats. *J Virol* **70**: 1542–1553.
26. Zuker M (2003). Mfold web server for nucleic acid folding and hybridization prediction. *Nucleic Acids Res.* **31**: 3406–3415.
27. Lusby E, Fife KH and Berns KI (1980). Nucleotide sequence of the inverted terminal repetition in adeno-associated virus DNA. *Journal of Virology* **34**: 402–409.
28. Snyder RO, Samulski RJ and Muzyczka N (1990). In vitro resolution of covalently joined AAV chromosome ends. *Cell* **60**: 105–113.
29. Straus SE, Sebring ED and Rose JA (1976). Concatemers of alternating plus and minus strands are intermediates in adenovirus-associated virus DNA synthesis. *Proc Natl Acad Sci U S A* **73**: 742–746.
30. McLaughlin SK, Collis P, Hermonat PL and Muzyczka N (1988). Adeno-associated virus general transduction vectors: analysis of proviral structures. *J Virol* **62**: 1963–1973.
31. Linden RM, Winocour E and Berns KI (1996). The recombination signals for adeno-associated virus site-specific integration. *Proc Natl Acad Sci U S A* **93**: 7966–7972.
32. King JA, Dubielzig R, Grimm D and Kleinschmidt JA (2001). DNA helicase-mediated packaging of adeno-associated virus type 2 genomes into preformed capsids. *EMBO J.* **20**: 3282–3291.
33. Im D-S and Muzyczka N (1990). The AAV origin binding protein Rep68 is an ATP-dependent site-specific endonuclease with DNA helicase activity. *Cell* **61**: 447–457.
34. Im DS and Muzyczka N (1992). Partial purification of adeno-associated virus Rep78, Rep52, and Rep40 and their biochemical characterization. *J Virol* **66**: 1119–1128.
35. Brister JR and Muzyczka N (2000). Mechanism of Rep-mediated adeno-associated virus origin nicking. *J Virol* **74**: 7762–7771.
36. Brister JR and Muzyczka N (1999). Rep-mediated nicking of the adeno-associated virus origin requires two biochemical activities, DNA helicase activity and transesterification. *J Virol* **73**: 9325–9336.
37. Beaton A, Palumbo P and Berns KI (1989). Expression from the adeno-associated virus p5 and p19 promoters is negatively regulated in trans by the rep protein. *J Virol* **63**: 4450–4454.
38. Pereira DJ, McCarty DM and Muzyczka N (1997). The adeno-associated virus (AAV) Rep protein acts as both a repressor and an activator to regulate AAV transcription during a productive infection. *J Virol* **71**: 1079–1088.

39. Ni TH, Zhou X, McCarty DM, Zolotukhin I and Muzyczka N (1994). In vitro replication of adeno-associated virus DNA. *J Virol* **68**: 1128–1138.
40. Chejanovsky N and Carter BJ (1989). Mutagenesis of an AUG codon in the adeno-associated virus rep gene: effects on viral DNA replication. *Virology* **173**: 120–128.
41. Myers MW and Carter BJ (1980). Assembly of adeno-associated virus. *Virology* **102**: 71–82.
42. Warrington KH, Gorbatyuk OS, Harrison JK, Opie SR, Zolotukhin S and Muzyczka N (2004). Adeno-Associated Virus Type 2 VP2 Capsid Protein Is Nonessential and Can Tolerate Large Peptide Insertions at Its N Terminus. *J Virol* **78**: 6595–6609.
43. Becerra SP, Rose JA, Hardy M, Baroudy BM and Anderson CW (1985). Direct mapping of adeno-associated virus capsid proteins B and C: a possible ACG initiation codon. *Proc Natl Acad Sci U S A* **82**: 7919–7923.
44. Becerra SP, Koczot F, Fabisch P and Rose JA (1988). Synthesis of adeno-associated virus structural proteins requires both alternative mRNA splicing and alternative initiations from a single transcript. *J Virol* **62**: 2745–2754.
45. Naumer M, Sonntag F, Schmidt K, Nieto K, Panke C, Davey NE *et al.* (2012). Properties of the adeno-associated virus assembly-activating protein. *J Virol* **86**: 13038–13048.
46. Xie Q, Bu W, Bhatia S, Hare J, Somasundaram T, Azzi A *et al.* (2002). The atomic structure of adeno-associated virus (AAV-2), a vector for human gene therapy. *Proc Natl Acad Sci U S A* **99**: 10405–10410.
47. Wobus CE, Hügler-Dörr B, Girod A, Petersen G, Hallek M and Kleinschmidt JA (2000). Monoclonal antibodies against the adeno-associated virus type 2 (AAV-2) capsid: epitope mapping and identification of capsid domains involved in AAV-2-cell interaction and neutralization of AAV-2 infection. *J Virol* **74**: 9281–9293.
48. Wu P, Xiao W, Conlon T, Hughes J, Agbandje-McKenna M, Ferkol T *et al.* (2000). Mutational analysis of the adeno-associated virus type 2 (AAV2) capsid gene and construction of AAV2 vectors with altered tropism. *J Virol* **74**: 8635–8647.
49. Kern A, Schmidt K, Leder C, Muller OJ, Wobus CE, Bettinger K *et al.* (2003). Identification of a Heparin-Binding Motif on Adeno-Associated Virus Type 2 Capsids. *J Virol* **77**: 11072–11081.
50. Lochrie MA, Tatsuno GP, Christie B, McDonnell JW, Zhou S, Surosky R *et al.* (2006). Mutations on the external surfaces of adeno-associated virus type 2 capsids that affect transduction and neutralization. *J Virol* **80**: 821–834.

51. Opie SR, Warrington KH, Agbandje-McKenna M, Zolotukhin S and Muzyczka N (2003). Identification of Amino Acid Residues in the Capsid Proteins of Adeno-Associated Virus Type 2 That Contribute to Heparan Sulfate Proteoglycan Binding. *J Virol* **77**: 6995–7006.
52. Gurda BL, DiMattia MA, Miller EB, Bennett A, McKenna R, Weichert WS *et al.* (2013). Capsid antibodies to different adeno-associated virus serotypes bind common regions. *J Virol* **87**: 9111–9124.
53. Bleker S, Sonntag F and Kleinschmidt JA (2005). Mutational analysis of narrow pores at the five-fold symmetry axes of adeno-associated virus type 2 capsids reveals a dual role in genome packaging and activation of phospholipase A2 activity. *J Virol* **79**: 2528–2540.
54. Pettersen EF, Goddard TD, Huang CC, Couch GS, Greenblatt DM, Meng EC *et al.* (2004). UCSF Chimera--a visualization system for exploratory research and analysis. *J Comput Chem* **25**: 1605–1612.
55. Cao M, You H and Hermonat PL (2014). The X gene of adeno-associated virus 2 (AAV2) is involved in viral DNA replication. *PLoS ONE* **9**: e104596.
56. Summerford C and Samulski RJ (1998). Membrane-associated heparan sulfate proteoglycan is a receptor for adeno-associated virus type 2 virions. *J Virol* **72**: 1438–1445.
57. Asokan A, Hamra JB, Govindasamy L, Agbandje-McKenna M and Samulski RJ (2006). Adeno-associated virus type 2 contains an integrin alpha5beta1 binding domain essential for viral cell entry. *J Virol* **80**: 8961–8969.
58. Qing K, Mah C, Hansen J, Zhou S, Dwarki V and Srivastava A (1999). Human fibroblast growth factor receptor 1 is a co-receptor for infection by adeno-associated virus 2. *Nat. Med.* **5**: 71–77.
59. Kashiwakura Y, Tamayose K, Iwabuchi K, Hirai Y, Shimada T, Matsumoto K *et al.* (2005). Hepatocyte growth factor receptor is a coreceptor for adeno-associated virus type 2 infection. *Journal of Virology* **79**: 609–614.
60. Akache B, Grimm D, Pandey K, Yant SR, Xu H and Kay MA (2006). The 37/67-kilodalton laminin receptor is a receptor for adeno-associated virus serotypes 8, 2, 3, and 9. *Journal of Virology* **80**: 9831–9836.
61. Summerford C, Bartlett JS and Samulski RJ (1999). AlphaVbeta5 integrin: a co-receptor for adeno-associated virus type 2 infection. *Nat. Med.* **5**: 78–82.
62. Qiu J and Brown KE (1999). Integrin alphaVbeta5 is not involved in adeno-associated virus type 2 (AAV2) infection. *Virology* **264**: 436–440.
63. Pillay S, Meyer NL, Puschnik AS, Davulcu O, Diep J, Ishikawa Y *et al.* (2016). An essential receptor for adeno-associated virus infection. *Nature* **530**: 108–112.

64. Summerford C and Samulski RJ (2016). AAVR: A Multi-Serotype Receptor for AAV. *Mol Ther* **24**: 663–666.
65. Bartlett JS, Wilcher R and Samulski RJ (2000). Infectious entry pathway of adeno-associated virus and adeno-associated virus vectors. *J Virol* **74**: 2777–2785.
66. Duan D, Li Q, Kao AW, Yue Y, Pessin JE and Engelhardt JF (1999). Dynamin is required for recombinant adeno-associated virus type 2 infection. *J Virol* **73**: 10371–10376.
67. Sanlioglu S, Benson PK, Yang J, Atkinson EM, Reynolds T and Engelhardt JF (2000). Endocytosis and nuclear trafficking of adeno-associated virus type 2 are controlled by rac1 and phosphatidylinositol-3 kinase activation. *J Virol* **74**: 9184–9196.
68. Douar AM, Poulard K, Stockholm D and Danos O (2001). Intracellular trafficking of adeno-associated virus vectors: routing to the late endosomal compartment and proteasome degradation. *J Virol* **75**: 1824–1833.
69. Nonnenmacher M and Weber T (2011). Adeno-associated virus 2 infection requires endocytosis through the CLIC/GEEC pathway. *Cell Host Microbe* **10**: 563–576.
70. Weinberg MS, Nicolson S, Bhatt AP, McLendon M, Li C and Samulski RJ (2014). Recombinant adeno-associated virus utilizes cell-specific infectious entry mechanisms. *J Virol* **88**: 12472–12484.
71. Xiao P-J and Samulski RJ (2012). Cytoplasmic trafficking, endosomal escape, and perinuclear accumulation of adeno-associated virus type 2 particles are facilitated by microtubule network. *J Virol* **86**: 10462–10473.
72. Ding W, Zhang LN, Yeaman C and Engelhardt JF (2006). rAAV2 traffics through both the late and the recycling endosomes in a dose-dependent fashion. *Mol Ther* **13**: 671–682.
73. Xiao W, Warrington KH, Hearing P, Hughes J and Muzyczka N (2002). Adenovirus-Facilitated Nuclear Translocation of Adeno-Associated Virus Type 2. *J Virol* **76**: 11505–11517.
74. Nonnenmacher M and Weber T (2012). Intracellular transport of recombinant adeno-associated virus vectors. *Gene Ther* **19**: 649–658.
75. Nonnenmacher ME, Cintrat J-C, Gillet D and Weber T (2015). Syntaxin 5-dependent retrograde transport to the trans-Golgi network is required for adeno-associated virus transduction. *J Virol* **89**: 1673–1687.
76. Akache B, Grimm D, Shen X, Fuess S, Yant SR, Glazer DS *et al.* (2007). A two-hybrid screen identifies cathepsins B and L as uncoating factors for adeno-associated virus 2 and 8. *Mol Ther* **15**: 330–339.

77. Sonntag F, Bleker S, Leuchs B, Fischer R and Kleinschmidt JA (2006). Adeno-associated virus type 2 capsids with externalized VP1/VP2 trafficking domains are generated prior to passage through the cytoplasm and are maintained until uncoating occurs in the nucleus. *J Virol* **80**: 11040–11054.
78. Girod A, Wobus CE, Zádori Z, Ried M, Leike K, Tijssen P *et al.* (2002). The VP1 capsid protein of adeno-associated virus type 2 is carrying a phospholipase A2 domain required for virus infectivity. *J Gen Virol* **83**: 973–978.
79. Grieger JC, Snowdy S and Samulski RJ (2006). Separate basic region motifs within the adeno-associated virus capsid proteins are essential for infectivity and assembly. *J Virol* **80**: 5199–5210.
80. Popa-Wagner R, Porwal M, Kann M, Reuss M, Weimer M, Florin L *et al.* (2012). Impact of VP1-specific protein sequence motifs on adeno-associated virus type 2 intracellular trafficking and nuclear entry. *J Virol* **86**: 9163–9174.
81. Stahnke S, Lux K, Uhrig S, Kreppel F, Hösel M, Coutelle O *et al.* (2011). Intrinsic phospholipase A2 activity of adeno-associated virus is involved in endosomal escape of incoming particles. *Virology* **409**: 77–83.
82. Kelich JM, Ma J, Dong B, Wang Q, Chin M, Magura CM *et al.* (2015). Super-resolution imaging of nuclear import of adeno-associated virus in live cells. *Mol Ther Methods Clin Dev* **2**: 15047.
83. Nicolson SC and Samulski RJ (2014). Recombinant adeno-associated virus utilizes host cell nuclear import machinery to enter the nucleus. *J Virol* **88**: 4132–4144.
84. Hansen J, Qing K and Srivastava A (2001). Infection of purified nuclei by adeno-associated virus 2. *Mol Ther* **4**: 289–296.
85. Johnson JS and Samulski RJ (2009). Enhancement of adeno-associated virus infection by mobilizing capsids into and out of the nucleolus. *J Virol* **83**: 2632–2644.
86. Lux K, Goerlitz N, Schlemminger S, Perabo L, Goldnau D, Endell J *et al.* (2005). Green Fluorescent Protein-Tagged Adeno-Associated Virus Particles Allow the Study of Cytosolic and Nuclear Trafficking. *J Virol* **79**: 11776–11787.
87. Schnepf BC, Jensen RL, Chen C-L, Johnson PR and Clark KR (2005). Characterization of adeno-associated virus genomes isolated from human tissues. *J Virol* **79**: 14793–14803.
88. Samulski RJ, Zhu X, Xiao X, Brook JD, Housman DE, Epstein N *et al.* (1991). Targeted integration of adeno-associated virus (AAV) into human chromosome 19. *EMBO J.* **10**: 3941–3950.
89. Kotin RM, Menninger JC, Ward DC and Berns KI (1991). Mapping and direct visualization of a region-specific viral DNA integration site on chromosome 19q13-qter. *Genomics* **10**: 831–834.

90. Weitzman MD, Kyöstiö SR, Kotin RM and Owens RA (1994). Adeno-associated virus (AAV) Rep proteins mediate complex formation between AAV DNA and its integration site in human DNA. *Proc Natl Acad Sci U S A* **91**: 5808–5812.
91. Weitzman MD (2006) in *Parvoviruses*, ed Kerr JR. (Hodder Arnold; Distributed in the U.S.A. by Oxford University Press, London, New York), p. 143-156.
92. Yakobson B, Hrynko TA, Peak MJ and Winocour E (1989). Replication of adeno-associated virus in cells irradiated with UV light at 254 nm. *J Virol* **63**: 1023–1030.
93. Yakobson B, Koch T and Winocour E (1987). Replication of adeno-associated virus in synchronized cells without the addition of a helper virus. *J Virol* **61**: 972–981.
94. Yalkinoglu AO, Heilbronn R, Bürkle A, Schlehofer JR and Zur Hausen H (1988). DNA amplification of adeno-associated virus as a response to cellular genotoxic stress. *Cancer Res* **48**: 3123–3129.
95. Meyers C, Mane M, Kokorina N, Alam S and Hermonat PL (2000). Ubiquitous human adeno-associated virus type 2 autonomously replicates in differentiating keratinocytes of a normal skin model. *Virology* **272**: 338–346.
96. Hastie E and Samulski RJ (2015). Adeno-associated virus at 50: a golden anniversary of discovery, research, and gene therapy success—a personal perspective. *Hum Gene Ther* **26**: 257–265.
97. Samulski RJ, Berns KI, Tan M and Muzyczka N (1982). Cloning of adeno-associated virus into pBR322: rescue of intact virus from the recombinant plasmid in human cells. *Proc Natl Acad Sci U S A* **79**: 2077–2081.
98. Hermonat PL and Muzyczka N (1984). Use of adeno-associated virus as a mammalian DNA cloning vector: transduction of neomycin resistance into mammalian tissue culture cells. *Proc Natl Acad Sci U S A* **81**: 6466–6470.
99. Dong JY, Fan PD and Frizzell RA (1996). Quantitative analysis of the packaging capacity of recombinant adeno-associated virus. *Hum Gene Ther* **7**: 2101–2112.
100. Brimble MA, Reiss UM, Nathwani AC and Davidoff AM (2015). New and improved AAVenues: current status of hemophilia B gene therapy. *Expert Opin Biol Ther*. 1–14.
101. Wang D, Zhong L, Nahid MA and Gao G (2014). The potential of adeno-associated viral vectors for gene delivery to muscle tissue. *Expert Opin Drug Deliv* **11**: 345–364.
102. Bourdenx M, Dutheil N, Bezard E and Dehay B (2014). Systemic gene delivery to the central nervous system using Adeno-associated virus. *Front Mol Neurosci* **7**: 50.

103. Carvalho LS and Vandenberghe LH (2015). Promising and delivering gene therapies for vision loss. *Vision Res* **111**: 124–133.
104. <http://www.abedia.com/wiley/vectors.php>.
105. Bryant LM, Christopher DM, Giles AR, Hinderer C, Rodriguez JL, Smith JB *et al.* (2013). Lessons learned from the clinical development and market authorization of Glybera. *Hum Gene Ther Clin Dev* **24**: 55–64.
106. <http://www.ema.europa.eu>.
107. Rolling F and Samulski RJ (1995). AAV as a viral vector for human gene therapy. Generation of recombinant virus. *Mol Biotechnol* **3**: 9–15.
108. Xiao X, Li J and Samulski RJ (1998). Production of high-titer recombinant adeno-associated virus vectors in the absence of helper adenovirus. *J Virol* **72**: 2224–2232.
109. Grimm D, Kern A, Rittner K and Kleinschmidt JA (1998). Novel tools for production and purification of recombinant adenoassociated virus vectors. *Hum Gene Ther* **9**: 2745–2760.
110. Wright JF (2009). Transient transfection methods for clinical adeno-associated viral vector production. *Hum Gene Ther* **20**: 698–706.
111. Graham FL, Smiley J, Russell WC and Nairn R (1977). Characteristics of a human cell line transformed by DNA from human adenovirus type 5. *J Gen Virol* **36**: 59–74.
112. Grieger JC, Soltys SM and Samulski RJ (2015). Production of Recombinant Adeno-associated Virus Vectors Using Suspension HEK293 Cells and Continuous Harvest of Vector From the Culture Media for GMP FIX and FLT1 Clinical Vector. *Mol Ther*.
113. Ayuso E, Mingozzi F and Bosch F (2010). Production, purification and characterization of adeno-associated vectors. *Curr Gene Ther* **10**: 423–436.
114. Clement N, Knop DR and Byrne BJ (2009). Large-scale adeno-associated viral vector production using a herpesvirus-based system enables manufacturing for clinical studies. *Hum Gene Ther* **20**: 796–806.
115. Mietzsch M, Grasse S, Zurawski C, Weger S, Bennett A, Agbandje-McKenna M *et al.* (2014). OneBac: platform for scalable and high-titer production of adeno-associated virus serotype 1-12 vectors for gene therapy. *Hum Gene Ther* **25**: 212–222.
116. Wright J (2014). Product-Related Impurities in Clinical-Grade Recombinant AAV Vectors: Characterization and Risk Assessment. *Biomedicines* **2**: 80–97.

117. Ayuso E, Mingozi F, Montane J, Leon X, Anguela XM, Haurigot V *et al.* (2010). High AAV vector purity results in serotype- and tissue-independent enhancement of transduction efficiency. *Gene Ther* **17**: 503–510.
118. Strobel B, Miller FD, Rist W and Lamla T (2015). Comparative analysis of cesium chloride- and iodixanol-based purification of recombinant Adeno-associated virus (AAV) vectors for preclinical applications. *Hum Gene Ther Methods*.
119. Rayaprolu V, Kruse S, Kant R, Venkatakrishnan B, Movahed N, Brooke D *et al.* (2013). Comparative analysis of adeno-associated virus capsid stability and dynamics. *J Virol* **87**: 13150–13160.
120. Potter M, Lins B, Mietzsch M, Heilbronn R, van Vliet K, Chipman P *et al.* (2014). A simplified purification protocol for recombinant adeno-associated virus vectors. *Mol Ther Methods Clin Dev* **1**: 14034.
121. Zolotukhin S, Byrne BJ, Mason E, Zolotukhin I, Potter M, Chesnut K *et al.* (1999). Recombinant adeno-associated virus purification using novel methods improves infectious titer and yield. *Gene Ther* **6**: 973–985.
122. Wang Q, Lock M, Prongay AJ, Alvira MR, Petkov B and Wilson JM (2015). Identification of an adeno-associated virus binding epitope for AVB sepharose affinity resin. *Mol Ther Methods Clin Dev* **2**: 15040.
123. Venkatakrishnan B, Yarbrough J, Domsic J, Bennett A, Bothner B, Kozyreva OG *et al.* (2013). Structure and dynamics of adeno-associated virus serotype 1 VP1-unique N-terminal domain and its role in capsid trafficking. *J Virol* **87**: 4974–4984.
124. Okada T, Nonaka-Sarukawa M, Uchibori R, Kinoshita K, Hayashita-Kinoh H, Nitahara-Kasahara Y *et al.* (2009). Scalable purification of adeno-associated virus serotype 1 (AAV1) and AAV8 vectors, using dual ion-exchange adsorptive membranes. *Hum Gene Ther* **20**: 1013–1021.
125. Kaludov N, Handelman B and Chiorini JA (2002). Scalable purification of adeno-associated virus type 2, 4, or 5 using ion-exchange chromatography. *Hum Gene Ther* **13**: 1235–1243.
126. Qu G, Bahr-Davidson J, Prado J, Tai A, Cataniag F, McDonnell J *et al.* (2007). Separation of adeno-associated virus type 2 empty particles from genome containing vectors by anion-exchange column chromatography. *J. Virol. Methods* **140**: 183–192.
127. Zolotukhin S, Potter M, Zolotukhin I, Sakai Y, Loiler S, Fraitjes TJ *et al.* (2002). Production and purification of serotype 1, 2, and 5 recombinant adeno-associated viral vectors. *Methods* **28**: 158–167.

128. Allay JA, Sleep S, Long S, Tillman DM, Clark R, Carney G *et al.* (2011). Good manufacturing practice production of self-complementary serotype 8 adeno-associated viral vector for a hemophilia B clinical trial. *Hum Gene Ther* **22**: 595–604.
129. Zhang H-G, Xie J, Dmitriev I, Kashentseva E, Curiel DT, Hsu H-C *et al.* (2002). Addition of Six-His-Tagged Peptide to the C Terminus of Adeno-Associated Virus VP3 Does Not Affect Viral Tropism or Production. *J Virol* **76**: 12023–12031.
130. Koerber JT, Jang J-H, Yu JH, Kane RS and Schaffer DV (2007). Engineering adeno-associated virus for one-step purification via immobilized metal affinity chromatography. *Hum Gene Ther* **18**: 367–378.
131. Croyle MA, Cheng X and Wilson JM (2001). Development of formulations that enhance physical stability of viral vectors for gene therapy. *Gene Ther* **8**: 1281–1290.
132. Sommer J (2003). Quantification of adeno-associated virus particles and empty capsids by optical density measurement. *Mol Ther* **7**: 122–128.
133. Zeltner N, Kohlbrenner E, Clément N, Weber T and Linden RM (2010). Near-perfect infectivity of wild-type AAV as benchmark for infectivity of recombinant AAV vectors. *Gene Ther* **17**: 872–879.
134. Hösel M, Broxtermann M, Janicki H, Esser K, Arzberger S, Hartmann P *et al.* (2012). Toll-like receptor 2-mediated innate immune response in human nonparenchymal liver cells toward adeno-associated viral vectors. *Hepatology* **55**: 287–297.
135. Mingozi F, Maus MV, Hui DJ, Sabatino DE, Murphy SL, Rasko JEJ *et al.* (2007). CD8(+) T-cell responses to adeno-associated virus capsid in humans. *Nat. Med.* **13**: 419–422.
136. Halbert CL, Metzger MJ, Lam S-L and Miller AD (2011). Capsid-expressing DNA in AAV vectors and its elimination by use of an oversize capsid gene for vector production. *Gene Ther* **18**: 411–417.
137. Samulski RJ, Chang LS and Shenk T (1989). Helper-free stocks of recombinant adeno-associated viruses: normal integration does not require viral gene expression. *J Virol* **63**: 3822–3828.
138. Allen JM, Debelak DJ, Reynolds TC and Miller AD (1997). Identification and elimination of replication-competent adeno-associated virus (AAV) that can arise by nonhomologous recombination during AAV vector production. *J Virol* **71**: 6816–6822.
139. Cao L, Liu Y, During MJ and Xiao W (2000). High-titer, wild-type free recombinant adeno-associated virus vector production using intron-containing helper plasmids. *J Virol* **74**: 11456–11463.

140. European Medicines Agency, Committee for Medicinal Products for Human Use (CHMP) (2012). Assessment Report of Glybera, INN-alipogene tiparvovec. Assessment Report. Procedure No. EMEA/H/C/002145.
141. Chadeuf G, Ciron C, Moullier P and Salvetti A (2005). Evidence for encapsidation of prokaryotic sequences during recombinant adeno-associated virus production and their in vivo persistence after vector delivery. *Mol Ther* **12**: 744–753.
142. Lecomte E, Tournaire B, Cogné B, Dupont J-B, Lindenbaum P, Martin-Fontaine M *et al.* (2015). Advanced Characterization of DNA Molecules in rAAV Vector Preparations by Single-stranded Virus Next-generation Sequencing. *Mol Ther Nucleic Acids* **4**: e260.
143. Hauck B, Murphy SL, Smith PH, Qu G, Liu X, Zelenia O *et al.* (2009). Undetectable transcription of cap in a clinical AAV vector: implications for preformed capsid in immune responses. *Mol Ther* **17**: 144–152.
144. Bauer S, Kirschning CJ, Häcker H, Redecke V, Hausmann S, Akira S *et al.* (2001). Human TLR9 confers responsiveness to bacterial DNA via species-specific CpG motif recognition. *Proc Natl Acad Sci U S A* **98**: 9237–9242.
145. Hyde SC, Pringle IA, Abdullah S, Lawton AE, Davies LA, Varathalingam A *et al.* (2008). CpG-free plasmids confer reduced inflammation and sustained pulmonary gene expression. *Nat Biotechnol* **26**: 549–551.
146. Miller DG, Rutledge EA and Russell DW (2002). Chromosomal effects of adeno-associated virus vector integration. *Nat Genet* **30**: 147–148.
147. Rabinowitz JE, Rolling F, Li C, Conrath H, Xiao W, Xiao X *et al.* (2002). Cross-Packaging of a Single Adeno-Associated Virus (AAV) Type 2 Vector Genome into Multiple AAV Serotypes Enables Transduction with Broad Specificity. *J Virol* **76**: 791–801.
148. Nathwani AC, Tuddenham EGD, Rangarajan S, Rosales C, McIntosh J, Linch DC *et al.* (2011). Adenovirus-associated virus vector-mediated gene transfer in hemophilia B. *N Engl J Med* **365**: 2357–2365.
149. Büning H, Huber A, Zhang L, Meumann N and Hacker U (2015). Engineering the AAV capsid to optimize vector-host-interactions. *Curr Opin Pharmacol* **24**: 94–104.
150. Girod A, Ried M, Wobus C, Lahm H, Leike K, Kleinschmidt J *et al.* (1999). Genetic capsid modifications allow efficient re-targeting of adeno-associated virus type 2. *Nat. Med.* **5**: 1052–1056.
151. Münch RC, Muth A, Muik A, Friedel T, Schmatz J, Dreier B *et al.* (2015). Off-target-free gene delivery by affinity-purified receptor-targeted viral vectors. *Nat Commun* **6**: 6246.

152. Perabo L, Buning H, Kofler DM, Ried MU, Girod A, Wendtner CM *et al.* (2003). In vitro selection of viral vectors with modified tropism: the adeno-associated virus display. *Mol Ther* **8**: 151–157.
153. Muller OJ, Kaul F, Weitzman MD, Pasqualini R, Arap W, Kleinschmidt JA *et al.* (2003). Random peptide libraries displayed on adeno-associated virus to select for targeted gene therapy vectors. *Nat Biotechnol* **21**: 1040–1046.
154. Sallach J, Di Pasquale G, Larcher F, Niehoff N, Rübsam M, Huber A *et al.* (2014). Tropism-modified AAV vectors overcome barriers to successful cutaneous therapy. *Mol Ther* **22**: 929–939.
155. Duan D, Yue Y, Yan Z, Yang J and Engelhardt JF (2000). Endosomal processing limits gene transfer to polarized airway epithelia by adeno-associated virus. *J Clin Invest* **105**: 1573–1587.
156. Yan Z, Zak R, Luxton, G. W. G., Ritchie TC, Bantel-Schaal U and Engelhardt JF (2002). Ubiquitination of both Adeno-Associated Virus Type 2 and 5 Capsid Proteins Affects the Transduction Efficiency of Recombinant Vectors. *J Virol* **76**: 2043–2053.
157. Zhong L, Li B, Jayandharan G, Mah CS, Govindasamy L, Agbandje-McKenna M *et al.* (2008). Tyrosine-phosphorylation of AAV2 vectors and its consequences on viral intracellular trafficking and transgene expression. *Virology* **381**: 194–202.
158. Zhong L, Li B, Mah CS, Govindasamy L, Agbandje-McKenna M, Cooper M *et al.* (2008). Next generation of adeno-associated virus 2 vectors: point mutations in tyrosines lead to high-efficiency transduction at lower doses. *Proc Natl Acad Sci U S A* **105**: 7827–7832.
159. Flotho A and Melchior F (2013). Sumoylation: a regulatory protein modification in health and disease. *Annu. Rev. Biochem.* **82**: 357–385.
160. Hölscher C, Sonntag F, Henrich K, Chen Q, Beneke J, Matula P *et al.* (2015). The SUMOylation Pathway Restricts Gene Transduction by Adeno-Associated Viruses. *PLoS Pathog* **11**: e1005281.
161. Schwartz RA, Palacios JA, Cassell GD, Adam S, Giacca M and Weitzman MD (2007). The Mre11/Rad50/Nbs1 complex limits adeno-associated virus transduction and replication. *J Virol* **81**: 12936–12945.
162. Cataldi MP and McCarty DM (2013). Hairpin-end conformation of adeno-associated virus genome determines interactions with DNA-repair pathways. *Gene Ther* **20**: 686–693.
163. Lentz TB and Samulski RJ (2015). Insight into the mechanism of inhibition of adeno-associated virus by the mre11/rad50/nbs1 complex. *J Virol* **89**: 181–194.
164. Iyama T and Wilson DM (2013). DNA repair mechanisms in dividing and non-dividing cells. *DNA Repair (Amst)* **12**: 620–636.

165. Stracker TH and Petrini JHJ (2011). The MRE11 complex: starting from the ends. *Nat Rev Mol Cell Biol* **12**: 90–103.
166. Cervelli T, Palacios JA, Zentilin L, Mano M, Schwartz RA, Weitzman MD *et al.* (2008). Processing of recombinant AAV genomes occurs in specific nuclear structures that overlap with foci of DNA-damage-response proteins. *J Cell Sci* **121**: 349–357.
167. Cataldi MP and McCarty DM (2010). Differential effects of DNA double-strand break repair pathways on single-strand and self-complementary adeno-associated virus vector genomes. *J Virol* **84**: 8673–8682.
168. Zentilin L, Marcello A and Giacca M (2001). Involvement of cellular double-stranded DNA break binding proteins in processing of the recombinant adeno-associated virus genome. *J Virol* **75**: 12279–12287.
169. Stracker TH, Carson CT and Weitzman MD (2002). Adenovirus oncoproteins inactivate the Mre11-Rad50-NBS1 DNA repair complex. *Nature* **418**: 348–352.
170. Wilkinson DE and Weller SK (2004). Recruitment of Cellular Recombination and Repair Proteins to Sites of Herpes Simplex Virus Type 1 DNA Replication Is Dependent on the Composition of Viral Proteins within Prereplicative Sites and Correlates with the Induction of the DNA Damage Response. *Journal of Virology* **78**: 4783–4796.
171. Lilley CE, Carson CT, Muotri AR, Gage FH and Weitzman MD (2005). DNA repair proteins affect the lifecycle of herpes simplex virus 1. *Proc Natl Acad Sci U S A* **102**: 5844–5849.
172. Millet R, Jolinon N, Nguyen X-N, Berger G, Cimorelli A, Greco A *et al.* (2015). Impact of the MRN Complex on Adeno-Associated Virus Integration and Replication during Coinfection with Herpes Simplex Virus 1. *J Virol* **89**: 6824–6834.
173. Sanlioglu S, Duan D and Engelhardt JF. Two Independent Molecular Pathways for Recombinant Adeno-Associated Virus Genome Conversion Occur after UV-C and E4orf6 Augmentation of Transduction.
174. Alexander IE, Russell DW and Miller AD (1994). DNA-damaging agents greatly increase the transduction of nondividing cells by adeno-associated virus vectors. *J Virol* **68**: 8282–8287.
175. Russell DW, Alexander IE and Miller AD (1995). DNA synthesis and topoisomerase inhibitors increase transduction by adeno-associated virus vectors. *Proc Natl Acad Sci U S A* **92**: 5719–5723.
176. Mano M, Ippodrino R, Zentilin L, Zacchigna S and Giacca M (2015). Genome-wide RNAi screening identifies host restriction factors critical for in vivo AAV transduction. *Proc Natl Acad Sci U S A* **112**: 11276–11281.

177. Lovric J, Mano M, Zentilin L, Eulalio A, Zacchigna S and Giacca M (2012). Terminal differentiation of cardiac and skeletal myocytes induces permissivity to AAV transduction by relieving inhibition imposed by DNA damage response proteins. *Mol Ther* **20**: 2087–2097.
178. Rahman SH, Bobis-Wozowicz S, Chatterjee D, Gellhaus K, Pars K, Heilbronn R *et al.* (2013). The nontoxic cell cycle modulator indirubin augments transduction of adeno-associated viral vectors and zinc-finger nuclease-mediated gene targeting. *Hum Gene Ther* **24**: 67–77.
179. Russell DW, Miller AD and Alexander IE (1994). Adeno-associated virus vectors preferentially transduce cells in S phase. *Proc Natl Acad Sci U S A* **91**: 8915–8919.
180. Nakai H, Storm TA and Kay MA (2000). Recruitment of single-stranded recombinant adeno-associated virus vector genomes and intermolecular recombination are responsible for stable transduction of liver in vivo. *J Virol* **74**: 9451–9463.
181. Ferrari FK, Samulski T, Shenk T and Samulski RJ (1996). Second-strand synthesis is a rate-limiting step for efficient transduction by recombinant adeno-associated virus vectors. *J Virol* **70**: 3227–3234.
182. Fisher KJ, Gao GP, Weitzman MD, DeMatteo R, Burda JF and Wilson JM (1996). Transduction with recombinant adeno-associated virus for gene therapy is limited by leading-strand synthesis. *J Virol* **70**: 520–532.
183. Wang Z, Ma H-I, Li J, Sun L, Zhang J and Xiao X (2003). Rapid and highly efficient transduction by double-stranded adeno-associated virus vectors in vitro and in vivo. *Gene Ther* **10**: 2105–2111.
184. McCarty DM, Fu H, Monahan PE, Toulson CE, Naik P and Samulski RJ (2003). Adeno-associated virus terminal repeat (TR) mutant generates self-complementary vectors to overcome the rate-limiting step to transduction in vivo. *Gene Ther* **10**: 2112–2118.
185. McCarty DM (2008). Self-complementary AAV vectors; advances and applications. *Mol Ther* **16**: 1648–1656.
186. Raj D, Davidoff AM and Nathwani AC (2011). Self-complementary adeno-associated viral vectors for gene therapy of hemophilia B: progress and challenges. *Expert Rev Hematol* **4**: 539–549.
187. Nash K, Chen W, McDonald WF, Zhou X and Muzyczka N (2007). Purification of host cell enzymes involved in adeno-associated virus DNA replication. *J Virol* **81**: 5777–5787.
188. Nash K, Chen W and Muzyczka N (2008). Complete in vitro reconstitution of adeno-associated virus DNA replication requires the minichromosome maintenance complex proteins. *J Virol* **82**: 1458–1464.

189. Nakai H, Yant SR, Storm TA, Fuess S, Meuse L and Kay MA (2001). Extrachromosomal Recombinant Adeno-Associated Virus Vector Genomes Are Primarily Responsible for Stable Liver Transduction In Vivo. *J Virol* **75**: 6969–6976.
190. Schnepf BC, Clark KR, Klemanski DL, Pacak CA and Johnson PR (2003). Genetic Fate of Recombinant Adeno-Associated Virus Vector Genomes in Muscle. *Journal of Virology* **77**: 3495–3504.
191. Miller DG, Petek LM and Russell DW (2003). Human gene targeting by adeno-associated virus vectors is enhanced by DNA double-strand breaks. *Mol Cell Biol* **23**: 3550–3557.
192. Russell DW (2003). AAV loves an active genome. *Nat Genet* **34**: 241–242.
193. Sanlioglu S, Benson P and Engelhardt JF (2000). Loss of ATM function enhances recombinant adeno-associated virus transduction and integration through pathways similar to UV irradiation. *Virology* **268**: 68–78.
194. Daya S, Cortez N and Berns KI (2009). Adeno-associated virus site-specific integration is mediated by proteins of the nonhomologous end-joining pathway. *J Virol* **83**: 11655–11664.
195. Song S, Lu Y, Choi Y-K, Han Y, Tang Q, Zhao G *et al.* (2004). DNA-dependent PK inhibits adeno-associated virus DNA integration. *Proc Natl Acad Sci U S A* **101**: 2112–2116.
196. Miller DG, Trobridge GD, Petek LM, Jacobs MA, Kaul R and Russell DW (2005). Large-scale analysis of adeno-associated virus vector integration sites in normal human cells. *J Virol* **79**: 11434–11442.
197. Nakai H, Montini E, Fuess S, Storm TA, Grompe M and Kay MA (2003). AAV serotype 2 vectors preferentially integrate into active genes in mice. *Nat Genet* **34**: 297–302.
198. Inagaki K, Lewis SM, Wu X, Ma C, Munroe DJ, Fuess S *et al.* (2007). DNA palindromes with a modest arm length of greater, similar 20 base pairs are a significant target for recombinant adeno-associated virus vector integration in the liver, muscles, and heart in mice. *J Virol* **81**: 11290–11303.
199. Kaepffel C, Beattie SG, Fronza R, van Logtenstein R, Salmon F, Schmidt S *et al.* (2013). A largely random AAV integration profile after LPLD gene therapy. *Nat. Med.* **19**: 889–891.
200. Yue Y and Duan D (2003). Double strand interaction is the predominant pathway for intermolecular recombination of adeno-associated viral genomes. *Virology* **313**: 1–7.
201. Choi VW, McCarty DM and Samulski RJ (2006). Host cell DNA repair pathways in adeno-associated viral genome processing. *J Virol* **80**: 10346–10356.

202. Duan D, Sharma P, Yang J, Yue Y, Dudus L, Zhang Y *et al.* (1998). Circular intermediates of recombinant adeno-associated virus have defined structural characteristics responsible for long-term episomal persistence in muscle tissue. *J Virol* **72**: 8568–8577.
203. Vincent-Lacaze N, Snyder RO, Gluzman R, Bohl D, Lagarde C and Danos O (1999). Structure of adeno-associated virus vector DNA following transduction of the skeletal muscle. *J Virol* **73**: 1949–1955.
204. Inagaki K, Ma C, Storm TA, Kay MA and Nakai H (2007). The role of DNA-PKcs and artemis in opening viral DNA hairpin termini in various tissues in mice. *J Virol* **81**: 11304–11321.
205. Song S, Laipis PJ, Berns KI and Flotte TR (2001). Effect of DNA-dependent protein kinase on the molecular fate of the rAAV2 genome in skeletal muscle. *Proc Natl Acad Sci U S A* **98**: 4084–4088.
206. Duan D, Yue Y and Engelhardt JF (2003). Consequences of DNA-Dependent Protein Kinase Catalytic Subunit Deficiency on Recombinant Adeno-Associated Virus Genome Circularization and Heterodimerization in Muscle Tissue. *J Virol* **77**: 4751–4759.
207. Afione SA, Conrad CK, Kearns WG, Chunduru S, Adams R, Reynolds TC *et al.* (1996). In vivo model of adeno-associated virus vector persistence and rescue. *J Virol* **70**: 3235–3241.
208. Flotte TR, Afione SA and Zeitlin PL (1994). Adeno-associated virus vector gene expression occurs in nondividing cells in the absence of vector DNA integration. *Am J Respir Cell Mol Biol* **11**: 517–521.
209. Penaud-Budloo M, Le Guiner C, Nowrouzi A, Toromanoff A, Chérel Y, Chenuaud P *et al.* (2008). Adeno-associated virus vector genomes persist as episomal chromatin in primate muscle. *J Virol* **82**: 7875–7885.
210. Clark KR, Sferra TJ, Lo W, Qu G, Chen R and Johnson PR (1999). Gene transfer into the CNS using recombinant adeno-associated virus: analysis of vector DNA forms resulting in sustained expression. *J Drug Target* **7**: 269–283.
211. Kobelt D, Schleef M, Schmeer M, Aumann J, Schlag PM and Walther W (2013). Performance of high quality minicircle DNA for in vitro and in vivo gene transfer. *Mol Biotechnol* **53**: 80–89.
212. Darquet AM, Cameron B, Wils P, Scherman D and Crouzet J (1997). A new DNA vehicle for nonviral gene delivery: supercoiled minicircle. *Gene Ther* **4**: 1341–1349.
213. Kreiss P, Cameron B, Darquet AM, Scherman D and Crouzet J (1998). Production of a new DNA vehicle for gene transfer using site-specific recombination. *Appl Microbiol Biotechnol* **49**: 560–567.

214. Bigger BW, Tolmachov O, Collombet JM, Fragkos M, Palaszewski I and Coutelle C (2001). An araC-controlled bacterial cre expression system to produce DNA minicircle vectors for nuclear and mitochondrial gene therapy. *J Biol Chem* **276**: 23018–23027.
215. Chen Z-Y, He C-Y, Ehrhardt A and Kay MA (2003). Minicircle DNA vectors devoid of bacterial DNA result in persistent and high-level transgene expression in vivo. *Mol Ther* **8**: 495–500.
216. Mayrhofer P, Blaesen M, Schleef M and Jechlinger W (2008). Minicircle-DNA production by site specific recombination and protein-DNA interaction chromatography. *J Gene Med* **10**: 1253–1269.
217. Rischmüller A, Viefhues M, Dieding M, Blaesen M, Schmeer M, Baier R *et al.* (2013) in *Minicircle and miniplasmid DNA vectors. The future of nonviral and viral gene transfer*, ed Schleef M. (Wiley-Blackwell, Weinheim, Germany), Pages 71–91.
218. Zhu J, Huang X and Yang Y (2009). The TLR9-MyD88 pathway is critical for adaptive immune responses to adeno-associated virus gene therapy vectors in mice. *J Clin Invest* **119**: 2388–2398.
219. Martino AT, Suzuki M, Markusic DM, Zolotukhin I, Ryals RC, Moghimi B *et al.* (2011). The genome of self-complementary adeno-associated viral vectors increases Toll-like receptor 9-dependent innate immune responses in the liver. *Blood* **117**: 6459–6468.
220. Kumagai Y, Takeuchi O and Akira S (2008). TLR9 as a key receptor for the recognition of DNA. *Adv Drug Deliv Rev* **60**: 795–804.
221. Wang J, Xie J, Lu H, Chen L, Hauck B, Samulski RJ *et al.* (2007). Existence of transient functional double-stranded DNA intermediates during recombinant AAV transduction. *Proc Natl Acad Sci U S A* **104**: 13104–13109.
222. Grimm D, Pandey K, Nakai H, Storm TA and Kay MA (2006). Liver transduction with recombinant adeno-associated virus is primarily restricted by capsid serotype not vector genotype. *J Virol* **80**: 426–439.
223. Mirkovitch J, Mirault M-E and Laemmli UK (1984). Organization of the higher-order chromatin loop: specific DNA attachment sites on nuclear scaffold. *Cell* **39**: 223–232.
224. Bode J *et al.*, eds (1995) *Scaffold/matrix-attached regions: structural properties creating transcriptionally active loci* (Elsevier).
225. Piechaczek C, Fetzer C, Baiker A, Bode J and Lipps HJ (1999). A vector based on the SV40 origin of replication and chromosomal S/MARs replicates episomally in CHO cells. *Nucleic Acids Res.* **27**: 426–428.

226. Schaarschmidt D, Baltin J, Stehle IM, Lipps HJ and Knippers R (2004). An episomal mammalian replicon: sequence-independent binding of the origin recognition complex. *EMBO J.* **23**: 191–201.
227. Grimm D (2003). Helper virus-free, optically controllable, and two-plasmid-based production of adeno-associated virus vectors of serotypes 1 to 6. *Mol Ther* **7**: 839–850.
228. Hacker UT, Gerner FM, Büning H, Hutter M, Reichenspurner H, Stangl M *et al.* (2001). Standard heparin, low molecular weight heparin, low molecular weight heparinoid, and recombinant hirudin differ in their ability to inhibit transduction by recombinant adeno-associated virus type 2 vectors. *Gene Ther* **8**: 966–968.
229. Hacker UT, Wingenfeld L, Kofler DM, Schuhmann NK, Lutz S, Herold T *et al.* (2005). Adeno-associated virus serotypes 1 to 5 mediated tumor cell directed gene transfer and improvement of transduction efficiency. *J Gene Med* **7**: 1429–1438.
230. William F. Scherer, Jerome T. Syverton, George O. Gey (1953). Studies on the propagation in vitro of poliomyelitis viruses. IV. Viral multiplication in a stable strain of human malignant epithelial cells (strain HeLa) derived from an epidermoid carcinoma of the cervix. *J Exp Med* **97**: 695–710.
231. Hanahan D (1983). Studies on transformation of *Escherichia coli* with plasmids. *J Mol Biol* **166**: 557–580.
232. Büning H, Perabo L, Coutelle O, Quadt-Humme S and Hallek M (2008). Recent developments in adeno-associated virus vector technology. *J Gene Med* **10**: 717–733.
233. Schnödt M, Schmeer M, Kracher B, Krüsemann C, Espinosa LE, Grünert A *et al.* (2016). DNA Minicircle Technology Improves Purity of Adeno-associated Viral Vector Preparations. *Mol Ther Nucleic Acids* **5**: e355.
234. Wright JF (2008). Manufacturing and characterizing AAV-based vectors for use in clinical studies. *Gene Ther* **15**: 840–848.
235. Stehle IM, Scinteie MF, Baiker A, Jenke, Andreas C W and Lipps HJ (2003). Exploiting a minimal system to study the epigenetic control of DNA replication: the interplay between transcription and replication. *Chromosome Res.* **11**: 413–421.
236. Baiker A, Maercker C, Piechaczek C, Schmidt SB, Bode J, Benham C *et al.* (2000). Mitotic stability of an episomal vector containing a human scaffold/matrix-attached region is provided by association with nuclear matrix. *Nat Cell Biol* **2**: 182–184.
237. Chen ZY, He CY, Meuse L and Kay MA (2004). Silencing of episomal transgene expression by plasmid bacterial DNA elements in vivo. *Gene Ther* **11**: 856–864.

238. Tan Y, Li S, Pitt BR and Huang L (1999). The inhibitory role of CpG immunostimulatory motifs in cationic lipid vector-mediated transgene expression in vivo. *Hum Gene Ther* **10**: 2153–2161.
239. Gaspar V, Melo-Diogo D de, Costa E, Moreira A, Queiroz J, Pichon C *et al.* (2015). Minicircle DNA vectors for gene therapy: advances and applications. *Expert Opin Biol Ther* **15**: 353–379.
240. Daya S and Berns KI (2008). Gene therapy using adeno-associated virus vectors. *Clin Microbiol Rev* **21**: 583–593.
241. Ward P, Elias P and Linden RM (2003). Rescue of the Adeno-Associated Virus Genome from a Plasmid Vector: Evidence for Rescue by Replication. *J Virol* **77**: 11480–11490.
242. Samulski RJ, Srivastava A, Berns KI and Muzyczka N (1983). Rescue of adeno-associated virus from recombinant plasmids: Gene correction within the terminal repeats of AAV. *Cell* **33**: 135–143.
243. Wang XS, Ponnazhagan S and Srivastava A (1995). Rescue and replication signals of the adeno-associated virus 2 genome. *J Mol Biol* **250**: 573–580.
244. Wang XS, Ponnazhagan S and Srivastava A (1996). Rescue and replication of adeno-associated virus type 2 as well as vector DNA sequences from recombinant plasmids containing deletions in the viral inverted terminal repeats: selective encapsidation of viral genomes in progeny virions. *J Virol* **70**: 1668–1677.
245. Ward P and Berns KI (1991). In vitro rescue of an integrated hybrid adeno-associated virus/simian virus 40 genome. *J Mol Biol* **218**: 791–804.
246. Hewitt FC and Samulski RJ (2010). Creating a novel origin of replication through modulating DNA-protein interfaces. *PLoS ONE* **5**: e8850.
247. Mingozi F and Büning H (2015). Adeno-Associated Viral Vectors at the Frontier between Tolerance and Immunity. *Front Immunol* **6**: 120.
248. Faust SM, Bell P, Cutler BJ, Ashley SN, Zhu Y, Rabinowitz JE *et al.* (2013). CpG-depleted adeno-associated virus vectors evade immune detection. *J Clin Invest* **123**: 2994–3001.
249. Zaiss A-K, Liu Q, Bowen GP, Wong NCW, Bartlett JS and Muruve DA (2002). Differential Activation of Innate Immune Responses by Adenovirus and Adeno-Associated Virus Vectors. *Journal of Virology* **76**: 4580–4590.
250. Hösel M. Personal communication.
251. Sudres M, Cire S, Vasseur V, Brault L, Da Rocha S, Boisgerault F *et al.* (2012). MyD88 signaling in B cells regulates the production of Th1-dependent antibodies to AAV. *Mol Ther* **20**: 1571–1581.

252. Garrels W, Talluri TR, Ziegler M, Most I, Forcato DO, Schmeer M *et al.* (2016). Cytoplasmic injection of murine zygotes with Sleeping Beauty transposon plasmids and minicircles results in the efficient generation of germline transgenic mice. *Biotechnol J* **11**: 178–184.
253. Jackson DA, Juranek S and Lipps HJ (2006). Designing nonviral vectors for efficient gene transfer and long-term gene expression. *Mol Ther* **14**: 613–626.
254. Hagedorn C, Wong S-P, Harbottle R and Lipps HJ (2011). Scaffold/matrix attached region-based nonviral episomal vectors. *Hum Gene Ther* **22**: 915–923.
255. Argyros O, Wong S-P and Harbottle RP (2011). Non-viral episomal modification of cells using S/MAR elements. *Expert Opin Biol Ther* **11**: 1177–1191.
256. Haase R, Argyros O, Wong S-P, Harbottle RP, Lipps HJ, Ogris M *et al.* (2010). pEPito: a significantly improved non-viral episomal expression vector for mammalian cells. *BMC Biotechnol.* **10**: 20.
257. Voigtlander R, Haase R, Mück-Hausl M, Zhang W, Boehme P, Lipps H-J *et al.* (2013). A Novel Adenoviral Hybrid-vector System Carrying a Plasmid Replicon for Safe and Efficient Cell and Gene Therapeutic Applications. *Mol Ther Nucleic Acids* **2**: e83.
258. Verghese SC, Goloviznina NA, Skinner AM, Lipps HJ and Kurre P (2014). S/MAR sequence confers long-term mitotic stability on non-integrating lentiviral vector episomes without selection. *Nucleic Acids Res.* **42**: e53.
259. Manthey D and Willecke K (2001). Transfection and expression of exogenous connexins in mammalian cells. *Methods Mol Biol* **154**: 187–199.
260. Rutledge EA and Russell DW (1997). Adeno-associated virus vector integration junctions. *J Virol* **71**: 8429–8436.
261. Kymäläinen H, Appelt JU, Giordano FA, Davies AF, Ogilvie CM, Ahmed SG *et al.* (2014). Long-term episomal transgene expression from mitotically stable integration-deficient lentiviral vectors. *Hum Gene Ther* **25**: 428–442.
262. Stehle IM, Postberg J, Rupprecht S, Cremer T, Jackson DA and Lipps HJ (2007). Establishment and mitotic stability of an extra-chromosomal mammalian replicon. *BMC Cell Biol.* **8**: 33.
263. Hagedorn C, Baiker A, Postberg J, Ehrhardt A, Lipps HJ (2012) *Handling S/MAR vectors.* <http://www.ncbi.nlm.nih.gov/pubmed/22661441>.
264. Jenke AC, Bok Hee C, Fetzer CP, Stehle IM, Jönsson F, Fackelmayer FO *et al.* (2002). An episomally replicating vector binds to the nuclear matrix protein SAF-A in vivo. *EMBO Rep.* **3**: 349–354.

265. Hauswirth WW and Berns KI (1977). Origin and termination of adeno-associated virus DNA replication. *Virology* **78**: 488–499.
266. Berns KI (1990). Parvovirus replication. *Microbiol Rev* **54**: 316–329.
267. Hong G, Ward P and Berns KI (1992). In vitro replication of adeno-associated virus DNA. *Proc Natl Acad Sci U S A* **89**: 4673–4677.
268. Ward P and Berns KI (1996). In vitro replication of adeno-associated virus DNA: enhancement by extracts from adenovirus-infected HeLa cells. *Journal of Virology* **70**: 4495–4501.
269. Yalkinoglu AO, Zentgraf H and Hubscher U (1991). Origin of adeno-associated virus DNA replication is a target of carcinogen-inducible DNA amplification. *J Virol* **65**: 3175–3184.
270. Ward P (2006) in *Parvoviruses*, ed Kerr JR. (Hodder Arnold; Distributed in the U.S.A. by Oxford University Press, London, New York), p. 190-211.
271. Jenke ACW, Stehle IM, Herrmann F, Eisenberger T, Baiker A, Bode J *et al.* (2004). Nuclear scaffold/matrix attached region modules linked to a transcription unit are sufficient for replication and maintenance of a mammalian episome. *Proc Natl Acad Sci U S A* **101**: 11322–11327.

# Appendix

## A. Significance values of Tukey *post hoc* comparison of means for ssAAV vectors

### 1. eGFP genomes

Vector preparation	Plasmid-Vector + Plasmid-Helper	Plasmid-Vector + MC-Helper	MC-Vector + Plasmid-Helper
Plasmid-Vector + Plasmid-Helper		0.6691	0.4343
Plasmid-Vector + MC-Helper	0.6691		0.0412 *
MC-Vector + Plasmid-Helper	0.4343	0.0412 *	
MC-Vector + MC-Helper	0.2290	0.0129 *	0.9795

### 2. Ratio vp:vg

Vector preparation	Plasmid-Vector + Plasmid-Helper	Plasmid-Vector + MC-Helper	MC-Vector + Plasmid-Helper
Plasmid-Vector + Plasmid-Helper		0.0732	0.2497
Plasmid-Vector + MC-Helper	0.0732		0.0145 *
MC-Vector + Plasmid-Helper	0.2497	0.0145 *	
MC-Vector + MC-Helper	0.1534	0.0105 *	0.9515

### 3. Transducing units (tu)

<b>Vector preparation</b>	Plasmid-Vector + Plasmid-Helper	Plasmid-Vector + MC-Helper	MC-Vector + Plasmid-Helper
Plasmid-Vector + Plasmid-Helper		0.238	< 0.001 ***
Plasmid-Vector + MC-Helper	0.238		< 0.001 ***
MC-Vector + Plasmid-Helper	< 0.001 ***	< 0.001 ***	
MC-Vector + MC-Helper	0.234	< 0.001 ***	< 0.001 ***

## B. Significance values of Tukey *post hoc* comparison of means for scAAV vectors

### 1. eGFP genomes

Vector preparation	MC-Vector + MC-Helper	Plasmid-Vector + MC-Helper	MC-Vector + Plasmid-Helper
MC-Vector + MC-Helper		0.00395 **	0.62261
Plasmid-Vector + MC-Helper	0.00395 **		0.00109 **
MC-Vector + Plasmid-Helper	0.62261	0.00109 **	
Plasmid-Vector + Plasmid-Helper	0.08486	0.18322	0.01515 *

### 2. Ratio vp:vg

Vector preparation	MC-Vector + MC-Helper	Plasmid-Vector + MC-Helper	MC-Vector + Plasmid-Helper
MC-Vector + MC-Helper		0.1243	0.9441
Plasmid-Vector + MC-Helper	0.1243		0.0578
MC-Vector + Plasmid-Helper	0.9441	0.0578	
Plasmid-Vector + Plasmid-Helper	0.3923	0.8181	0.1949

### 3. Transducing units (tu)

Vector preparation	MC-Vector + MC-Helper	Plasmid-Vector + MC-Helper	MC-Vector + Plasmid-Helper
MC-Vector + MC-Helper		< 0.001 ***	0.276
Plasmid-Vector + MC-Helper	< 0.001 ***		< 0.001 ***
MC-Vector + Plasmid-Helper	0.276	< 0.001 ***	
Plasmid-Vector + Plasmid-Helper	< 0.001 ***	0.956	< 0.001 ***

### 4. Ratio vp:tu

Vector preparation	MC-Vector + MC-Helper	Plasmid-Vector + MC-Helper	MC-Vector + Plasmid-Helper
MC-Vector + MC-Helper		0.03318 *	0.77174
Plasmid-Vector + MC-Helper	0.03318 *		0.00909 **
MC-Vector + Plasmid-Helper	0.77174	0.00909 **	
Plasmid-Vector + Plasmid-Helper	0.01898 *	0.97593	0.00562 **

## Danksagung

Herzlich bedanken möchte ich mich bei meiner Doktormutter Prof. Dr. Hildegard Büning für die Ermöglichung dieser Arbeit, die freundliche Aufnahme in die Arbeitsgruppe, die engagierte Betreuung meiner Doktorarbeit und ihre vielfältige Unterstützung zu jeder (Tages-)Zeit.

Prof. Dr. Dagmar Mörsdorf danke ich für die Bereitschaft, meine Doktorarbeit zu betreuen und sie so zu ermöglichen. Vielen Dank an Prof. Uhlirova für die Übernahme des Zweitgutachtens. Beiden danke ich für ihre Unterstützung als Tutorinnen während meiner Arbeit und für die anregenden Diskussionen bei den Tutorentreffen.

Riesiger Dank gilt auch allen Kooperationspartnern: Dr. Martin Schleef, Dr. Marco Schmeer und dem Team von PlasmidFactory im MC-Projekt, Dr. Claudia Hagedorn und Prof. Dr. Hans J. Lipps im S/MAR-Projekt und Dr. Tobias Riet und Prof. Dr. Hinrich Abken im T-Zell-Projekt. Die Zusammenarbeit mit euch hat viel Spaß gemacht und ich habe von euch und durch die gemeinsame Arbeit sehr viel gelernt.

Lieben Dank an alle früheren und jetzigen Mitglieder der AG Büning für ihre große Hilfsbereitschaft, ihre tatkräftige Unterstützung, den wissenschaftlichen Austausch und die tolle Zeit im Labor. Besonders bedanken möchte ich mich bei Dr. Marianna Hösel (auch für ihre Hilfe bei den Experimenten und die hilfreichen Diskussionen) und Nadja Meumann, meiner Leidens- und Lachensgenossin, die mit mir in den letzten Monaten die Stellung gehalten haben. Herzlicher Dank an die „Räumchen-Insassen“ und die Gourmets der Ebene 5, Nadja, Elli, Alex, Viki, Johannes und Petra für das Teilen von Freud und Leid, Spiel und Spaß und immer gutem Essen.

Ganz herzlich danke ich meinen Eltern Claudia und Werner Schnödt, meinen Geschwistern Christina und Michael, meiner Familie und Freunden für die liebevolle Unterstützung – ihr seid die Besten!  
Lieber Marcus, vielen Dank für alles!

# Erklärung

Ich versichere, dass ich die von mir vorgelegte Dissertation selbständig angefertigt, die benutzten Quellen und Hilfsmittel vollständig angegeben und die Stellen der Arbeit – einschließlich Tabellen, Karten und Abbildungen –, die anderen Werken im Wortlaut oder dem Sinn nach entnommen sind, in jedem Einzelfall als Entlehnung kenntlich gemacht habe; dass diese Dissertation noch keiner anderen Fakultät oder Universität zur Prüfung vorgelegen hat; dass sie – abgesehen von unten angegebenen Teilpublikationen – noch nicht veröffentlicht worden ist, sowie, dass ich eine solche Veröffentlichung vor Abschluss des Promotionsverfahrens nicht vornehmen werde. Die Bestimmungen der Promotionsordnung sind mir bekannt. Die von mir vorgelegte Dissertation ist von Prof. Dr. Dagmar Mörsdorf und Prof. Dr. Hildegard Büning betreut worden.

## Teilpublikationen:

**Schnödt M**, Schmeer M, Kracher B, Krüseemann C, Espinosa LE, Grünert A, Fuchsluger T, Rischmüller A, Schleef M and Büning H (2016). DNA Minicircle Technology Improves Purity of Adeno-associated Viral Vector Preparations. *Mol Ther Nucleic Acids* **5**: e355. DOI 10.1038/mtna.2016.60

Aus dieser Publikation sind große Teile der Kapitel 4.1 und 5.1, sowie der Anhang übernommen. Der Text wurde teilweise im Wortlaut übernommen. Alle Abbildungen und Tabellen, die aus der Publikation übernommen wurden, sind im Einzelnen gekennzeichnet.

Hagedorn C \*, **Schnödt M** \*, Boehme P, Abdelrazik H, Lipps HJ, Büning H (2016). S/MAR element improves but is not required for episomal long-term persistence of Adeno-associated viral (AAV) vector genomes in proliferating cells. *Gene Ther*, revised manuscript under review  
(\* equal contribution)